Studies on Development of MgB_2 Superconducting Wires with Improved In-Field Critical Current Density and Electromechanical Properties

Thesis submitted to

Cochin University of Science and Technology (CUSAT)

in partial fulfillment of the requirements for the award of the degree of

Doctor of Philosophy

in **Physics** Under the **Faculty of Science**

by

SYJU THOMAS

Under the supervision of

Dr. U. Syamaprasad

National Institute for Interdisciplinary Science and Technology
(Council of Scientific and Industrial Research)
Thiruvananthapuram-695019

May 2016

Studies on Development of MgB_2 Superconducting Wires with Improved In-Field Critical Current Density and Electromechanical Properties

Ph. D. Thesis
May 2016

Author:

Syju Thomas

Material Science and Technology Division

National Institute for Interdisciplinary Science and Technology (CSIR)

Trivandrum-695019

Email: syjuthomas@gmail.com

Tel: +91 9745331849

Supervising guide:

Dr. U. Syamaprasad

Former Chief Scientist

Material Science and Technology Division

National Institute for Interdisciplinary Science and Technology (CSIR)

Trivandrum-695019

Email: syamcsir@gmail.com

Tel: +91 471 2741830

DECLARATION

I, **Syju Thomas**, hereby declare that, the thesis entitled "**Studies on Development of MgB_2 Superconducting Wires with Improved In-Field Critical Current Density and Electromechanical Properties**" is a bonafide record of the research work done by me under the supervision and guidance of Dr. U. Syamaprasad, Retired Chief Scientist, National Institute for Interdisciplinary Science and Technology (CSIR), Trivandrum and no part of this dissertation has been submitted previously for the award of any degree in any other University.

Syju Thomas

Place: Trivandrum
Date: 17-05-2016

CERTIFICATE

Certified that the work embodied in the thesis entitled, "**Studies on Development of MgB_2 Superconducting Wires with Improved In-Field Critical Current Density and Electromechanical Properties**" is an authentic record of the research work carried out by **Mr. Syju Thomas**, Applied Superconductivity Group, Materials Science and Technology Division, CSIR - National Institute for Interdisciplinary Science and Technology (NIIST), Trivandrum, under my supervision in partial fulfillment of the requirement for the degree of Doctor of Philosophy of the Cochin University of Science and Technology and further that no part of this thesis has been presented previously for the award of any other degree.

U. Syamaprasad
(Research Guide)
Former Chief Scientist
CSIR-NIIST, Trivandrum

Place: Trivandrum
Date: 18-05-2016

Dedicated to my family…

Acknowledgements

Firstly, I would like to express my sincere gratitude to my supervising guide, Dr. U. Syamaprasad, Chief Scientist (Rtd.), Applied Superconductivity Group, National Institute for Interdisciplinary Science and Technology (CSIR), Trivandrum, for the continuous support on my research, for his patience, motivation, and immense knowledge. Without his support I could not have completed my Ph.D. work successfully.

I would like to thank Dr. A. Ajayghosh, Director, NIIST (CSIR); Dr. Suresh Das and Dr. B. C. Pai, former Directors, for providing all the necessary facilities to carry out this work.

I thank Dr. Manoj Raama Varma, Senior Principal Scientist, NIIST (CSIR) for his support and co-operation after the retirement of my guide.

I would like to thank Dr. Prabhakar Rao P., Chief Scientist & Head, Materials Science and Technology Division (MSTD), NIIST (CSIR); Dr. M. L. P. Reddy, Dr. M. T. Sebastian, and Dr. K. G. K. Warrier, former Heads of MSTD.

Next, I wish to sincerely thank Mr. P. Guruswamy (Rtd.), Technical Officer at Applied Superconductivity Group, NIIST (CSIR), for his encouragement and support.

I also extend my heartfelt thanks to Mr. M. R. Chandran, Mr.Robert Philip, Mr. Kiran Mohan and Mr. Peer Mohammad for extending different instrumental facilities such as SEM, HRTEM and optical microscope.

I sincerely thank Dr. A. Sundaresan, Professor, Chemistry and Physics of Materials Unit, Jawaharlal Nehru Centre for Advanced Scientific Research (JNCASR), Bangalore; Dr. S. B. Roy, Raja Ramanna Centre for Advanced Technology (RRCAT), Indore and Dr. S. Pradhan, Institute for Plasma Research (IPR), Gandhinagar, for experimental equipment support and collaboration. I thank Dr. K. P. Vijayakumar, Emeritus Professor, Department of Physics, Cochin University of Science and Technology, Cochin, for his valuable suggestions at various stages of work

I thank my fellow labmates Dr. K Vinod, Dr. Neson Varghese, Dr. K M Devadas, S Rahul, Dr. P M Sarun, Dr. P M Aswathi, Dr. J B Anooja, Dr. R Shabna, M B Basim, A Sivaprakash, S Santhoshkumar, late Mr. V F Vinu, G R Anuraghi, K T Jackson, S L Vinu, M Maheshkumar, M Firozkhan and Dinesh Jose for the stimulating

discussions, technical supports and cheerful moments. I sincerely thank Dr. R P Aloysius, Dr. A Biju and Dr. S Vinu for all their help and support.

I thank all my friends in NIIST who helped me scientifically as well as personally. I am also grateful to the NIIST administration for facilitating all the timely help.

I sincerely acknowledge University Grants Commission (UGC) for providing the research fellowship and thus an opportunity to do the present work.

Finally, I must express my very profound gratitude to my family for providing me with unfailing support and continuous encouragement throughout my years of study.

PREFACE

Since its discovery in 1911, superconductivity has been experimentally fascinating and theoretically challenging phenomenon. The accidental and unexpected discoveries of new superconductors have been creating waves of excitement and research outputs for decades. The efforts for better theoretical understanding and exploitation of possibilities for applications hold this field always active. The applications of superconductors cover a wide area: from lossless power transmission to high speed transportation and very high field magnets to extremely low field sensors. The efforts in realization of stable nuclear fusion reactor with the aid of superconducting magnets are being keenly watched by the world in the scenario of energy crisis.

Although hundreds of superconductors have been discovered, only few of them are practically useful. The NbTi (T_C = 9 K) and Nb_3Sn (T_C = 18 K) are the most commonly used superconductors to make high field magnets. The easiness in conductor fabrication gives NbTi an upperhand. But being low temperature superconductors, they need costly liquid He to maintain its superconducting state. Later in 1980s cuprate based superconductors with T_C higher than liquid Nitrogen were discovered. But the intrinsic problems such as high anisotropy and weak link granularity make the long length conductor fabrication difficult. In 2001 the discovery of superconductivity in MgB_2 by Akimitsu group, Japan evoked curiosity of many researchers to transform it to practical appliances. In addition to the high transition temperature (39 K), the favorable properties such as, low anisotropy, strong intergrain links and cheaper raw materials have made this superconductor as a potential candidate for developing various devices.

The usefulness of a superconductor is determined by its capacity to carry high current in high magnetic fields. Though MgB_2 possesses a self-field J_C of 10^5 - 10^6 A/cm^2 at 4.2 K, it falls rapidly on application of high magnetic fields due to poor flux pinning ability and lower upper critical field (H_{C2}). So it is necessary to improve the in-field current carrying capacity ($J_C(H)$) of the superconductor for the applications where high magnetic field is present. To make superconducting magnets, designers adopt two

approaches depending on the nature of material, wind & react method and react & wind method. The latter one is easier and cheaper, but if the superconductor is brittle type, as the coil diameter lowers the current carrying capacity will be reduced fast. So that magnet making will be easier if bending strain tolerance of reacted wires is improved.

The objective of the present thesis is to develop MgB_2 wires with enhanced in-field critical current density and to study and improve the bending strain tolerance of MgB_2 wires prepared by various approaches.

The thesis is organized into 7 chapters. The introductory chapter describes the phenomenon of superconductivity, underlying theories and applications of superconductors. The chapter 2 discusses the features and significance of MgB_2 superconductor with its present status. Details of preparative techniques and characterizations used for present work are described in the chapter 3.

The efforts to improve $J_C(H)$ of MgB_2 by chemical addition are presented in chapter 4. Bulk form of MgB_2 was prepared for the study and magnetic measurements were used to characterize superconducting properties. In the first section of the chapter it is identified that 0.1 atomic % of nano-carbon is ideal for $J_C(H)$ improvement of MgB_2. The following sections present, achievement of further improvement of $J_C(H)$ by co-doping of various nano-additives with nano-carbon.

For most of the practical applications superconductors has to be made in the form of wires. Chapter 5 presents the results of fabrication of MgB_2 mono-filamentary and multi-filamentary wires. The sheath, barrier and reaction temperature were optimized. Both self-field and in-field characterization of transport properties of multi-filamentary wires was done. The results obtained from the studies on the bulk MgB_2 to enhance $J_C(H)$ were successfully carried over to wire samples and it is presented in the last section of this chapter.

Chapter 6 details the studies on the effect of bending strain on current carrying property of the MgB_2 wires. The first section of the chapter presents the results of studies on the Fe sheathed mono-filamentary wires. In the following section, the achievement of a significant improvement on J_C with bending strain in multi-filamentary wires by

increasing the number of filaments is presented. Last section of the chapter presents a novel and effective technique towards the improvement of bending strain tolerance-the excess Mg addition. In this method the stoichiometry of the Mg was deliberately increased from 1 Mg to 6 Mg and heat treatment was done at 600 $^{\circ}$C. The result was a geometry, in which micrometer sized MgB_2 cores embedded in the Mg matrix with very high bent strain tolerance. Finally the chapter 7 summarizes the work with main conclusions and future scope and directions of work in the area.

Contents

Chapter 1

Superconductivity: The Phenomenon and Applications

1.1 Quick Retrospect

The first successful liquefaction of helium was done by Dutch physicist Kamerlingh Onnes in 1908 at university of Leiden. By decreasing the boiling off pressure of liquid helium, he could bring down its temperature to 0.9 K. The ability to achieve a temperature of just few decimals of kelvin above absolute zero opened up a new frontier of science – low temperature physics.

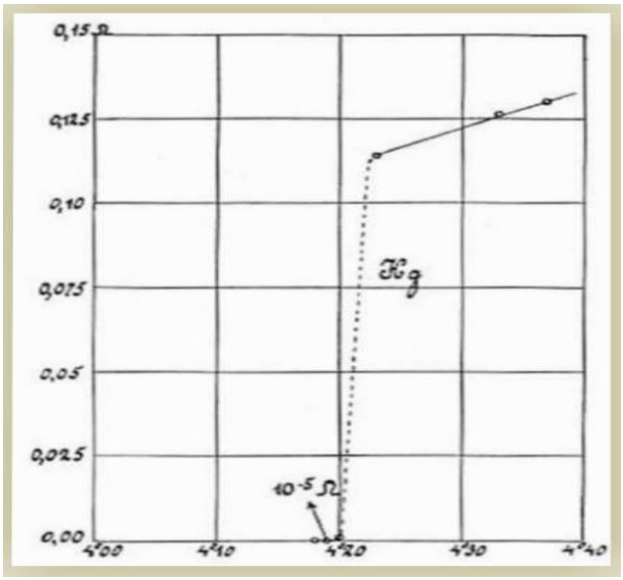

Figure 1.1: The Historic Plot done by Onnes in October 1911 showing the Resistance vs Temperature plot of mercury

In 1911, in an effort to settle down the logical dispute about the behavior of electrical conductivity of metals at very low temperatures he carried out low temperature resistance measurements of pure metal wires. He wisely chose mercury as a candidate because high purity mercury can be obtained by distillation and also it

was expected to have a high enough resistance to measure at low temperatures. While measuring the resistance of mercury with decreasing the temperature, he could observe a precipitous drop in resistance at 4.2 K. The drop was too enormous to measure or practically zero and too abrupt i.e. within few hundredths of a Kelvin [1]. Kamerlingh Onnes declared that the mercury had passed into a new state - the superconductive state, as he called it. Thus the phenomenon of vanishing of electrical resistance of a material below a particular temperature was called superconductivity and the materials which exhibit superconductivity were called superconductors. The temperature at which a material transits from normal state to superconductive state was termed as critical temperature (T_C) of that material.

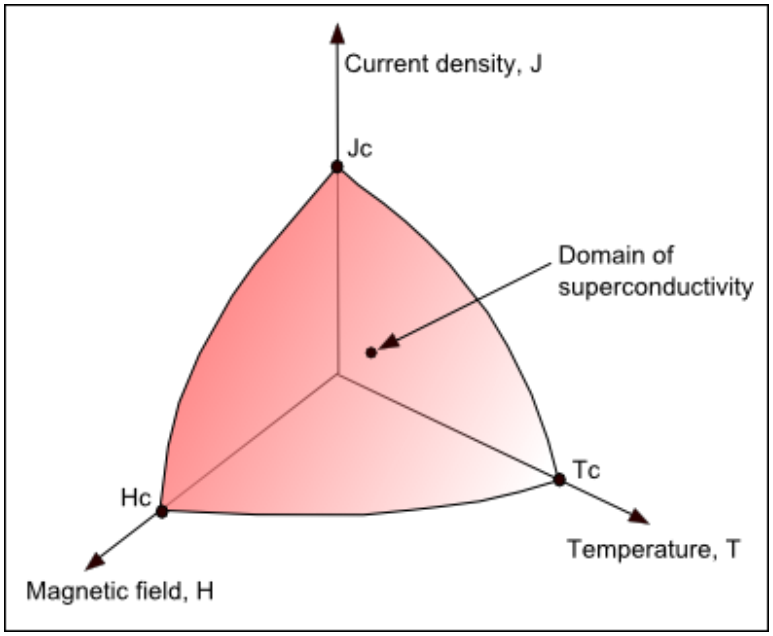

Figure 1.2: The critical surface of a superconductor. The point inside the surface is the domain of superconductivity

Onnes was well aware of the potential of his discovery. He dreamt of electromagnets capable of producing huge fields without any joule dissipation. But he was displeased to see that even in the presence of a very small magnetic field the material lost its superconducting state. This critical limit of the magnetic field was called critical field (H_C) of the superconductor. The same collapse of superconductivity was observed when the material was passed with a current beyond a critical limit known as critical current (I_C). These critical values, each depending on each other, set a limitation to superconductors to lie within a surface known as critical surface to exhibit its superconductivity.

In 1933, Walther Meissner and R. Ochsenfeld discovered that superconductors are able to completely expel the magnetic field from within it, provided the field is below a threshold level called critical field (H_C) [2]. They found that, whatever be the path chosen to apply the field, the field expulsion takes place. This is the result of the thermodynamic reversibility of the superconducting transition. Therefore a superconductor is not only a material with zero resistivity but a perfect diamagnet also. This finding was a milestone in superconductivity and paved the way to further development of the subject in both theoretical and experimental aspects.

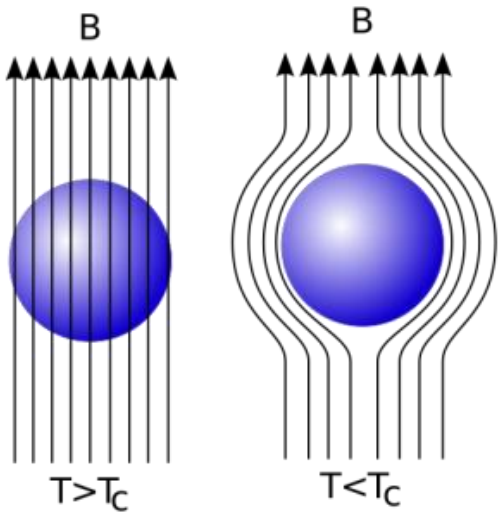

Figure 1.3: The Meissner effect showing the exclusion of magnetic field from within a superconductor when temperature below the T_C

The first noticeable effort to explain the Meissner effect was done by London brothers by their phenomenological theory in 1935 [3]. The important contribution of the theory was the term λ, the penetration depth of the superconductor. London's equations allow penetration of finite magnetic field into the superconductor and this field decays to *1/e* th of its original value over a distance of λ. But the theory was unsuccessful to give an account to the existence of the positive surface energy between superconducting and normal regions.

In 1950, a more comprehensive theory was put forward by Ginzburg and Landau, by considering the property of coherence of the superconducting electrons [4]. The theory introduced a complex order parameter with non-zero value in superconductive transition state, and related to the density of superconducting

electrons. The GL theory put forward an effective way to study the properties of a superconductor.

One of the major successes of the theory was in 1957, when Abrikosov solved the GL equations to show the existence of negative surface energy, between superconducting and normal phases [5]. This made him to predict the presence of a new class of superconductors known as type II superconductors, which allows the penetration of magnetic field into it and creates normal regions and at the same time maintains the superconducting regions too. This allows the type II superconductors to withstand high magnetic fields of the order of tesla. Several alloys were confirmed to be type II superconductors and Onnes' dream became realistic.

But a major drawback of the GL theory was its silence towards the microscopic changes and properties in a superconductor transition. The occurrence of energy gap and phenomena like isotopic effect were not well understood due to absence of such a microscopic theory until the publication of the well-known BCS theory. In 1957 Bardeen, Cooper and Schrieffer, from USA could bring out a microscopic theory to explain the superconductive transition at critical temperature [6]. They described a mechanism of phonon exchange interaction between two electrons to form a bound state known as cooper pair and which is capable of moving without resistance. They could explain the isotopic effect and band gap successfully.

Another important theoretical advancement came in 1962, when Brian D. Josephson, who was a graduate student of Cambridge University, predicted that the supercurrent can flow between two superconductors separated by an insulator. This prediction was experimentally confirmed later and now known as Josephson effect [7]. 1980s were an unparalleled decade for superconductivity due to unexpected and astonishing discoveries of new superconductors. The discovery of high temperature cuprate superconductors in 1986 by Alex Muller and George Bednorz evoked the researchers to search for new superconductors worldwide [8]. Also, this high temperature superconductivity demanded new theoretical models other than BCS theory for the complete understanding of the phenomenon. The search for new superconductors continued with all possible combinations. To the excitement of all, in 2001, a simple diatomic compound, sitting in the shelf for half a century was found to be superconducting at a fairly high critical temperature of 39 K [9]. The compound

was MgB_2 and found to have potential to replace low temperature superconductors. Researchers started worldwide efforts to extract the maximum from it. The present thesis work describes the results of a few such efforts done.

1.2 BCS Theory of Superconductivity

One year before the publication of BCS theory Cooper had introduced the 'cooper pair problem', which was the first step towards the development of BCS theory [10]. Cooper theoretically showed that, there exists a fundamental instability in the ground state of the electron gas if the electron system develops a net attractive interaction to form bound pairs called Cooper pairs, by overcoming their mutual Coulomb repulsion. Whatever smaller the interaction is, the effect of this is to push far down the energy levels just above the Fermi level E_F. The split off of this state far below E_F means that a free-electron gas with random occupation of state is unstable to the formation of pairs when an attractive interaction is introduced.

Bardeen, Cooper and Schrieffer, in 1957, showed that the electron pair could be formed mediated by lattice vibrations [6]. The theory states, at sufficiently lower temperatures, an electron moving with momentum $\boldsymbol{k}$ through the lattice can distort the lattice and get scattered. This creates a virtual phonon and a second electron, with a momentum $\boldsymbol{k'}$, absorbs this phonon momentum at some distance away. If the difference in energies of above two electrons is equal to $\hbar\omega_D$, where ω_D is the Debye frequency of the lattice, they will exhibit an attractive interaction. Thus a Cooper pair can be formed by electron-phonon-electron interaction. The energetically most favored combination for this phonon exchange occurs when the electrons have equal and opposite momentum and with spins antiparallel. Since the total spin of Cooper pair is zero, they obey Bose-Einstein distribution law and all the pairs can be in the same ground state, represented by a single wave function. The real space extent of this wave packet is given by $\xi \sim 0.18\hbar v_F/k_BT_C$. This is known as the coherence length or simply the size of a Cooper pair. If the system is disturbed, it responds as a giant unit rather than single particles.

The pairs can be disrupted due to many causes like thermal (k_BT) excitations, electromagnetic absorption or injection of electrons. The minimum energy for this

disruption to be happened for one pair of electron at $T = 0$ turns to be $\Delta_0 \sim 1.8 k_B T_C$, Δ_0 is called as the energy gap at absolute zero.

1.3 Ginzburg-Landau parameter and Type II superconductivity

Earlier in the theoretical development of superconductivity, Ginzburg and Landau had developed a powerful formulation of the problem. They defined a term order parameter which behaves like a wave function ψ, and obeys the relation $|\psi|^2 = n_s$, where n_s is the local density of superconducting electrons. They expanded an expression for free energy in terms of order parameter and minimized it to arrive Ginzburg-Landau equation [4].

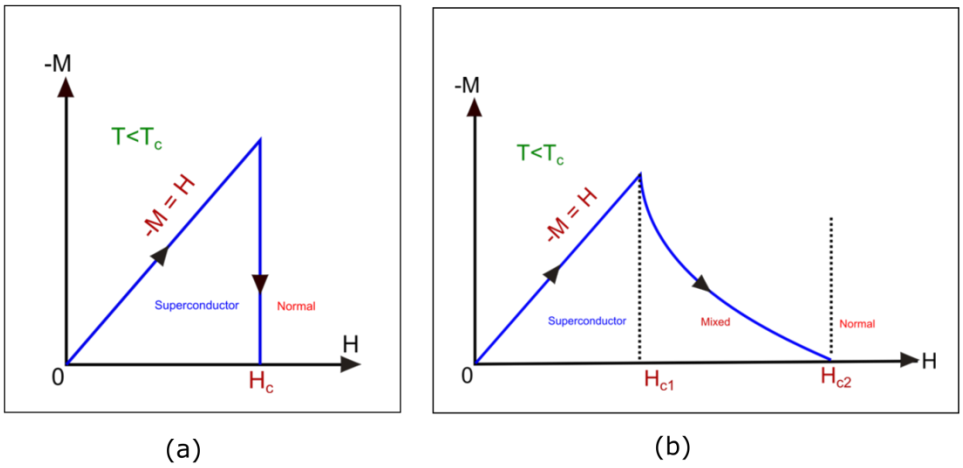

Figure 1.4: The magnetic behavior of (a) Type I and (b) Type II superconductors

A key factor deciding whether a superconductor is type I or type II is the boundary energy between the superconducting and normal region. If the superconducting-normal metal boundary has a positive surface energy, the system will minimize the area of boundary and perfect expulsion of the external field will be the result (figure 1.4a). These are called type I or soft superconductors.

If the superconductor-normal metal boundary has a negative surface energy, the material will try to maximize the amount of superconductor-normal metal boundary area. This causes the material to partially allow the passage of field lines through it when the applied field is above the lower critical field H_{C1} (figure1.4b). As the result there will be co-existing superconducting and normal areas. The volume

proportion of the normal areas of this intermediate state increases with the applied field and at upper critical field H_{C2}, the material becomes normal.

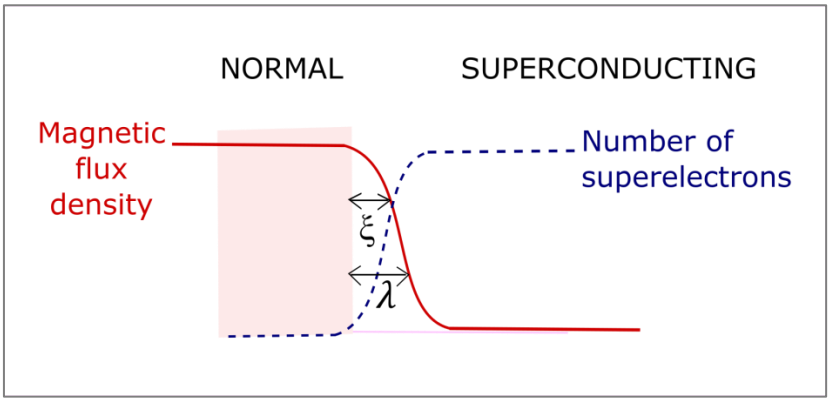

Figure 1.5: Illustration of coherence length (ξ) and penetration depth (λ) at asuperconductor-normal metal boundary

The density of superconducting electrons does not change abruptly but only gradually over a distance called coherence length ξ. This means, a sharp boundary between normal and superconducting regions does not exist. The coherence length ξ is a characteristic length of a superconducting material just like λ-the penetration depth, another characteristic length. In their original paper, Ginzburg and Landau showed that the ratio of these two characteristic lengths determines the onset of occurrence of negative surface energy. This ratio is called Ginzburg-Landau parameter given by $\kappa = \lambda/\xi$. For $\kappa > 0.71$, the material favors mixed state and shows type II superconductivity and if $\kappa < 0.71$, the material will be of type I.

The vortex state

In type II superconductors, beyond the H_{C1}, small normal state zones are formed and the excess magnetic field lines are localized along these cores of normal zones with circulating current on their surfaces, which keep the superconducting state of the areas outside the core.

Abrikosov in 1957, based on GL theory predicted that the flux entering the type II superconductor breaks into quantized units of flux ϕ_0, variously called flux quantum, fluxon, fluxoid or flux vortex [11]. The minimum unit of this flux that can enter has a magnitude of, $\phi_0 = 2.07 \times 10^{-15}$ Tm^2. Figure 1.6 shows the model of a single flux core. It is like a cylindrical shaped normal state material with circulating

supercurrent around at distance λ from the center of vortex. The circulating current is the origin of the name flux vortex. The cylindrical core has a diameter twice the coherence length (2ξ). The magnetic flux resides within the core and decays to the superconducting bulk over a distance of London penetration depth λ.

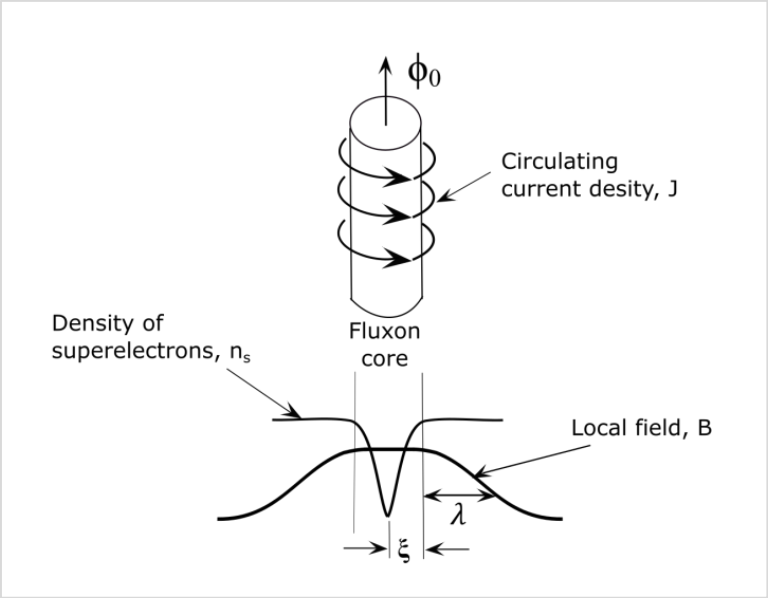

Figure 1.6: Model of a single flux core. The core has a radius ξ

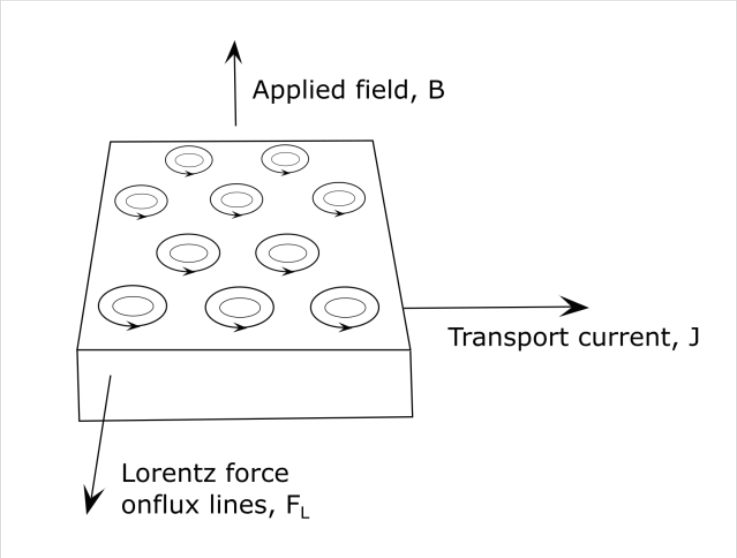

Figure 1.7: The directions of magnetic field, transport current and Lorentz force on triangular flux line lattice in a superconducting slab

When the applied field increases, the number density of the vortex lines also increases and there will be significant mutual repulsive force between them. This

causes the flux vortices to arrange themselves into a lattice like arrangement. This periodic structure is called flux line lattice (FLL) and was predicted by Abrikosov [11]. He found that the most favorable configuration of this lattice is "triangular" to minimize the free energy (figure 1.7).

1.4 Flux flow and flux pinning in type II superconductors

When a transport current is applied to a superconducting fluxon lattice, where the current flow is perpendicular to the applied magnetic field, the flux vortices experience an interactive force with the transport current. The magnitude and the direction of this force is given by Lorentz's law for the force on a charged particle moving through a magnetic field, $\boldsymbol{F_L} = \boldsymbol{J}\times\boldsymbol{B}$. Where F_L is the Lorentz's force density and J and B are the transport current density and magnetic field, respectively. The F_L has unit of newton per cubic meter and acts in a direction perpendicular to the direction of both $\boldsymbol{J}$ and $\boldsymbol{B}$ (figure 1.7).

The effect of this force is to move flux line across the superconductor. The movement of flux lines corresponds to change in flux density and from fundamental axioms of electromagnetics; this creates an induced electric field in the direction of transport current. The magnitude of this induced field is given by $E = n_f \phi_0 v_f$, where n_f is the number of fluxons and v_f is the velocity of fluxons (the voltage is given by product of electric field and length along the direction of current).

The consequence of this flux flow is that this superconductor can no longer support a transport current with zero dissipation. The flow of normal electrons in the flux core dissipates heat energy and the material becomes normal. But if we could prevent the movement of FLL under the influence of Lorentz force, the zero resistance condition can be sustained even when high transport current is passed through. There exists such an opposing force to Lorentz force in any inhomogeneous superconducting material. This is known as flux pinning force and the effect of this force is to restrain the FLL by pinning it in place against the Lorentz force.

As the current density is increased the Lorentz's force on the pinned flux line is also increased and at some critical current density, the F_L exceeds the flux pinning force density F_P and creates dissipation loss in the material. Hence the bulk pinning

force density F_P (N/m^3) can be defined as the critical Lorentz force density, i.e. $F_P = |F_{LC}| = J_C \times B$. But if the applied field is higher than certain limit known as irreversibility field (B_{irr}), flux pinning becomes ineffective even at very small transport current. In other words, the critical current density becomes practically zero at B_{irr}. The irreversibility field of a superconductor is often very lower than H_{C2}. It is not an intrinsic property but can be increased by increasing the flux pinning ability of the bulk superconductor.

There are various mechanisms by which FLL may be pinned. Generally, these depend on the microstructural features that interact with the individual flux lines. Normal conducting precipitates, inclusions, voids, and grain boundaries are examples of some microstructural features which can provide pinning force against the movement of FLL and are called as “flux pinners”.

To create a flux line within the superconductor, the system should provide energy to convert the core of the flux with radius ξ to normal state. This energy (per unit length of flux line) is called condensation energy. If the superconducting matrix contains normal precipitates/inclusions/voids of diameter in the range of 2ξ, it acts as a potential well of lower energy to flux line and the flux line is pinned to this so as to save the condensation energy [12]. Whereas in grain boundaries a different flux pinning mechanism is proposed [12, 13]. Grain boundaries are strong scatterers of normal electrons and thereby reducing the mean free path at grain boundaries. When the mean free path l is less than the coherence length ξ, there exists a relation between them given by $\xi \propto l^{0.5}$. This means, the coherence length is reduced at grain boundaries and hence the condensation energy too. Therefore, grain boundaries also act as flux pinning centers.

To get the picture complete, the superconductor should be considered as bulk and all the flux line –flux line interactions and flux line – inclusion/grain boundary interactions are to be considered. The various theories and models to explain these have evolved into a new branch of superconductivity-the vortex dynamics.

1.5 Superconducting Materials

Soon after the discovery of superconductivity in Hg, Onnes himself discovered the phenomenon in more elements and alloys within next two years. He observed the superconductivity in Pb (T_C = 7.3 K), Sn (3.7 K) and also in various alloys such as HgAu, HgCd, HgSn and PbSn [14]. Today thousands of materials have been known to be superconducting within a wide spectrum of transition temperatures ranging from few milli kelvins to 165 K. Regarding the elements, 31 of them are found to be superconducting at ambient pressure and the highest transition temperature (9.2 K) is observed in Nb [15, 16]. But varying the ambient conditions and natural form, it is interesting to note that more than half of the elements in periodic table are superconducting. This variation of conditions can be the application of high pressure, irradiation or transformation of material into thin film/fine powder/amorphous state etc. Besides the pure elements, materials in almost all categories have shown superconductivity in one condition or the other. These include metallic alloys, and compounds, metallic glasses, intermetallics, ceramics, organic and inorganic polymers, various forms of carbon such as carbon nanotubes and fullerenes (under doping) etc.

Table 1.1: T_C s of selected superconductors under different classifications

Type/Class	Material	T_C
Elements	Hg	4.2
	Nb	9.2
	Li (under pressure)	20
	Pd (after irradiation)	3.2
	W (thin film)	5.5
Alloys	NbTi	9.0
	MoTc	16.0
A-15 type (A_3B)	Nb_3Sn	18.2

	V_3Ga	14.8
	Nb_3Ge	23.2
Laves phase (AB_2)	ZrV_2	9.6
	$LaOs_2$	8.9
Chevrel phase	$PbMo_6S_8$	12.6
	$Sn_{1.2}Mo_6S_8$	14.2
Heavy electron systems	UPd_2Al_3	2.0
Oxides	$Ba(PbBi)O_3$	13
	$LiTi_2O_4$	13.7
Borides	ZrB_{12}	5.8
	YRh_4B_4	11.3
	MgB_2	39
Cuprates	$YBa_2Cu_3O_7$	92
	$Bi_2Sr_2Ca_1Cu_2O_8$	80
	$Bi_2Sr_2Ca_2Cu_3O_{10}$	110
	$Hg_2Sr_2Ca_2Cu_3O_{10}$	135
Organic materials	[a]$(TMTSF)PF_6$	0.9
	[b]$(BEDT\text{-}TF)_2Cu[N(CN)_2]Br$	0.6
Doped Fullerenes	$Rb_{2.7}\ Tl_{2.2}C_{60}$	45
	CS_3C_{60}	47.4
Oxypnictides	$LaFeAsO_{0.9}F_{0.1}$	26
	$SmFeAsO_{0.85}F_{0.15}$	55

[a] TMTSF = tetra-methyl-tetra-selenium-fulvalene
[b] BEDT-TTF = bis-ethylene-dithia-tetra-thiafulvalene

Another noticeable class of superconductors is the A-15 type superconductors. They are binary compounds of formula A_3B and with A-15 structure. In this group of superconductors, generally the A ions are niobium (Nb) or vanadium (V) and B ions are, for example tin (Sn), aluminium (Al), germanium (Ge) or gallium (Ga). The superconductivity in V_3Si at 17.1 K was discovered by Hardy and Hulm in 1953 and Nb_3Sn was found to be superconducting around 18 K by Mathias *et al*. in 1957 [17, 18]. About 47 A-15 superconductors are known now but of which practically important materials are Nb_3Sn and V_3Ga due to their high critical current density [19]. The A-15 superconductor Nb_3Ge was the material with highest recorded T_C (23 K) until the discovery of high temperature superconductors [20]. The tabulation done by Roberts in 1976 lists several thousands of superconducting alloys and compounds, almost all with critical temperature below 20 K and assumed to be described by BCS theory [21].

The discovery of superconductivity in an organic compound in 1980 grabbed the attention of scientific community. Though the phenomenon was observed at 1.2 K and at high pressure, its existence was enough for the excitement. More excitements were on the way in 80s. In 1986, George Bednorz and Alex Muller published an article that galvanized the area of superconductivity. They discovered a new class of materials called cuprates and the system they synthesized (La-Ba-Cu-O) had an unusually high T_C of 30 K [8]. Their discovery made an outbreak of activities around the world to cook new ceramic cuprates, being insulators at room temperature, those were unexplored until then. In 1987, a research team substituted Yttrium for Lanthanum in Bednorz-Muller system and achieved superconductivity at an incredibly higher T_C of 92 K [22]. Simply, this material (now known as YBCO) can be kept warmer than liquid nitrogen without losing superconductivity. Other important additions to this group are Ba-Sr-Ca-Cu-O (BSCCO) [23], Ta-Ba-Ca-Cu-O (TBCCO) [24], and Hg-Ba-Ca-Cu-O (HBCCO) [25]. Among them, the mercuric-cuprate (discovered in 1993) exhibits a T_C of 135 K at normal pressure; under extreme pressure T_C could be increased up to 165 K [26].

In 2001, it was again a surprise in the field when an ordinary binary compound known for decades was identified as an extra ordinary superconductor with high potential for practical applications-the magnesium diboride (MgB_2) superconductor. The measured T_C, 39 K is the highest for any elemental or binary alloy superconductors [9]. The latest significant addition to the list of superconductors is a family of pnictides. These are iron-based superconductors and discovered in 2006 by a Japanese group [27, 28]. By doping, the T_C of these compounds have been increased up to 55 K [29]. Very high values of H_{C2} (>100 T) have made this type of superconductors a subject of active research [30]. The table 1.1 provides list of selected superconductors under various classifications.

1.6 Applications of Superconductors

Onnes had conceived the idea of very high field magnets at the very moment of the discovery of this fascinating phenomenon. But the superconducting materials discovered during his age were not good enough to fulfill his ambition. It was in 1954 that G.B. Yntema could develop the first successful superconducting magnet using Nb

wire [31]. He demonstrated a field of 0.71 T at 4.2 K and announced the beginning of engineering superconductivity. Later, the discovery of ductile superconducting alloy – NbTi flourished the field due to the easiness in long length wire drawing. Although the initial efforts aimed at developing superconductors in the form of coils to generate high magnetic fields, now engineers and scientists are exploiting them for a wide variety of applications. The unique properties such as, zero resistance to direct current, the ability to carry high currents, high sensitivity to magnetic field, expulsion of external magnetic field, very low resistance at high frequencies, very low signal dispersion etc. have made superconductors as the only choice for obtaining high performance in various applications.

Superconducting magnets are very compact and have high field strength when compared with the conventional electromagnets with copper cables. So the conventional magnets can be readily replaced with superconducting ones in many applications. Magnetic Resonance Imaging (MRI) is a radiation free noninvasive imaging technique used in medical field. The core requirement of an MRI instrument is a high field magnet with high homogeneity and stability of the field. The superconductor magnets are well suited for this and are being used. Currently, NbTi alloys are mainly used in MRI instruments. A counterpart of MRI in research field is the NMR device. It is a very important diagnostic tool in many research areas and requires very high magnetic fields. Nb_3Sn is usually employed for this requirement. In mining industries, magnetic separation of magnetic contaminants is very common. Technical advances have led to the development of high gradient magnetic separators (HGMS) with the aid of superconducting magnets.

The demand from high energy physics community has always propelled engineering superconductivity from late 1960's onwards. High energy particle accelerators (atom smashers) with tera-electron volt (TeV) energy regime and capable to guide the particle in circular orbit of many kilometers in diameter wouldn't have been realized without superconducting magnets. Large Hadron Collider (LHC) of CERN, the world's largest particle accelerator has used tons of superconducting wires to construct its 1232 dipole magnets and 392 quadrupole magnets [32].

The most important project which is capable to change the future of mankind and where superconductor technology is inevitable is the international Thermonuclear

Experimental Reactor (ITER) project. The project team is engaged to develop fusion reactor where many millions of electron volts of energy/nucleon (equivalent to several million degree Celsius of temperature) is to be supplied. The temperature of this range can be achieved by magnetic plasma confinement, using superconducting magnets. ITER demands about ten thousand tons of magnets for this purpose and these magnets are made of NbTi and Nb_3Sn [33]. Magnetic refrigeration (where adiabatic demagnetization process is involved) is another area where superconducting magnets are effectively being used. Temperatures as low as micro kelvins has been achieved by making use of magneto caloric effect.

Power industry is another sector which has started to exploit the benefits of superconductor technologies recently. Lossless electric power transmission is possible by replacing conventional copper/aluminum transmission cables. A significant progress using HTS cable has already taken place in this arena. World's first commercial power grid with HTS cable has been demonstrated in US, which has a capacity of 574 megawatts (enough to power ~300,000 homes) [34]. The local power grid may sometimes suffer to unexpected high power surges beyond many times the rated current. This 'fault' current due to short circuit is capable to damage many devices in power grid. Superconductor Fault Current Limiters (SFCLs) are a solution to this and under development for commercialization [35]. When an overcurrent passes through, SFCLs sense it and switch to normal resistive state from superconducting state, thereby reducing the high current levels [12].

Conventional transformers in power grids cause energy loss as heat and they are bulky too. Efficient and compact superconductor transformers can replace them easily. Energy storage devices are useful in power grids where supply-demand mismatch is frequent. Superconducting Magnetic Energy Storage (SMES) devices in small scale are in use for many years where mega joules of energy can be stored in magnetic field without any dissipation [36]. Another technique is to store excess electrical energy as kinetic energy in massive flywheels with frictionless superconductor bearings. The magnetic levitation due to Meissner effect is used here with bulk HTS superconductor bearings. Such devises are demonstrated and under development in various scales. Magnetic levitation has been successfully applied in transportation too; such as Maglev trains which can literally 'fly' over the tracks [37].

Having high T_C, H_{irr} and the ability to grow into large grains, YBCO is the preferred material in this regard. The field expulsion property of superconductors also finds application in magnetic shielding [36].

Since its development in 1960's, Superconducting Quantum Interference Devices (SQUIDs) are approved as the most sensitive devices to measure not only the magnetic field but a number of electromagnetic properties. In SQUIDs and most of other electronics applications, superconductors are used in thin film form and are small scale devices. The working of SQUIDs is based on two superconducting phenomena - the flux quantization and Josephson Effect. By Josephson Effect, the cooper pairs can tunnel through a resistive barrier between two superconducting regions. When the current is smaller than a critical current I_C, there will be no voltage drop across the junction. As soon as the limit exceeds, there will be a non-zero ac voltage across the junction. Detection and measurement of this change from one state to another is the core of many applications based on Josephson Effect. SQUIDs can measure incredibly small fields (~ 10^{-15} T) and voltages (~ 10^{-12} V) [38]. SQUIDs find applications in geomagnetism and biomagnetism (detecting and mapping of magnetic fields due to biological activities like neurological current) [section 9.3.4 and 9.3.3 of ref. 36]. SQUID based magnetometers and susceptometers are widely used for characterizations in material science.

The Josephson junction can be switched very fast (in few picoseconds) between 2 states. Rapid Single Flux Quantum (RSFQ) logic, where voltage pulse of typically few picosecond width across the junction is regarded as "1" state and the absence of voltage is regarded as "0" state, is considered as the future of supercomputers. It is estimated that RSFQ based chips need only $1/10000^{th}$ power to operate and are ~ 10^3 times faster on comparing with the conventional complementary metal oxide semiconductor (CMOS) chips [39]. A key area of technological application of superconductors is in high frequency devices, especially in the range of micro and millimeter range wave frequencies. A superconductor microwave transmission line has a low surface resistance so that low strength signals also can pass through without much attenuation. Unlike the normal conductors, superconductors have frequency independent penetration depth (London penetration length, λ) which enables them to carry signals without phase dispersion.

Superconductor cavity resonators and filters (coupled resonators with closely spaced resonance frequencies) are other important applications of superconductors in electronics [40].

Admitting that most of the above mentioned applications are developed with early discovered NbTi, Nb_3Sn and HTS materials, the MgB_2 superconductor is a potential candidate to replace them in many areas. The high T_C and low cost of production make this a tough competitor to low temperature superconductors. The advent of cryogen free cryocoolers in market is a good reason to go with MgB_2 superconductor. The status of being a 'light weight superconductor' makes MgB_2 useful in specific applications like in space. MgB_2 based Josephson junctions for SQUID and RSFQ logic are subjects of intense study today [41].

REFERENCES

[1] H. K. Onnes, "The Superconductivity of Mercury," *Comm. Phys. Lab. Leiden,* vol. 122b, 1911.

[2] W. Meissner, Oschenfeld, R., "Ein neuer Effekt bei Eintritt der Supraleitfähigkeit," *Naturwissenschaften,* vol. 21, pp. 787-789, 1933.

[3] F. London and H. London, "The Electromagnetic Equations of the Supraconductor," *Proceedings of the Royal Society of London A: Mathematical, Physical and Engineering Sciences,* vol. 149, pp. 71-88, 1935-03-01 1935.

[4] V. L. Ginzburg and D. Landau, "On the theory of superconductivity," *Zh. Eksp. Teor. Fiz.,* vol. 20, pp. 1064-1082, 1950.

[5] A. A. Abrikosov, "On the Magnetic Properties of Superconductors of the Second Group," *Soviet Physics-JETP,* vol. 5, 1957.

[6] N. C. J. Bardeen, J. R. Schreiffer, "Theory of Superconductivity," *Physical Review,* vol. 108, 1957.

[7] B. D. Josephson, "Possible new effects in superconducting tunneling," *Physics Letters,* vol. 10, 1962.

[8] G. Bednorz and K. A. Muller, "Possible high T_C superconductivity in the Ba-La-Cu system," *Zeitschrift für Physik B,* vol. 64, pp. 189-197, 1986.

[9] J. Nagamatsu, N. Nakagawa, T. Muranaka, Y. Zenitani, and J. Akimitsu, "Superconductivity at 39 K in magnesium diboride," *Nature,* vol. 410, pp. 63-64, 03/01/ 2001.

[10] L. N. Cooper, "Bound electron pairs in a degenerate Fermi gas," *Phys. Rev.,* vol. 104, pp. 1189-1190, 1956.

[11] A. A. Abrikosov, "On the Magnetic properties of superconductors of the second group," *Soviet Physics-JETP,* vol. 5, pp. 1174-1182, 1957.

[12] P. J. Lee, *Engineering Superconductivity*: Wiley, 2001.

[13] A. S. Brito, G. Zerweck, and O. F. Lima, "High critical flux density gradients near the surface of superconducting niobium," *Journal of Low Temperature Physics,* vol. 36, pp. 33-46.

[14] H. K. Onnes, "Further experiments with liquid helium. H. On the electrical resistance of pure metals etc. VIII. ," vol. 133a-133d, 1913.

[15] C. Buzea and K. Robbie, "Assembling the puzzle of superconducting elements: A Review," *Superconductor Science & Technology,* vol. 18, p. R1, 2005.

[16] J. Tuoriniemi, "superconductor lithium," *Nature* vol. 447, 2007.

[17] G. F. Hardy and J. K. Hulm, "Superconducting Silicides and Germanides," *Physical Review,* vol. 89, pp. 884-884, 02/15/ 1953.

[18] B. T. Matthias, T. H. Geballe, S. Geller, and E. Corenzwit, "Superconductivity of Nb_3Sn," *Physical Review,* vol. 95, pp. 1435-1435, 09/15/ 1954.

[19] J. Muller, "A15 type superconductors," *Reports on Progress in Physics,* vol. 43, 1980.

[20] R. J. Cohn, "Record superconductor at 22.3 K," *physics today,* vol. 26, 1973.

[21] B. W. Roberts, " Survey of Superconductive Materials and Critical Evaluation of Selected Properties," *Journal of Physical and Chemical Reference Data,* vol. 5, pp. 581-821, 1976.

[22] X. D. Wu, D. Dijkkamp, S. B. Ogale, A. Inam, E. W. Chase, P. F. Miceli, *et al.*, "Epitaxial ordering of oxide superconductor thin films on (100) SrTiO3 prepared by pulsed laser evaporation," *Applied Physics Letters,* vol. 51, pp. 861-863, 1987.

[23] H. Maeda, Y. Tanaka, M. Fukutomi, and T. Asano, "A new high-r. oxide superconductor without a rare earth element," *Japanese Journal of Applied Physics.,* vol. 27, p. L2, 1988.

[24] Z. Z. Sheng and A. M. Hermann, "Bulk superconductivity at 120 K in the Tl-Ca/Ba-Cu-O system," *Nature,* vol. 332, pp. 138-139, 1988.

[25] A. Schilling, M. Cantoni, J. D. Guo, and H. R. Ott, "Superconductivity above 130 K in the Hg-Ba-Ca-Cu-O system," *Nature,* vol. 363, pp. 56-58, 05/06/print 1993.

[26] C. W. Chu, L. Gao, F. Chen, Z. J. Huang, R. L. Meng, and Y. Y. Xue, "Superconductivity above 150 K in $HgBa_2Ca_2Cu_3O_{8+\delta}$ at high pressures," *Nature,* vol. 365, pp. 323-325, 09/23/ 1993.

[27] Y. Kamihara, H. Hiramatsu, M. Hirano, R. Kawamura, H. Yanagi, T. Kamiya, *et al.*, "Iron-Based Layered Superconductor: LaOFeP," *Journal of the American Chemical Society,* vol. 128, pp. 10012-10013, 08/01/ 2006.

[28] Y. Kamihara, T. Watanabe, M. Hirano, and H. Hosono, "Iron-Based Layered Superconductor $La[O_{1-x}F_x]FeAs$ (x = 0.05−0.12) with Tc = 26 K," *Journal of the American Chemical Society,* vol. 130, pp. 3296-3297, 03/01/ 2008.

[29] R. Zhi-An, C. Guang-Can, D. Xiao-Li, Y. Jie, L. Wei, Y. Wei, *et al.*, "Superconductivity and phase diagram in iron-based arsenic-oxides ReFeAsO 1−δ (Re = rare-earth metal) without fluorine doping," *EPL (Europhysics Letters),* vol. 83, p. 17002, 2008.

[30] P. M. Aswathy, J. B. Anooja, P. M. Sarun, and U. Syamaprasad, "An overview on iron based superconductors," *Superconductor Science and Technology,* vol. 23, p. 073001, 2010.

[31] G. B. Yntema, "Nb Supermagnets," *Physical Review*, vol. 98, 1955.

[32] *http://home.cern/topics/large-hadron-collider*.

[33] *http://www.iter.org/mach/magnets*.

[34] *http://www.ccas-web.org/superconductivity/electicpower/*.

[35] Y. Xin, W. Z. Gong, H. Hong, Y. Q. Gao, X. Y. Niu, J. Y. Zhang, *et al.*, "Development of a 220 kV/300 MVA superconductive fault current limiter," *Superconductor Science and Technology*, vol. 25, p. 105011, 2012.

[36] P. Seidel, Ed., *Applied Superconductivity: Handbook on Devices and Applications*: Wiley, 2015.

[37] R. D. Thornton, "Efficient and Affordable Maglev Opportunities in the United States," *Proceedings of the IEEE*, vol. 97, pp. 1901-1921, 2009.

[38] H. Weinstock, Ed., *SQUID Sensors: Fundamentals, Fabrication and Applications*: Kluwer Academic Publishers, 1996.

[39] P. Bunyk, K. Likharev, and D. Zinoviev, "RSFQ Technology: Physics And Devices," *International Journal of High Speed Electronics and Systems*, vol. 11, pp. 257-305, 2001.

[40] R. W. Simon, R. B. Hammond, S. J. Berkowitz, and B. A. Willemsen, "Superconducting microwave filter systems for cellular telephone base stations," *Proceedings of the IEEE*, vol. 92, pp. 1585-1596, 2004.

[41] S. A. Cybart, T. J. Wong, E. Y. Cho, J. W. Beeman, C. S. Yung, B. H. Moeckly, *et al.*, "Large scale two-dimensional arrays of magnesium diboride superconducting quantum interference devices," *Applied Physics Letters*, vol. 104, p. 182604, 2014.

Chapter 2

The MgB_2 Superconductor: Assets, Achievements and Prospects

2.1 The discovery and the distinctiveness of MgB_2 superconductor

It was in January 2001, Prof. J. Akimitsu and crew of Aoyama Gakuin University, Tokyo, Japan revealed that cooling below 39 K makes MgB_2 a superconductor [1]. The unusually high T_C in a simple binary compound was a great surprise to entire physics community. This material was known for decades [2] and even had been synthesized in single crystal form [3] but was waiting 'to be tested' for superconductivity. The specific heat capacity of MgB_2 was also reported earlier and tabulated from 18 to 305 K [4], but no feature related to a transition was reported. In short, MgB_2 got the 'old material but new superconductor' status. The transition temperature 39 K is the highest observed T_C in any binary compound and is near to double of the second highest material. It was also the highest T_C ever observed in any non-cuprate superconductors at the time of discovery. After the discovery, the scientific community - both theorists and experimentalists - rose to the occasion and within one and a half year basic physical properties of MgB_2 were delineated [5]. The opening of a new temperature window between LHe and LN temperatures catalyzed the technological research due to the possibility of usage of liquid hydrogen (~20 K) or liquid neon (~27 K) or fairly inexpensive closed cycle refrigerators.

It was not only the high transition temperature that attracted the scientists and engineers to this material, but certain other properties too and some of them make it very distinctive. Following the discovery, many researches showed that the $H_{C2}(T)$ curve of the doped MgB_2 is at par with or surpasses that of Nb_3Sn in the entire temperature range

[6, 7]. The engineers' favorite superconductor alloy NbTi has an H_{C2} of 10-12 T and which is less than H_{C2} of MgB_2 even at its pure form [7, 8]. In addition to this, considering the lower transition temperature of these, MgB_2 is a potential candidate to replace them in many applications. Within a couple of weeks of knowing the superconductivity in MgB_2, Canfield *et al*. produced MgB_2 wire segments by reacting boron fibers with Mg vapor [9]. They measured a critical current density > 10^5 A/cm^2. In thin film form, this value again increases at least by an order of 10 [10, 11]. These values of J_C are high enough to make use in many devices.

Table 2.1: Basic superconducting parameters of MgB_2 superconductor. Average value is given for anisotropic parameters

Superconducting transition temperature, T_C	39 K*
Coherence length, ξ	5 nm*
Penetration depth, λ	140 nm*
Ginzburg-Landau parameter, κ	≈ 25
Electron mean free path, l	≈ 60 nm*
Residual resistivity ratio RRR = ρ(300 K)/ ρ(42 K)	≈ 20
Debye temperature, Θ_D	340 K
Isotope effect constant, α	0.32
Lower critical field H_{C1}	30 mT
Upper critical field H_{C2}, clean sample (l>>ξ)	15 T*
dirty sample (l<<ξ)	30 T*
Irreversibility field H_{irr}, clean sample	7 T*
dirty sample	15 T*
Critical current density J_C	4×10^5 Acm^{-2}*

*Values are taken from [12]

When compared with the HTS materials, the T_C of MgB_2 is not that great. But the long length conductor fabrication using HTS materials is very difficult due to their high anisotropic nature. The 'first generation HTS wires' made from BSCCO use expensive Ag sheath and they require a uniaxial texturing too [13]. The huge cost of production prevented this to be a great success in market. The 'second generation HTS wires' made

from YBCO use coated conductor technique and a biaxial texturing is preferred [13]. But since the HTS grains are not weak link-free, very long length fabrication is still difficult. The conductor fabrication of MgB_2 is easier when compared to the HTS. The raw materials Mg and B are abundant in nature and are of low cost. No expensive sheath material such as Ag is required for MgB_2 wire manufacturing. The lower anisotropy and weak link-free boundaries make it easy to draw round wires in very long length. The weak link-free nature of the MgB_2 is explained by its quite large coherence length, $\xi > 5$ *nm* [14, 15]. Besides the low cost of raw materials, the synthesis of MgB_2 is also easier. The material can be synthesized at temperatures as low as ~ 650 °C (in comparison to HTS) with ~ 30 minutes duration, whereas HTS materials often require multi-step processes, higher temperatures and longer durations. Also, the MgB_2 is not very sensitive to minor variations in sintering temperature.

The MgB_2 has a lower value of normal state resistivity (~ 0.38 μΩcm at 42 K). This gives a chance to increase core area and hence the current carrying capacity of superconductor wire/current leads without compromising the quench protection. Magnesium and its alloys are well known for their 'lightweight' and being used in many automobile parts. Similarly, MgB_2 has also a status as 'lightweight superconductor'. Hence the MgB_2 becomes convenient in certain specific situations where 'weightlessness' is also important, like space related applications. Moreover, MgB_2 is a particularly attractive material for its two superconducting energy gaps [15]. Though multiple energy gap had been predicted earlier [16], MgB_2 is the first material containing intrinsic multiple gaps. Table 2.1 lists values of basic superconducting parameters of MgB_2.

2.2 Crystal and electronic structures of MgB_2

2.2.1 Crystal structure of MgB_2

MgB_2 has simple AlB_2-type crystal structure, characterized by lattice parameters a = 3.08 Å and c = 3.51 Å and described by space group p6/mmm[2, 17]. The structure

can be viewed as alternate stacking of boron honeycomb planes and magnesium triangular planes (figure 2.1).

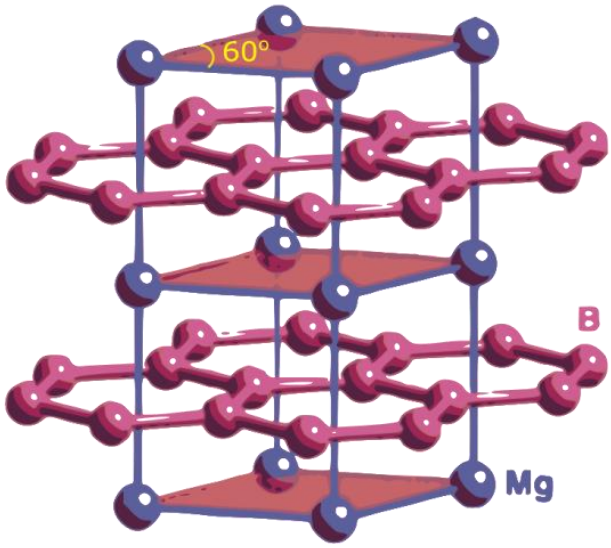

Figure 2.1: Schematic crystal structure of MgB_2

Each Mg atom is at the center of a hexagonal prism formed by B atoms with a B-Mg distance of 2.5 Å. In the two dimensional honeycomb lattice formed by boron layers, each boron atom is surrounded by three other boron atoms and forming an equilateral triangle where B-B distance is 1.78 Å. The Mg layers form a triangular lattice where Mg-Mg distance is the lattice parameter *a*. in the unit cell the atomic position of Mg is at (0,0,0) (Wyckoff symbol 1a) and the positions of B is given by (1/3, 2/3, 1/2) and (2/3, 1/3, 1/2) (Wyckoff symbol 2d) [18, 19]. The crystal structure of MgB_2 has been investigated under various conditions by X-ray diffraction and high resolution neutron diffraction. These studies show that the hexagonal structure remains unchanged at temperatures as low as 2 K and at pressures as high as 40 GPa [20, 21]. It is observed that the thermal expansion coefficient along *c*-axis is about two times larger than that along *a*-axis [21]. This anisotropy is related with the difference in bond strength, i.e. the B-B bonds are more rigid than Mg-B bonds. Within the boron layers the bonding is strongly covalent and between boron and magnesium bonding is more metallic like.

2.2.2 Electronic structure of MgB_2

The band structure of the MgB_2 has been calculated by several groups soon after the discovery of the superconductivity [22-27]. The Mg ions in the triangular lattice donate electrons to the conduction band but Mg atomic orbitals have only a little to do with the conduction process. The electronic structure of MgB_2 is mainly determined by the honeycomb planes of boron atoms. These in-plane boron atoms are held together by covalent bonds. The band structure of MgB_2 is similar to that of graphite. It is formed by three σ bands (in-plane sp_xp_y hybridization) and two π bands (bonding and anti-bonding p_z hybridization). The σ band corresponds to the 2D covalent bond existing between boron atoms in honeycomb structure. The σ electrons are restricted to the boron layer and conducts along this plane. The π bands connect adjacent boron honeycomb layers and thus allow metallic conduction perpendicular to the bond sheets. The 2D covalent band are partially filled and mainly of hole type. The π band comprises of both electrons and holes as charge carriers [23, 26, 27].

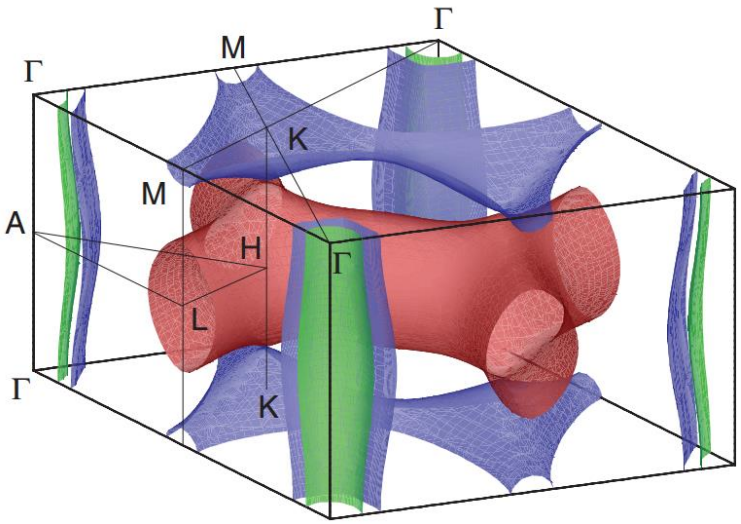

Figure 2.2: Calculated Fermi surface topology of MgB_2

The band structure can be conveniently represented in the momentum space by Fermi surface as shown in the figure 2.2 [24, 28]. The Fermi surface of MgB_2 consists of four distinctive sheets. The green and blue cylindrical sheets (hole type) come from the

bonding $p_{x,y}$ bands. They are shown as split into eight pieces around the four vertical Γ-Γ lines. The π bands form two tubular networks: the blue tubular network (hole type) from the bonding p_z bands and the red (electron like) tubular network from the anti-bonding p_z band.

2.3 Mechanism of superconductivity

An effective method to probe into the mechanism of superconductivity is to study isotope effect i.e. the change of T_C with isotope mass according to the relation $T_C \sim M^{\alpha}$, where α is isotropic coefficient. The boron isotope effect was studied by Bud'ko *et al.* [29] and observed 1.0 K shift in T_C between $Mg^{11}B_2$ and $Mg^{10}B_2$ samples. Hinks *et al.* [30] estimated the isotope coefficient (α) for both B and Mg and came out with values of 0.30 and 0.02, respectively. These results show that MgB_2 is a phonon mediated superconductor and the B phonons are responsible for the pairing. The Mg phonons apparently contribute little to the overall pairing.

There are four distinctive optical phonon modes for MgB_2 denoted by B_{1g}, E_{2g}, A_{2u} and E_{1u}, corresponding to the in-plane and out-of-plane displacement of B or Mg atoms. Among these, the high energy (~ 570 meV) optical phonon E_{2g} has the great impact on the MgB_2 as it couples very strongly to the electrons in 2Dσ band near the Fermi level [22, 24, 31, 32]. Although, the total isotopic coefficient $\alpha_B + \alpha_{Mg} \sim 0.32$ is a significantly varied value from typical value of a BCS superconductor ($\alpha = 0.5$). This difference has been studied in various works and was suggested to be the result of possible anharmonicity of boron E_{2g} phonon mode and multi-band superconductivity in this material.

Two-gap superconductivity

A striking feature of the MgB_2 is the presence of two kinds of superconductivity gaps. Signs of it was first observed in specific heat measurement under magnetic fields done by Bouquet *et al.* [33]. Various other characterizations like point-contact spectra [34], electronic Raman spectra [35], photo emission spectra [36], scanning tunneling spectra [37], angle-resolved photo emission spectra (ARPES) [38], tunnel junction

characteristics etc. are in good agreement with the presence and the values of two distinct superconducting energy gaps of MgB_2. These two energy gaps are the natural result of two different strengths in electron-phonon coupling: the strong electron-phonon coupling in 2Dσ bands and the weak coupling in the 3Dπ bands. The average values of gap at 4 K are 6.8 meV for σ sheets and 1.8 meV for the π sheets.

Although very weak, the electrons in σ and π bands interact through scattering from states in one band to states in other band and through Coulomb repulsion. Due to this small interaction, both the bands become superconducting at same temperature and no two separate T_C is observed [5]. The two energy bands in MgB_2 open three scattering channels of different scattering rates: the intraband scattering within σ and π bands and the inter-band scattering between within σ and π bands. Upon tuning these scattering rates, it is possible to attain high H_{C2} values. This is a major advantage of having multi-energy gap superconductivity.

2.4 Preparation of MgB_2 bulk and wires

The low cost of raw materials and easiness of preparation are the main attractions towards large scale production of MgB_2. Since its discovery, MgB_2 has been prepared in a number of forms for various purposes. They include bulk, wire, tape, single crystal, thin film etc. and each of them have been prepared through different routes. The Mg and B differ greatly in their physical properties. Boron has a melting point of 2050 °C and the Mg has a melting point 650 °C and boiling point 1090 °C. Therefore, it is impossible for a liquid-liquid reaction to occur. But Mg starts evaporation at temperatures even below its melting point. It has been shown that the 80 % of formation of MgB_2 can be completed at temperatures as low as 550 °C during a heat treatment duration of 13 hours [39].

The two general approaches towards synthesis of MgB_2 are *in situ* and *ex situ* processes. In *in situ* method the reactants Mg and B are mixed in atomic ratio of 1:2 and heat treated (usually at 600 to 900 °C) to form MgB_2. The *in situ* method ensures better grain connectivity and also enables chemical doping effectively. But due to the difference in theoretical densities of reactants (Mg ~ 1.74 g/cm^3, B ~ 2.34 g/cm^3) and product (2.63

g/cm^3) and due to the high volatile nature of Mg, the density of the normally prepared sample will be much lower than that of its theoretical density. This causes to reduce effective cross-sectional area and limits current carrying capacity.

In *ex situ* approach, commercially available/as prepared MgB_2 powder is pelletized or drawn into wires and sintered at high temperatures of 800 – 1200 °C for 1 – 5 hrs. *Ex situ* sample gives high homogeneity and density but requires very high temperatures for grain connectivity. The chemical doping is also difficult in *ex situ* method.

2.4.1 Bulk samples

MgB_2 in bulk form is required to study the basic properties and also for *ex situ* wire fabrications. In the *in situ* preparation of bulk sample the mixture of precursors is enclosed in metal tube (Nb/Fe/SS/Ta) or in quartz tube or in foils/ampules and heat treated usually in the temperature range 650 – 1000 °C range for 0.5 to 3 hours duration. The precursors may be in pellet or powder form and the heat treatment is usually done in vacuum or argon atmosphere. Low temperature synthesis also has been reported by several groups using metallic dopants such as copper, silver, tin etc. [39-44]. These metallic dopants form magnesium alloys with lower melting point and work as carrier to enhance contact with boron. Instead of Mg and B, sources of these such as MgH_2 have also been used as starting materials to avoid oxygen contamination [45]. In order to reduce the porosity of the samples prepared in *in situ* method and thus to increase the density of the samples, methods like high pressure sintering (HPS) [46-48], hot isostatic pressing (HIP) [49, 50] and 2-stage sintering [51-53] have been tried. In HPS and HIP methods, high pressure in the range of 0.5-5 GPa is applied on the sample during the heat treatment. Employing these methods, samples with density near to theoretical density are reported. However, extension of this method from bulk to long length wire making is difficult.

Microstructure has serious role in flux pinning of MgB_2 superconductors. Reducing the grain size increases the density of grain boundaries in bulk sample and

enhances grain boundary pinning. Mechanical alloying/high energy milling is proven to be an effective method to synthesis MgB_2 bulk with fine grain size [54-56]. In this method, the quality of the sample depends on various factors like size of the bowl and balls, ball to powder ratio, speed and duration of milling and the milling medium. But there can be contaminations from ball, bowl and milling medium.

The Powder In Sealed Tube (PIST) method, developed by our group, has been employed in this work for the synthesis of MgB_2 bulk [57]. Here, the reactants are concealed in stainless steel tubes of desired size and heat treated at 850 °C for 2 hours. The method offers an easier way to synthesize large quantities of MgB_2 in a short time without any inert or vacuum atmosphere.

2.4.2 Wire/Tape samples

Fabrication of long length wires is essential for most of the superconductor based applications where high magnetic field is necessary. Being a 21st century superconductor, MgB_2 has the advantage of having accumulated experiences of superconductor wire making over fifty years. Since a brittle type material, MgB_2 cannot be drawn into fine wires like ductile NbTi. But the low anisotropy and weak link-free boundaries enable us to make MgB_2 wires without any texturing as in the case of HTS materials. As in the case of Nb_3Sn-the brittle Al-5 superconductor-Powder In Tube (PIT) method is most suitable and widely used in the wire making of MgB_2 also. Wires of several kilometer length have been fabricated and commercially available now. Other than PIT method, the diffusion method and the coating technique are two main approaches towards preparation of MgB_2 for conductor application.

Powder In Tube (PIT) method

The PIT method is the most convenient and popular method to fabricate MgB_2 wires in short and long lengths [58-65]. In PIT method, Mg+2B mixture (*in situ* approach) or pre-reacted MgB_2 (*ex situ* approach) is filled and compacted in suitable metal tube and rolled/drawn into required length and diameters. Different sheath metals such as Fe, Cu, Ag, Nb, Ti or alloys like SS, monel etc. [58-60, 62, 65-68] have been

used to fabricate MgB_2 wires by various groups. The sheath metal must mechanically support the brittle superconductor core inside and should be ductile enough to be cold-worked. Intermediate heat treatment may be done during the cold working so as to release the structural stress developed in metallic matrix [51, 69]. The final heat treatment is done at suitable temperatures for the sintering of the MgB_2 powder (*ex situ*) or to form MgB_2 phase (*in situ*). Besides the monofilamentary wires, multifilamentary wires are also made by PIT technique where bundles of monofilamentary wires are stacked inside another metal tube along with additional stabilizers such as copper filaments. This composite is rolled/drawn and heat treated. Multifilamentary wires have superior J_C values, better uniaxial and bending strain tolerance and good thermal stability.

Diffusion Technique

Just within a couple of weeks after the declaration of superconductivity in MgB_2, Canfield *et al.* prepared MgB_2 wire segments by diffusion technique[9]. They diffused Mg vapor to tungsten cored boron fiber to form MgB_2. Giunchi *et al.* developed another technique known as 'Internal Mg Diffusion' (IMD) process or 'Mg-Reactive Liquid Infiltration' (Mg-RLI), in which they cold worked boron filled tube with Mg rod embedded axially in it [70, 71]. On heat treatment, Mg gets diffused into boron and a 'layered core' is formed. Though the wires made by diffusion technique have shown good J_C values, the method is most suitable for short length sample preparation. Various groups project IMD as a substitute to PIT technique and the mechanical and flux pinning behaviors of these wires have been studied [72-74].

Coating Technique

Coated conductor fabrication is a common technique in second generation high T_C wires made with materials like YBCO. The observation of very large H_{C2} and T_C in hybrid physical-chemical vapor deposited (HPCVD) thin films made several research groups to think about fabrication of coated conductors of MgB_2 as an alternative to PIT wires and tapes. Polycrystalline MgB_2 coated conductor fibers, deposited by HPCVD on SiC fibers, reported by Ferrando *et al*., show H_{C2} of 55 T and H_{irr} of 40 T [75]. Ranot *et*

al. has reported a J_C of 10^7 A/cm^2 and 10^5 A/cm^2 in MgB_2 coated superconducting tapes fabricated on textured Cu (001) with and without SiC doping [76]. Different metallic substrates SS, Fe, Nb, Cu etc. have been used for coated conductor development [77-80]. The above results suggests the technique is worth for further consideration but scaling up of this technique in not straight forward compared to PIT technique.

2.5 Efforts to improve superconducting properties of MgB_2

The freedom to choose the 'operating point' of a superconductor device depends on the volume enclosed by its critical surface. So, enlarging this volume is a primary concern of any researcher. This can be achieved by improving the critical parameters such as T_C, H_{C2} and J_C and by holding the $J_C(H)$ curve from falling steeply with increase of external field. Various methods like irradiating with high energy beams, varying synthesis condition, doping with elements or compounds, varying microstructure, applying external pressure, introducing defects and strain etc. are being tried to improve superconducting properties of various materials. The MgB_2 also cannot be an exception especially due to its poor in-field behavior and low flux pinning in pristine form.

2.5.1 Efforts to improve transition temperature T_C

The T_C in MgB_2 is unusually higher than any other borides or non-cuprate superconductors. One of the greatest achievements of the BCS theory is that it could relate the T_C of a material with two physical constants (k_B, Boltzmann constant and ħ, Planck constant) and three material parameters:

$$k_B T_c = 1.13\hbar\omega_D e^{-1/VN(E_F)}$$

where ω_D is the Debye frequency, V is the electron-phonon attractive interaction and $N(E_F)$ is the density of electron states at Fermi energy E_F which determines number of electrons that can participate in superconducting phenomenon. Presence of high energy phonons ($\hbar\omega_D$) and strong electron-phonon interaction (V) are the main reasons for high value of T_C in MgB_2. But various efforts have been done for further improvement of the T_C of MgB_2.

Substitution of ^{11}B with ^{10}B was studied by Bud'ko *et al.* and observed an upward shift of 1 K in T_C [29]. But, isotope substitution of Mg has negligible effect on the T_C as the E_{2g} phonon mode, mainly responsible for electron-phonon coupling, is from boron plane [30]. Isotope substitution increased the characteristic frequency ω_D and hence increases the T_C. Unfortunately, other than isotope substitution no methods show a significant improvement in T_C of this material. Similar to most of the other BCS superconductors application of external pressure decreases the T_C of MgB_2 at a rate dT_C/dP = -1.*6* K/GPa and which is in agreement with the theoretical calculations [81-83]. The pressure induced charge variation, changes in phonon modes and electron-phonon coupling are the reasons for decrease in T_C. N. Hur *et al.* reports a slight increase in T_C of MgB_2 thin films under tensile strain [84]. This can be understood when the tensile strain is viewed as negative pressure. The irradiation by energetic ions also has negative influence on T_C [85, 86].

Doping ternary elements into crystal lattice is the most attempted method to increase the superconducting properties of MgB_2, but none of them favored improvement of T_C. Elements such as Al, Li, Si, Ca, Nb, Mn, Co, Ni, Ag, Sc, Zr, Sn, Ti, Pb, Be etc. [87-98] were tried to replace Mg atom from the lattice but only Al is substituted at the site successfully. Boron can be easily replaced by carbon atom by doping many varieties of carbon sources. Both Al and C substitution dope electron. This leads to reduction in overall hole density and hence suppress T_C and both gaps [99]. Al substitution mainly affects intraband scattering of π bands, while the C substitution has a large impact on both π and σ bands and is able to drive the system into dirty limit. In single band s-wave (where net angular momentum of cooper pair is zero) superconductors only magnetic scattering has pair-breaking effect, thus decreasing T_C. But, in two band s-wave superconductors like MgB_2, interband scattering even due to nonmagnetic impurities is predicted to suppress T_C down [100].

2.5.2 Improvement of H_{C2} and J_C(H) of MgB_2

Though the efforts to improve T_C of MgB_2 were all in vain, researchers could improve other important properties such as $J_C(H)$, H_{C2} and H_{irr} by various methods. The bulk and wire MgB_2 samples synthesized just after the discovery of superconductivity

proved that the material is suitable to be engineered for practical applications, as it showed a self-field J_C of 10^6 A/m^2 and H_{C2} in the range of 15-20 T. In thin films, the observed J_C is in the order of 10^7 A/m^2. Though pristine MgB_2 exhibits high J_C values at zero field, its value degrades very fast with increase in external field, especially fields above 3 T, due to poor flux pinning and low irreversibility field. This can make it less suitable for magnet applications, where high fields are mandatory. In pure MgB_2, the flux pinning is provided only by grain boundaries and that too becomes ineffective at high fields. The H_{C2} is the primary factor that sets the upper limit to H_{irr}, but due to lack of proper flux pinning in MgB_2, the value of H_{irr} is limited to only about half of the value of H_{C2}. The H_{C2} of MgB_2 superconductor is its intrinsic property and it can be varied by changing the density of states or tuning the inter and intraband scattering rates by doping or creating defects [101, 102]. The $J_C(H)$ of the MgB_2 is controlled by two closely related but distinguishable mechanisms: H_{C2} and flux pinning.

Various methods like changing synthesis route, reactants properties, heat treatment profile, irradiation with high energy beams, chemical doping etc. have been tried to improve in-field properties of MgB_2 superconductor. To exploit grain boundary pinning, preparation of MgB_2 with fine grain size was tried and found to be effective. Low temperature synthesis [54, 103, 104], mechanical alloying [55, 56, 105], reducing size of Mg/B powders [106-108] etc. are the usual methods to attain this. Irradiating MgB_2 with high energy neutrons [109-111]/protons [112, 113]/ions [114, 115] were tried by various groups and improved in-field properties were observed. Irradiation creates strong artificial pinning centers in the form of atomic scale crystal defects. Eisterer *et al.* [111] reported an increase in H_{C2} from 17 to 24 T by neutron irradiation, while Bugoslavsky *et al.* [113] showed an improved $J_C(H)$ behavior after irradiating with proton. Though irradiation experiments are found to be effective, it reduces low field J_C and T_C significantly, and the method is not scalable for long length wire production.

Chemical doping was found to be most convenient, cheaper, easily achievable and highly reproducible method for the improvement of in-field properties of MgB_2. Volume of works have been reported on the chemical addition/substitution in MgB_2 to enhance the infield properties. The chemical doping was not a great success in HTS materials due

to their large anisotropy and small coherence length, but MgB_2 is free from these limitations. Also unlike HTS materials, the flux lines to be pinned in MgB_2 have string-like morphology as in LTS materials and can be pinned on particles, defects, precipitates etc. This opens a wide window of opportunities to experiment with MgB_2 and a variety of dopants.

Various metallic elements including Fe, Mo, Cu, Ag and Y were doped on MgB_2 by Jin *et al.* [61] to study the $J_C(H)$ behavior, but the result was negative, as not only any of them get substituted in the lattice but forms secondary phases at grain boundaries and hinder the supercurrent flow also. Zhao *et al*. [116] reported an improved J_C at 4 K with Ti and Zr additions in MgB_2 and this is attributed to the sintering-aid and flux pinning properties of added metals. Though substitution of Mg with Al decreases the T_C as discussed earlier, a low doping level of Al is found to enhance the J_C [117]. Various advantages of metallic addition were reported such as accelerated phase formation, grain refinement, connectivity improvement, lowering of sintering temperature and flux pinning [118-122].

The carbon is the only element which can replace boron from MgB_2 lattice. Various forms of elemental carbon and carbon containing compounds have been doped in MgB_2 to improve $J_C(H)$ characteristics. As described earlier, the C-substitution has great impact on σ and π band scattering and can drive the system into dirty limits. This causes a significant increase in H_{C2} at the expense of few kelvins in T_C. Enhancement of H_{C2} from 15 to 30 T has been observed in MgB_2 single crystal with 5 % carbon doping [123]. C-doped wires and carbon nanotube doped samples also have shown H_{C2} beyond 30 T [124, 125]. Another advantage of carbon doping is the creation of structural defects caused by carbon substitution because of its different ionic radii. These structural defects and strains serve as good flux pinners and improve the $J_C(H)$ and H_{irr}. But due to the low solubility of C in MgB_2, high temperature heat treatment is often required for a significant amount of substitution. This causes grain growth and hence reduces boundary pinning. Another disadvantage is the significant reduction in T_C, which causes a decreased $J_C(H)$, especially when the superconductor has to be operated at 20-30 K temperature range.

The doping of nano-SiC, reported by Dou *et al*., is found to be a successful method to improve H_{irr} and flux pinning properties [126-128]. Various groups have confirmed the considerable improvement in the superconducting properties of SiC doped MgB_2 in different forms including bulk, wires, thin films etc. [129-132]. A dual reaction method has been proposed to explain the enhanced superconducting properties of MgB_2 with SiC doping, based on J_C dependence on the sintering temperature [133]. The SiC decomposes and easily gets substituted into MgB_2 lattice at temperatures as low as 600 °C with the formation of secondary phase Mg_2Si. The secondary phases would be good flux pinners if their size matches the coherence length and their spacing matches the vortex distance in desired field range. Accordingly, the nano-sized reaction product Mg_2Si and the excess carbon are observed to be serving as good flux pinners. In short, the defects created by C-substitution, presence of nano-inclusions and smaller grain size due to low temperature synthesis are the sources of flux pinning in SiC doped MgB_2. In SiC doped wires, at 20 K and 2 T, a J_C in the order of $10^5 A/cm^2$ has been obtained, which is comparable to the best Ag/Bi-2223 tapes [128]. Other than SiC and elemental carbon sources such as nano-carbon, nano-diamond, carbon nanotube (CNT), graphite, graphene etc. [134-138], remarkable results have been obtained from carbon containing compounds like B_4C [139], TiC [140] and a number of organic compounds. The organic compounds have low melting point and hence no high temperature heat treatment is required for carbon substitution. They are cheaper and may be coated on boron powder for better homogeneity, using an appropriate solvent. A good number of organic compounds including sugar [141], acetone [142], benzene [143], toluene [143], paraffin [144], stearates [145] and different organic acids [146-152] have been tried and came out with positive results.

Though not substantial, a noticeable increment on superconducting properties is observed with various silicides ($ZrSi_2$, WSi_2, Mg_2Si) and borides (TiB_2, NbB_2, ZrB_2, WB). Another class of dopants which is tried on MgB_2 is the ‘oxides’. They include a number of metal oxides such as Fe_2O_3, Co_3O_4, TiO_2, Al_2O_3, ZrO_2, SbO_3, SiO_2 etc. and various rare earth oxides (REO) like Y_2O_3, Ho_2O_3, Dy_2O_3, Pr_6O_{11}, Nd_2O_3, Eu_2O_3 etc.[153-157] A few results from REO doping are noteworthy. REO forms respective

borides on heat treatment and which are observed to be pinning flux lines effectively. The Ho_2O_3 doped sample has shown a $J_C \sim 1.2 \times 10^5$ A/cm^2 at 5 T and 5 K. Graphene oxide (GO) and reduced graphene oxide (rGO) have also been tried with positive results from the class 'oxides' [158, 159].

Combined addition or co-doping of two or more dopants with specific individual effects has been tried in MgB_2 with various combinations. The combination of additives is generally found as: a carbon source + metal/metal oxide/REO/another carbon source [160-165]. The amount of carbon substitution is found to be increased on co-doping. Co-doping also provides excess flux pinning agents in grains to improve $J_C(H)$ and H_{irr}.

2.6 Applications of MgB_2 superconductor

A significant progress, both theoretical and experimental, has been achieved in MgB_2 in past years as a result of rigorous research. The operability of MgB_2 based devices in 20-30 K temperature range considerably reduces the expense of cooling when compared with the Nb-based LTS materials. The enormous progress made in cryogen-free cooling techniques with large cooling power and good reliability, as in Gifford-McMahon (GM) and pulse-tube coolers (PTC) is readily applicable to MgB_2 based devices. The effort and cost of fabrication of MgB_2 is very low when compared with the HTS materials. Relying on the projection of Columbus Superconductors, Genova, MgB_2 conductor fabrication is at least ten times cheaper than HTS. Therefore, MgB_2 can challenge both HTS and LTS materials for the applications in moderate fields (< 5 T) in the temperature domain of 20-30 K. In various devices such as FCLs, MRI magnets, motors, generators, superconducting transformers etc., MgB_2 can easily replace LTS and HTS materials. The first real technical application of MgB_2 wire was as a low thermal conduction current lead in an X-ray spectrometer (XRS) on the American-Japanese research satellite ASTRO-E2 [166]. For space applications, MgB_2 is highly recommended because of its light weight. The low cost to performance ratio of MgB_2 attracted the industry and now wires of several kilometers length fabricated in single batch are commercially available. Several test runs of MgB_2 coils for low field ($\leq$ 1.5 T), cryogen-free MRI magnets are reported [167, 168]. A cryogen-free 0.5 T/56 cm patient

gap MgB_2 MRI magnet, operated at 20 K, has been fabricated by ASG superconductors for Standup Open MRI of Pensacola, FL, USA and is now commercially available [169]. The mammoth projects such as Large Hadron Collider (LHC) and International Thermonuclear Experimental Reactor (ITER) now consider MgB_2 superconductor as a replacement to conventional ones in coming upgrades.

Extensive research is being done on MgB_2 thin films for practical applications such as Josephson junctions and SQUIDs. The higher T_C than Nb-based superconductors gives MgB_2 special attention in this area. Reports are available on fabrication of SQUIDs with single layer MgB_2 films [170, 171]. MgB_2 is also considered for ultra-high speed digital circuits with a limiting clock speed of 1 THz and operable at 20 K [172, 173]. Superconducting RF cavities is another potential electronic application of MgB_2 where Nb is the most commonly used material now. Promising results are available in this regard also [174, 175].

2.7 Objectives of the present work

MgB_2 is a superconductor which is free from the limitations of conductor fabrication in HTS materials and at the same time has a T_C twice higher than LTS materials. Though a BCS superconductor, in terms of transition temperature, it is neither an LTS superconductor nor an HTS conductor. The T_C of 39 K makes it suitable to use with cryogen-free cryocoolers. But due to weaker flux pinning in its pure form, MgB_2 shows a deprived $J_C(H)$ performance with increase in external field. This should be improved before we go for conductor fabrication for high field applications. Another disadvantage of MgB_2 superconductor is its brittle nature and hence the inferior electromechanical properties i.e. significant deterioration of J_C under stress and strain. During device fabrication and operation the conductor is subjected to various stress and strain. For the ductile superconductors like NbTi, magnet designers can adopt ‘react and wind’ approach due to its very high bending strain tolerance, while for brittle type superconductors, to avoid degradation of J_C, ‘wind and react’ method is desirable . The first approach is more comfortable in terms of winding, insulation and selection of materials for mandrel, sensors etc. In ‘wind and react’ approach, the final winding may

be different, smaller diameter than that during the reaction and if high bending strain tolerance is not maintained, winding of magnets with smaller bore size is not possible. Therefore, the electromechanical property of a superconductor is also important in device fabrication.

The present work addresses the above two limitations of the MgB_2 superconductor namely, the poor $J_C(H)$ behavior and electromechanical properties. The specific objectives of the work can be summarized as below.

- Enhance the in-field critical current density of MgB_2 bulk sample prepared by PIST method. Exploit the advantages of co-doping technique towards this.
- Prepare MgB_2 wires, in both mono and multifilamentary forms with low cost materials and to enhance transport $J_C(H)$ properties based on the studies in bulk.
- Study and improve electromechanical properties of MgB_2 wires prepared by various approaches with focus on bending strain tolerance.

REFERNCES

[1] J. Nagamatsu, N. Nakagawa, T. Muranaka, Y. Zenitani, and J. Akimitsu, "Superconductivity at 39 K in magnesium diboride," *Nature*, vol. 410, pp. 63-64, 03/01/ 2001.

[2] M. E. Jones and R. E. Marsh, "The preparation and structure of magnesium boride, MgB_2," *J. Am. Chem. Soc.*, vol. 76, pp. 1434-1436, 1954.

[3] N. E. Filonenko, V. I. Ivanov, L. I. Fel'dgun, M. I. Sokhor, and L. F. Vereshchagin, "Magnesium borides prepared under superhigh-pressure conditions," *Doklady Akademii Nauk SSSR*, vol. 175, pp. 1266-1269, Aug 1967.

[4] R. M. Swift and D. White, "Low Temperature Heat Capacities of Magnesium Diboride (MgB_2) and Magnesium Tetraboride (MgB_4)," *J. Am. Chem. Soc.*, vol. 79, 1957.

[5] S. L. Bud'ko and P. C. Canfield, "Superconductivity of magnesium diboride," *Physica C-Superconductivity and Its Applications*, vol. 385, pp. 1-2, 2003.

[6] X. S. Huang, W. Mickelson, B. C. Regan, and A. Zettl, "Enhancement of the upper critical field of MgB_2 by carbon-doping," *Solid State Communications*, vol. 136, pp. 278-282, Oct 2005.

[7] M. D. Sumption, M. Bhatia, M. Rindfleisch, M. Tomsic, S. Soltanian, S. X. Dou, *et al.*, "Large upper critical field and irreversibility field in MgB_2 wires with SiC additions," *Applied Physics Letters*, vol. 86, Feb 28 2005.

[8] G. Fuchs, K. H. Muller, A. Handstein, K. Nenkov, V. N. Narozhnyi, D. Eckert, *et al.*, "Upper critical field and irreversibility line in superconducting MgB_2," *Solid State Communications*, vol. 118, pp. 497-501, 2001.

[9] P. C. Canfield, D. K. Finnemore, S. L. Bud'ko, J. E. Ostenson, G. Lapertot, C. E. Cunningham, *et al.*, "Superconductivity in dense MgB_2 wires," *Physical Review Letters*, vol. 86, pp. 2423-2426, Mar 12 2001.

[10] S. H. Moon, J. H. Yun, H. N. Lee, J. I. Kye, H. G. Kim, W. Chung, *et al.*, "High critical current densities in superconducting MgB_2 thin films," *Applied Physics Letters*, vol. 79, p. 2429, 2001.

[11] S. K. Gupta, S. Sen, A. Singh, D. K. Aswal, J. V. Yakhmi, E. M. Choi, *et al.*, "I-V characteristic measurements to study the nature of the vortex state and dissipation in MgB_2 thin films," *Physical Review B,* vol. 66, Sep 1 2002.

[12] P. C. Canfield, S. L. Bud'ko, and D. K. Finnemore, "An overview of the basic physical properties of MgB_2," *Physica C-Superconductivity and Its Applications,* vol. 385, pp. 1-7, Mar 1 2003.

[13] P. Seidel, Ed., *Applied Superconductivity: Handbook on Devices and Applications*: Wliey, 2015.

[14] D. C. Larbalestier, L. D. Cooley, M. O. Rikel, A. A. Polyanskii, J. Jiang, S. Patnaik, *et al.*, "Strongly linked current flow in polycrystalline forms of the superconductor MgB_2," *Nature,* vol. 410, pp. 186-189, Mar 8 2001.

[15] W. Pickett, "Superconductivity: Mind the double gap," *Nature,* vol. 418, pp. 733-734, 08/15/ 2002.

[16] H. Suhl, B. T. Matthias, and L. R. Walker, "Bardeen-Cooper-Schrieffer Theory of Superconductivity in the Case of Overlapping Bands," *Physical Review Letters,* vol. 3, pp. 552-554, 12/15/ 1959.

[17] B. Cristina and Y. Tsutomu, "Review of the superconducting properties of MgB_2," *Superconductor Science and Technology,* vol. 14, p. R115, 2001.

[18] A. L. Ivanovskii, "Band structure and properties of superconducting MgB_2 and related compounds (A review)," *Physics of the Solid State,* vol. 45, pp. 1829-1859.

[19] D. Tzeli and A. Mavridis, "Ab initio investigation of the electronic and geometric structure of magnesium diboride, MgB_2," *Journal of Physical Chemistry A,* vol. 109, pp. 10663-10674, Dec 1 2005.

[20] P. Bordet, M. Mezouar, M. Núñez-Regueiro, M. Monteverde, M. Núñez-Regueiro, N. Rogado, *et al.*, "Absence of a structural transition up to 40 GPa in MgB_2 and the relevance of magnesium nonstoichiometry," *Physical Review B,* vol. 64, 2001.

[21] J. D. Jorgensen, D. G. Hinks, and S. Short, "Lattice properties of MgB_2 versus temperature and pressure," *Physical Review B,* vol. 63, Jun 1 2001.

[22] J. M. An and W. E. Pickett, "Superconductivity of MgB_2: Covalent bonds driven metallic," *Physical Review Letters*, vol. 86, pp. 4366-4369, May 7 2001.

[23] K. D. Belashchenko, M. van Schilfgaarde, and V. P. Antropov, "Coexistence of covalent and metallic bonding in the boron intercalation superconductor MgB_2," *Physical Review B*, vol. 64, Sep 1 2001.

[24] J. Kortus, Mazin, II, K. D. Belashchenko, V. P. Antropov, and L. L. Boyer, "Superconductivity of metallic boron in MgB_2," *Physical Review Letters*, vol. 86, pp. 4656-4659, May 14 2001.

[25] G. Satta, G. Profeta, F. Bernardini, A. Continenza, and S. Massidda, "Electronic and structural properties of superconducting MgB_2, $CaSi_2$, and related compounds," *Physical Review B*, vol. 64, Sep 1 2001.

[26] P. Ravindran, P. Vajeeston, R. Vidya, A. Kjekshus, and H. Fjellvåg, "Detailed electronic structure studies on superconducting MgB_2 and related compounds," *Physical Review B*, vol. 64, 2001.

[27] J. Akimitsu and T. Muranaka, "Superconductivity in MgB_2," *Physica C-Superconductivity and Its Applications*, vol. 388, pp. 98-102, May 2003.

[28] H. Rosner, J. M. An, W. E. Pickett, and S. L. Drechsler, "Fermi surfaces of diborides: MgB_2 and ZrB_2," *Physical Review B*, vol. 66, Jul 1 2002.

[29] S. L. Bud'ko, G. Lapertot, C. Petrovic, C. E. Cunningham, N. Anderson, and P. C. Canfield, "Boron isotope effect in superconducting MgB_2," *Physical Review Letters*, vol. 86, pp. 1877-1880, Feb 26 2001.

[30] D. G. Hinks, H. Claus, and J. D. Jorgensen, "The complex nature of superconductivity in MgB_2 as revealed by the reduced total isotope effect," *Nature*, vol. 411, pp. 457-460, May 24 2001.

[31] K. P. Bohnen, R. Heid, and B. Renker, "Phonon dispersion and electron-phonon coupling in MgB_2 and AlB_2," *Physical Review Letters*, vol. 86, pp. 5771-5774, Jun 18 2001.

[32] Y. Kong, O. V. Dolgov, O. Jepsen, and O. K. Andersen, "Electron-phonon interaction in the normal and superconducting states of MgB_2," *Physical Review B*, vol. 64, Jul 1 2001.

[33] F. Bouquet, R. A. Fisher, N. E. Phillips, D. G. Hinks, and J. D. Jorgensen, "Specific heat of $Mg^{11}B_2$: Evidence for a second energy gap," *Physical Review Letters*, vol. 87, Jul 23 2001.

[34] P. Szabo, P. Samuely, J. Kacmarcik, T. Klein, J. Marcus, D. Fruchart, *et al.*, "Evidence for two superconducting energy gaps in MgB_2 by point-contact spectroscopy," *Physical Review Letters*, vol. 87, Sep 24 2001.

[35] X. K. Chen, M. J. Konstantinović, J. C. Irwin, D. D. Lawrie, and J. P. Franck, "Evidence for Two Superconducting Gaps in MgB_2," *Physical Review Letters*, vol. 87, p. 157002, 09/21/ 2001.

[36] S. Tsuda, T. Yokoya, T. Kiss, A. Chainani, Y. Takano, K. Togano, *et al.*, "Superconducting gap of MgB_2 observed using ultrahigh-resolution photoemission spectroscopy," *Physica B-Condensed Matter*, vol. 312, pp. 150-151, Mar 2002.

[37] M. Iavarone, G. Karapetrov, A. E. Koshelev, W. K. Kwok, G. W. Crabtree, D. G. Hinks, *et al.*, "Two-band superconductivity in MgB_2," *Physical Review Letters*, vol. 89, Oct 28 2002.

[38] S. Souma, Y. Machida, T. Sato, T. Takahashi, H. Matsui, S. C. Wang, *et al.*, "Direct observation of superconducting gaps in MgB_2 by angle-resolved photoemission spectroscopy," *Physica C-Superconductivity and Its Applications*, vol. 408, pp. 102-103, Aug 2004.

[39] Z. Ma and Y. Liu, "The varied kinetics mechanisms in the synthesis of MgB_2 from elemental powders by low-temperature sintering," *Materials Chemistry and Physics*, vol. 126, pp. 114-117, Mar 15 2011.

[40] J. Shimoyama, K. Hanafusa, A. Yamamoto, Y. Katsura, S. Horii, K. Kishio, *et al.*, "Catalytic effect of silver addition on the low temperature phase formation of MgB_2," *Superconductor Science & Technology*, vol. 20, pp. 307-311, Apr 2007.

[41] Z. Q. Ma, Y. C. Liu, Q. Z. Shi, Q. Zhao, and Z. M. Gao, "The accelerated formation of MgB_2 bulks with high critical current density by low-temperature Cu-doping sintering," *Superconductor Science & Technology*, vol. 21, Jun 2008.

[42] Z. Ma, H. Jiang, and Y. Liu, "The acceleration of low-temperature sintering of MgB_2 bulks with high critical density by minor Sn doping," *Superconductor Science & Technology*, vol. 23, Feb 2010.

[43] Z. Ma, Y. Liu, and Z. Gao, "The synthesis and grain connectivity of lamellar MgB_2 grains by Cu-activated sintering at low temperature," *Scripta Materialia*, vol. 63, pp. 399-402, Aug 2010.

[44] A. Yamamoto, J. Shimoyama, S. Ueda, Y. Katsura, S. Horii, and K. Kishio, "Improved critical current properties observed in MgB_2 bulks synthesized by low-temperature solid-state reaction," *Superconductor Science & Technology*, vol. 18, pp. 116-121, Jan 2005.

[45] T. Nakane, H. Kitaguchi, H. Fujii, and H. Kumakura, "Improvement of ex-situ MgB_2 powder in tube processed tapes using MgH_2 powder," *Physica C-Superconductivity and Its Applications*, vol. 445, pp. 784-787, Oct 1 2006.

[46] T. A. Prikhna, W. Gawalek, Y. M. Savchuk, A. B. Surzhenko, M. Zeisberger, V. E. Moshchil, *et al.*, "High pressure synthesis and sintering of MgB_2," *IEEE Transactions on Applied Superconductivity*, vol. 13, pp. 3506-3509, Jun 2003.

[47] T. Prikhna, W. Gawalek, Y. Savchuk, A. Soldatov, V. Sokolovsky, M. Eisterer, *et al.*, "Effects of High Pressure on the Physical Properties of MgB_2," *Journal of Superconductivity and Novel Magnetism*, vol. 24, pp. 137-150, Jan 2011.

[48] F. Y. Li, R. J. Wang, S. C. Li, L. C. Chen, J. L. Zhu, Z. X. Liu, *et al.*, "Ultrasound studies of MgB_2 superconductor under hydrostatic pressure," *Physical Review B*, vol. 65, Apr 1 2002.

[49] T. C. Shields, K. Kawano, D. Holdom, and J. S. Abell, "Microstructure and superconducting properties of hot isostatically pressed MgB_2," *Superconductor Science & Technology*, vol. 15, pp. 202-205, Feb 2002.

[50] A. T. Findikoglu, A. Serquis, L. Civale, X. Z. Liao, Y. T. Zhu, M. E. Hawley, *et al.*, "Microwave performance of high-density bulk MgB_2," *Applied Physics Letters*, vol. 83, pp. 108-110, Jul 7 2003.

[51] L. An, C.-p. Chen, X.-g. Li, and Q.-r. Feng, "High-density MgB_2 superconducting bulk samples prepared at ambient pressure," *Frontiers of Physics in China*, vol. 2, pp. 81-84.

[52] M. Maeda, Y. Zhao, S. X. Dou, Y. Nakayama, T. Kawakami, H. Kobayashi, *et al.*, "Fabrication of highly dense MgB_2 bulk at ambient pressure," *Superconductor Science & Technology*, vol. 21, Mar 2008.

[53] D. Shan, Q. Wang, G. Liu, X. Xiong, J. Li, G. Yan, *et al.*, "Effects of B Powder on the MgB_2 Superconductor Prepared by Two-Step PIT," *Rare Metal Materials and Engineering*, vol. 42, pp. 1278-1281, Jun 2013.

[54] W. Hassler, C. Rodig, C. Fischer, B. Holzapfel, O. Perner, J. Eckert, *et al.*, "Low temperature preparation of MgB_2 tapes using mechanically alloyed powder," *Superconductor Science & Technology*, vol. 16, pp. 281-284, Feb 2003.

[55] W. Haessler, B. Birajdar, W. Gruner, M. Herrmann, O. Perner, C. Rodig, *et al.*, "MgB_2 bulk and tapes prepared by mechanical alloying: influence of the boron precursor powder," *Superconductor Science & Technology*, vol. 19, pp. 512-520, Jun 2006.

[56] Y. F. Wu, Y. F. Lu, G. Yan, J. S. Li, Y. Feng, H. P. Tang, *et al.*, "Improved superconducting properties in bulk MgB_2 prepared by high-energy milling of Mg and B powders," *Superconductor Science & Technology*, vol. 19, pp. 1215-1218, Nov 2006.

[57] R. G. A. Kumar, K. Vinod, R. P. Aloysius, and U. Syamaprasad, "A simple and inexpensive method for rapid synthesis of MgB_2 superconductor," *Materials Letters*, vol. 60, pp. 3328-3331, Dec 2006.

[58] B. A. Glowacki, M. Majoros, M. Vickers, J. E. Evetts, Y. Shi, and I. McDougall, "Superconductivity of powder-in-tube MgB_2 wires," *Superconductor Science & Technology*, vol. 14, pp. 193-199, Apr 2001.

[59] W. Goldacker, S. I. Schlachter, S. Zimmer, and H. Reiner, "High transport currents in mechanically reinforced MgB_2 wires," *Superconductor Science & Technology*, vol. 14, pp. 787-793, Sep 2001.

[60] G. Grasso, A. Malagoli, C. Ferdeghini, S. Roncallo, V. Braccini, A. S. Siri, *et al.*, "Large transport critical currents in unsintered MgB_2 superconducting tapes," *Applied Physics Letters*, vol. 79, pp. 230-232, Jul 9 2001.

[61] S. Jin, H. Mavoori, C. Bower, and R. B. van Dover, "High critical currents in iron-clad superconducting MgB_2 wires," *Nature,* vol. 411, pp. 563-565, May 31 2001.

[62] H. Kumakura, A. Matsumoto, H. Fujii, and K. Togano, "High transport critical current density obtained for powder-in-tube-processed MgB_2 tapes and wires using stainless steel and Cu–Ni tubes," *Applied Physics Letters,* vol. 79, p. 2435, 2001.

[63] A. K. Pradhan, Y. Feng, Y. Zhao, N. Koshizuka, L. Zhou, P. X. Zhang, *et al.*, "Transport behavior and critical current densities in MgB_2 wires," *Applied Physics Letters,* vol. 79, pp. 1649-1651, Sep 10 2001.

[64] S. Soltanian, X. L. Wang, I. Kusevic, E. Babic, A. H. Li, M. J. Qin, *et al.*, "High-transport critical current density above 30 K in pure Fe-clad MgB_2 tape," *Physica C,* vol. 361, pp. 84-90, Sep 1 2001.

[65] H. Suo, C. Beneduce, M. Dhallé, N. Musolino, J.-Y. Genoud, and R. Flükiger, "Large transport critical currents in dense Fe- and Ni-clad MgB_2 superconducting tapes," *Applied Physics Letters,* vol. 79, p. 3116, 2001.

[66] P. Kovac, I. Husek, and T. Melisek, "Transport currents of two-axially rolled and post-annealed MgB_2/Fe wires at 4.2 K," *Superconductor Science & Technology,* vol. 15, pp. 1340-1344, Sep 2002.

[67] R. Nast, S. I. Schlachter, S. Zimmer, H. Reiner, and W. Goldacker, "Mechanically reinforced MgB_2 wires and tapes with high transport currents," *Physica C-Superconductivity and Its Applications,* vol. 372, pp. 1241-1244, Aug 1 2002.

[68] P. Kovac, I. Husek, L. Kopera, T. Melisek, A. Rosova, and E. Dobrocka, "Properties of in situ made MgB_2 in Nb or Ti sheath," *Superconductor Science & Technology,* vol. 26, Feb 2013.

[69] B. H. Jun, Y. J. Kim, K. S. Tan, J. H. Kim, X. Xu, S. X. Dou, *et al.*, "Influence of intermediate annealing on the microstructure of in situ MgB_2/Fe wire," *Physica C-Superconductivity and Its Applications,* vol. 468, pp. 1825-1828, Sep 15 2008.

[70] G. Giunchi, "High density MgB_2 obtained by reactive liquid Mg infiltration," *International Journal of Modern Physics B,* vol. 17, pp. 453-460, Mar 10 2003.

[71] G. Giunchi, S. Ceresara, G. Ripamonti, A. Di Zenobio, S. Rossi, S. Chiarelli, *et al.*, "High performance new MgB_2 superconducting hollow wires," *Superconductor Science & Technology,* vol. 16, pp. 285-291, Feb 2003.

[72] L. Gozzelino, B. Minetti, R. Gerbaldo, G. Ghigo, F. Laviano, G. Lopardo, *et al.*, "Pinning properties in pure and SiC doped MgB_2 bulk obtained by reactive Mg liquid infiltration technique," *Physica C-Superconductivity and Its Applications,* vol. 460, pp. 604-605, Sep 1 2007.

[73] G. Nishijima, S. J. Ye, A. Matsumoto, K. Togano, H. Kumakura, H. Kitaguchi, *et al.*, "Mechanical properties of MgB_2 superconducting wires fabricated by internal Mg diffusion process," *Superconductor Science & Technology,* vol. 25, May 2012.

[74] G. Z. Li, M. D. Sumption, J. B. Zwayer, M. A. Susner, M. A. Rindfleisch, C. J. Thong, *et al.*, "Effects of carbon concentration and filament number on advanced internal Mg infiltration-processed MgB_2 strands," *Superconductor Science & Technology,* vol. 26, Sep 2013.

[75] V. Ferrando, P. Orgiani, A. V. Pogrebnyakov, J. Chen, Q. Li, J. M. Redwing, *et al.*, "High upper critical field and irreversibility field in MgB_2 coated-conductor fibers," *Applied Physics Letters,* vol. 87, Dec 19 2005.

[76] M. Ranot and W. N. Kang, "MgB_2 coated superconducting tapes with high critical current densities fabricated by hybrid physical-chemical vapor deposition," *Current Applied Physics,* vol. 12, pp. 353-363, Mar 2012.

[77] H. Abe, K. Nishida, M. Imai, H. Kitazawa, and K. Yoshii, "Superconducting properties of MgB_2 films electroplated to stainless steel substrates," *Applied Physics Letters,* vol. 85, pp. 6197-6199, Dec 20 2004.

[78] M. Auinger and G. Gritzner, "Magnesium diboride films on iron substrates," *Superconductor Science and Technology,* vol. 21, p. 015006, 2008.

[79] L.-P. Chen, F. Li, T. Guo, C.-G. Zhuang, D. Yao, L.-L. Ding, *et al.*, "Deposition of MgB_2 superconducting films on different metal substrates," *Chinese Physics Letters,* vol. 24, pp. 2074-2076, Jul 2007.

[80] C. Zhuang, D. Yao, F. Li, K. Zhang, Q. Feng, and Z. Gan, "Study of micron-thick MgB_2 films on niobium substrates," *Superconductor Science & Technology,* vol. 20, pp. 287-291, Mar 2007.

[81] B. Lorenz, R. L. Meng, and C. W. Chu, "High-pressure study on MgB_2," *Physical Review B,* vol. 64, Jul 1 2001.

[82] I. Loa and K. Syassen, "Calculated elastic and electronic properties of MgB_2 at high pressures," *Solid State Communications,* vol. 118, pp. 279-282, 2001 2001.

[83] T. Tomita, J. J. Hamlin, J. S. Schilling, D. G. Hinks, and J. D. Jorgensen, "Dependence of T-c on hydrostatic pressure in superconducting MgB_2," *Physical Review B,* vol. 64, Sep 1 2001.

[84] N. Hur, P. A. Sharma, S. Guha, M. Z. Cieplak, D. J. Werder, Y. Horibe, *et al.*, "High-quality MgB_2 films on boron crystals with onset Tc of 41.7 K," *Applied Physics Letters,* vol. 79, pp. 4180-4182, Dec 17 2001.

[85] M. Putti, M. Affronte, C. Ferdeghini, P. Manfrinetti, C. Tarantini, and E. Lehmann, "Observation of the crossover from two-gap to single-gap superconductivity through specific heat measurements in neutron-irradiated MgB_2," *Physical Review Letters,* vol. 96, Feb 24 2006.

[86] R. H. T. Wilke, S. L. Bud'ko, P. C. Canfield, J. Farmer, and S. T. Hannahs, "Systematic study of the superconducting and normal-state properties of neutron-irradiated MgB_2," *Physical Review B,* vol. 73, Apr 2006.

[87] C. H. Cheng, Y. Yang, C. Ke, and H. T. Lin, "Iron doping effect on superconducting properties of MgB_2," *Physica C-Superconductivity and Its Applications,* vol. 470, pp. 1092-1095, Nov 1 2010.

[88] S. Agrestini, C. Metallo, M. Filippi, G. Campi, C. Sanipoli, S. De Negri, *et al.*, "Sc doping of MgB_2: the structural and electronic properties of $Mg_{1-x}Sc_xB_2$," *Journal of Physics and Chemistry of Solids,* vol. 65, pp. 1479-1484, Aug-Sep 2004.

[89] A. Tampieri, G. Celotti, S. Sprio, and D. Rinaldi, "Effects of Cu and other metallic dopings on the superconducting properties of MgB_2," *International Journal of Modern Physics B,* vol. 17, pp. 438-445, Mar 10 2003.

[90] B. Q. Fu, Y. Feng, G. Yan, Y. Zhao, A. K. Pradhan, C. H. Cheng, *et al.*, "High critical current density in Ti-doped MgB_2/Ta/Cu tape by powder-in-tube process," *Journal of Applied Physics,* vol. 92, pp. 7341-7344, Dec 15 2002.

[91] M. R. Cimberle, M. Novak, P. Manfrinetti, and A. Palenzona, "Magnetic characterization of sintered MgB_2 samples: effect of substitution or 'doping' with Li, Al and Si," *Superconductor Science & Technology,* vol. 15, pp. 43-47, Jan 2002.

[92] A. Tampieri, G. Celotti, S. Sprio, D. Rinaldi, G. Barucca, and R. Caciuffo, "Effects of copper doping in MgB_2 superconductor," *Solid State Communications,* vol. 121, pp. 497-500, 2002.

[93] W. H. Xie and D. S. Xue, "A first-principles study of MgB_2: the effect of pressure and substitution," *Journal of Physics-Condensed Matter,* vol. 13, pp. 11679-11687, Dec 17 2001.

[94] Y. Zhao, Y. Feng, C. H. Cheng, L. Zhou, Y. Wu, T. Machi, *et al.*, "High critical current density of MgB_2 bulk superconductor doped with Ti and sintered at ambient pressure," *Applied Physics Letters,* vol. 79, pp. 1154-1156, Aug 20 2001.

[95] Y. Feng, Y. Zhao, A. K. Pradhan, C. H. Cheng, J. K. F. Yau, L. Zhou, *et al.*, "Enhanced flux pinning in Zr-doped MgB_2 bulk superconductors prepared at ambient pressure," *Journal of Applied Physics,* vol. 92, pp. 2614-2619, Sep 1 2002.

[96] C. H. Cheng, Y. Zhao, X. T. Zhu, J. Nowotny, C. C. Sorrell, T. Finlayson, *et al.*, "Chemical doping effect on the crystal structure and superconductivity of MgB_2," *Physica C-Superconductivity and Its Applications,* vol. 386, pp. 588-592, Apr 15 2003.

[97] D. W. Gu, Y. M. Cai, J. K. F. Yau, Y. G. Cui, T. Wu, G. Q. Yuan, *et al.*, "Effect of Pb substitution in bulk superconducting MgB_2," *Physica C-Superconductivity and Its Applications,* vol. 386, pp. 643-647, Apr 15 2003.

[98] H. L. Li, K. Q. Ruan, S. Y. Li, Y. Yu, C. Y. Wang, and L. Z. Cao, "Upper critical field and the effect of Li doping on the activation energy in MgB_2," *Physica C-Superconductivity and Its Applications,* vol. 386, pp. 560-564, Apr 15 2003.

[99] R. S. Gonnelli, D. Daghero, G. A. Ummarino, M. Tortello, D. Delaude, V. A. Stepanov, *et al.*, "Point-contact Andreev-reflection spectroscopy in MgB_2: The role of substitutions," *Physica C-Superconductivity and Its Applications,* vol. 456, pp. 134-143, Jun 1 2007.

[100] A. A. Golubov and I. I. Mazin, "Effect of magnetic and nonmagnetic impurities on highly anisotropic superconductivity," *Physical Review B,* vol. 55, pp. 15146-15152, 06/01/ 1997.

[101] A. Gurevich, "Enhancement of the upper critical field by nonmagnetic impurities in dirty two-gap superconductors," *Physical Review B,* vol. 67, p. 184515, 05/16/ 2003.

[102] A. Gurevich, S. Patnaik, V. Braccini, K. H. Kim, C. Mielke, X. Song, *et al.*, "Very high upper critical fields in MgB_2 produced by selective tuning of impurity scattering," *Superconductor Science & Technology,* vol. 17, pp. 278-286, Feb 2004.

[103] L. Yongchang, L. Feng, M. Zongqing, C. Ning, L. Huijun, B. Shaon, *et al.*, "Significantly enhanced critical current density in nano-MgB_2 grains rapidly formed at low temperature with homogeneous carbon doping," *Superconductor Science and Technology,* vol. 28, p. 055005, 2015.

[104] J. H. Kim, S. X. Dou, J. L. Wang, D. Q. Shi, X. Xu, M. S. A. Hossain, *et al.*, "The effects of sintering temperature on superconductivity in MgB_2/Fe wires," *Superconductor Science & Technology,* vol. 20, pp. 448-451, May 2007.

[105] A. Kario, R. Nast, W. Haessler, C. Rodig, C. Mickel, W. Goldacker, *et al.*, "Critical current density enhancement in strongly reactive ex situ MgB_2 bulk and tapes prepared by high energy milling," *Superconductor Science & Technology,* vol. 24, Jul 2011.

[106] M. Vignolo, G. Romano, A. Martinelli, C. Bernini, and A. S. Siri, "A Novel Process to Produce Amorphous Nanosized Boron Useful for MgB_2 Synthesis," *IEEE Transactions on Applied Superconductivity,* vol. 22, Aug 2012.

[107] K. Vinod, N. Varghese, R. G. A. Kumar, U. Syamaprasad, and S. B. Roy, "Influence of Mg particle size on the reactivity and superconducting properties of

in situ MgB_2," *Journal of Alloys and Compounds,* vol. 464, pp. 33-37, Sep 22 2008.

[108] H. Yamada, M. Hirakawa, H. Kumakura, A. Matsumoto, and H. Kitaguchi, "Critical current densities of powder-in-tube MgB_2 tapes fabricated with nanometer-size Mg powder," *Applied Physics Letters,* vol. 84, pp. 1728-1730, Mar 8 2004.

[109] I. Pallecchi, V. Ferrando, C. Tarantini, M. Putti, C. Ferdeghini, Y. Zhu, *et al.*, "Increased in-field critical current density in neutron-irradiated MgB_2 films," *Superconductor Science & Technology,* vol. 22, Jan 2009.

[110] I. Pallecchi, C. Tarantini, H. U. Aebersold, V. Braccini, C. Fanciulli, C. Ferdeghini, *et al.*, "Enhanced flux pinning in neutron irradiated MgB_2," *Physical Review B,* vol. 71, Jun 2005.

[111] M. Eisterer, M. Zehetmayer, S. Tonies, H. W. Weber, M. Kambara, N. H. Babu, *et al.*, "Neutron irradiation of MgB_2 bulk superconductors," *Superconductor Science & Technology,* vol. 15, pp. L9-L12, Feb 2002.

[112] G. K. Perkins, Y. Bugoslavsky, A. D. Caplin, J. Moore, T. J. Tate, R. Gwilliam, *et al.*, "Effects of proton irradiation and ageing on the superconducting properties of single crystalline and polycrystalline MgB_2," *Superconductor Science & Technology,* vol. 17, pp. 232-235, Jan 2004.

[113] Y. Bugoslavsky, L. F. Cohen, G. K. Perkins, M. Polichetti, T. J. Tate, R. Gwilliam, *et al.*, "Enhancement of the high-magnetic field critical current density of superconducting MgB_2 by proton irradiation," *Nature,* vol. 411, pp. 561-563, May 31 2001.

[114] Y.-B. Wang, C. Xue, and Q.-R. Feng, "The effects of Ti ion-irradiation on critical current and flux pinning in MgB_2 thin film," *Acta Physica Sinica,* vol. 61, 2012 2012.

[115] N. Chikumoto, A. Yamamoto, M. Konczykowski, and M. Murakami, "Effect of heavy-ion irradiation on the pinning properties of MgB_2," *Physica C-Superconductivity and Its Applications,* vol. 388, pp. 167-168, May 2003.

[116] Y. Zhao, Y. Feng, D. X. Huang, T. Machi, C. H. Cheng, K. Nakao, *et al.*, "Doping effect of Zr and Ti on the critical current density of MgB_2 bulk

superconductors prepared under ambient pressure," *Physica C-Superconductivity and Its Applications,* vol. 378, pp. 122-126, Oct 1 2002.

[117] A. Berenov, A. Serquis, X. Z. Liao, Y. T. Zhu, D. E. Peterson, Y. Bugoslavsky, *et al.*, "Enhancement of critical current density in low level Al-doped MgB_2," *Superconductor Science & Technology,* vol. 17, pp. 1093-1096, Oct 2004.

[118] Q. Zhao, Y. Liu, and Q. Cai, "Influence of Ni addition on the process of phase formation in MgB_2 bulk," *Applied Physics a-Materials Science & Processing,* vol. 107, pp. 877-883, Jun 2012.

[119] J. C. Grivel, N. H. Andersen, P. G. A. P. Pallewatta, Y. Zhao, and M. von Zimmermann, "Influence of Bi, Se and Te additions on the formation temperature of MgB_2," *Superconductor Science & Technology,* vol. 25, Jan 2012.

[120] Y. Takikawa, M. Takeda, M. Migita, M. Uehara, T. Kuramoto, and Y. Kimishima, "Effect of W-addition on pinning property of MgB_2," *Physica C-Superconductivity and Its Applications,* vol. 471, pp. 905-907, Nov 2011.

[121] J. C. Grivel, A. Abrahamsen, and J. Bednarcik, "Effects of Cu or Ag additions on the kinetics of MgB_2 phase formation in Fe-sheathed wires," *Superconductor Science & Technology,* vol. 21, Mar 2008.

[122] T. Goto, H. Katoh, K. Watanabe, and G. Nishijima, "Eeffects of Zr, In and SiC addition on the critical current in filamentary MgB_2 superconductors by suspension spinning," in *Advances in Cryogenic Engineering, Vols 50a and B*. vol. 711, U. Balachandran, Ed., ed, 2004, pp. 569-576.

[123] T. Muranaka and J. Akimitsu, "Superconductivity in MgB_2," *Zeitschrift Fur Kristallographie,* vol. 226, pp. 385-394, 2011.

[124] A. Serquis, G. Serrano, S. M. Moreno, L. Civale, B. Maiorov, F. Balakirev, *et al.*, "Correlated enhancement of H_{C2} and J(c) in carbon nanotube doped MgB_2," *Superconductor Science & Technology,* vol. 20, pp. L12-L15, Apr 2007.

[125] R. Wilke, S. Bud'ko, P. Canfield, D. Finnemore, R. Suplinskas, and S. Hannahs, "Systematic Effects of Carbon Doping on the Superconducting Properties of $Mg(B_{1-x}C_x)_2$," *Physical Review Letters,* vol. 92, 2004.

[126] S. X. Dou, J. Horvat, S. Soltanian, X. L. Wang, M. J. Qin, S. H. Zhou, *et al.*, "Transport critical current density in Fe-sheathed nano-SiC doped MgB_2 wires,"

IEEE Transactions on Applied Superconductivity, vol. 13, pp. 3199-3202, Jun 2003.

[127] S. X. Dou, A. V. Pan, S. Zhou, M. Ionescu, H. K. Liu, and P. R. Munroe, "Substitution-induced pinning in MgB_2 superconductor doped with SiC nano-particles," *Superconductor Science & Technology,* vol. 15, pp. 1587-1591, Nov 2002.

[128] S. X. Dou, S. Soltanian, J. Horvat, X. L. Wang, S. H. Zhou, M. Ionescu, *et al.*, "Enhancement of the critical current density and flux pinning of MgB_2 superconductor by nanoparticle SiC doping," *Applied Physics Letters,* vol. 81, pp. 3419-3421, Oct 28 2002.

[129] H.-L. Suo, L. Ma, J.-M. Jiang, Y.-M. Li, Z.-L. Zhang, M. Liu, *et al.*, "High critical current densities in SiC doped In-Situ MgB_2 wires prepared by continuous tube forming and filling technique," *IEEE Transactions on Applied Superconductivity,* vol. 17, pp. 2822-2825, Jun 2007.

[130] L. B. S. Da Silva, G. Serrano, A. Serquis, V. C. V. Metzner, and D. Rodrigues, Jr., "Study of TaB2 and SiC additions on the properties of MgB_2 superconducting bulks," *Superconductor Science & Technology,* vol. 28, Feb 2015.

[131] X. H. Zeng, A. V. Pogrebnyakov, M. H. Zhu, J. E. Jones, X. X. Xi, S. Y. Xu, *et al.*, "Superconducting MgB_2 thin films on silicon carbide substrates by hybrid physical-chemical vapor deposition," *Applied Physics Letters,* vol. 82, pp. 2097-2099, Mar 31 2003.

[132] N. Varghese, K. Vinod, U. Syamaprasad, and S. B. Roy, "Doping effect of nano-SiC on structural and superconducting properties of MgB_2 bulks prepared by PIST method in air," *Journal of Alloys and Compounds,* vol. 484, pp. 734-738, Sep 18 2009.

[133] S. X. Dou, O. Shcherbakova, W. K. Yoeh, J. H. Kim, S. Soltanian, X. L. Wang, *et al.*, "Mechanism of enhancement in electromagnetic properties of MgB_2 by nano SiC doping," *Physical Review Letters,* vol. 98, Mar 2 2007.

[134] X. Xu, S. X. Dou, X. L. Wang, J. H. Kim, J. A. Stride, M. Choucair, *et al.*, "Graphene doping to enhance the flux pinning and supercurrent carrying ability of

a magnesium diboride superconductor," *Superconductor Science & Technology*, vol. 23, Aug 2010.

[135] S. X. Dou, W. K. Yeoh, J. Horvat, and M. Ionescu, "Effect of carbon nanotube doping on critical current density of MgB_2 superconductor," *Applied Physics Letters*, vol. 83, pp. 4996-4998, Dec 15 2003.

[136] C. H. Cheng, H. Zhang, Y. Zhao, Y. Feng, X. F. Rui, P. Munroe, *et al.*, "Doping effect of nano-diamond on superconductivity and flux pinning in MgB_2," *Superconductor Science & Technology*, vol. 16, pp. 1182-1186, Oct 2003.

[137] H. L. Xu, Y. Feng, Z. Xu, G. Yan, L. Z. Cao, and X. G. Li, "Enhancement of critical current density in graphite doped MgB_2 wires," *Chinese Physics Letters*, vol. 21, pp. 2511-2513, Dec 2004.

[138] S. J. Balaselvi, N. Gayathri, A. Bharathi, V. S. Sastry, and Y. Hariharan, "Stoichiometric carbon substitution in MgB_2," *Superconductor Science & Technology*, vol. 17, pp. 1401-1405, Dec 2004.

[139] P. Lezza, C. Senatore, and R. Fluekiger, "Improved critical current densities in B_4C doped MgB_2 based wires," *Superconductor Science & Technology*, vol. 19, pp. 1030-1033, Oct 2006.

[140] A. Yamamoto, J.-i. Shimoyama, S. Ueda, S. Horii, and K. Kishio, "Doping effects of TiC and Mo_2C on critical current properties of MgB_2 tapes," *IEEE Transactions on Applied Superconductivity*, vol. 16, pp. 1411-1414, Jun 2006.

[141] S. Zhou, A. V. Pan, D. Wexler, and S. X. Dou, "Sugar coating of boron powder for efficient carbon doping of MgB_2 with enhanced current-carrying performance," *Advanced Materials*, vol. 19, pp. 1373-1376, May 21 2007.

[142] D. Wang, Y. Ma, Z. Gao, X. Zhang, L. Wang, E. Mossang, *et al.*, "Enhancement of the High-Field J(c) properties of MgB_2/Fe Tapes by Acetone Doping," *Journal of Superconductivity and Novel Magnetism*, vol. 22, pp. 671-676, Oct 2009.

[143] H. Yamada, N. Uchiyama, H. Kumakura, H. Kitaguchi, and A. Matsumoto, "Superconducting properties of aromatic hydrocarbon-added powder-in-tube MgB_2/Fe tapes," *IEEE Transactions on Applied Superconductivity*, vol. 17, pp. 2850-2853, Jun 2007.

[144] C. H. Jiang, S. X. Dou, Z. X. Cheng, and X. L. Wang, "Light carbon doping by oxygen-free paraffin wax to enhance the current density of MgB_2 in the entire field regime," *Superconductor Science and Technology*, vol. 21, p. 065017, 2008.

[145] Z. Gao, Y. Ma, X. Zhang, D. Wang, Z. Yu, K. Watanabe, *et al.*, "Strongly enhanced critical current density in MgB_2/Fe tapes by stearic acid and stearate doping," *Superconductor Science & Technology*, vol. 20, pp. 485-489, May 2007.

[146] S. M. Lee, S. M. Hwang, C. M. Lee, W. Kim, J. Joo, J. H. Lim, *et al.*, "Enhancement in the Critical Current Density of C-Doped MgB_2 Wire Using a Polyacrylic Acid Dopant," *Journal of Nanoscience and Nanotechnology*, vol. 12, pp. 1406-1410, Feb 2012.

[147] C. M. Lee, S. M. Lee, G. C. Park, J. Joo, J. H. Lim, W. N. Kang, *et al.*, "Investigation of lauric acid dopant as a novel carbon source in MgB_2 wire," *Physica C-Superconductivity and Its Applications*, vol. 470, pp. 1438-1441, Nov 1 2010.

[148] H.-H. Sun, Y. Yang, L. Wang, C. H. Cheng, Y. Feng, and Y. Zhao, "Evidence of delta l pinning induced by citric acid doping in MgB_2 superconductor," *Acta Physica Sinica*, vol. 59, pp. 3488-3493, May 2010.

[149] A. Motaman, M. S. A. Hossain, X. Xu, K. W. See, K. C. Chung, and S. X. Dou, "A comprehensive study of the pinning mechanisms of MgB_2 wires treated with malic acid and their relationships with lattice defects," *Superconductor Science & Technology*, vol. 26, p. 085013, Aug 2013.

[150] H. Agil, O. Cicek, E. Ertekin, A. Motaman, M. S. A. Hossain, S. X. Dou, *et al.*, "Effects of MgO on the Electronic and Superconducting Properties in Succinic Acid ($C_4H_6O_4$) Doped MgB_2 Bulks," *Journal of Superconductivity and Novel Magnetism*, vol. 26, pp. 1525-1529, May 2013.

[151] A. Vajpayee, V. P. S. Awana, G. L. Bhalla, P. A. Bhobe, A. K. Nigam, and H. Kishan, "Superconducting properties of adipic-acid-doped bulk MgB_2 superconductor," *Superconductor Science & Technology*, vol. 22, Jan 2009.

[152] M. S. A. Hossain, J. H. Kim, X. L. Wang, X. Xu, G. Peleckis, and S. X. Dou, "Enhancement of flux pinning in a MgB_2 superconductor doped with tartaric acid," *Superconductor Science & Technology*, vol. 20, pp. 112-116, Jan 2007.

[153] C. Yao, X. Zhang, D. Wang, Z. Gao, L. Wang, Y. Qi, *et al.*, "Doping effects of Nd_2O_3 on the superconducting properties of powder-in-tube MgB_2 tapes," *Superconductor Science & Technology,* vol. 24, May 2011.

[154] J. Wang, Y. Bugoslavsky, A. Berenov, L. Cowey, A. D. Caplin, L. F. Cohen, *et al.*, "High critical current density and improved irreversibility field in bulk MgB_2 made by a scaleable, nanoparticle addition route," *Applied Physics Letters,* vol. 81, pp. 2026-2028, Sep 9 2002.

[155] C. Cheng and Y. Zhao, "Enhancement of critical current density of MgB_2 by doping Ho_2O_3," *Applied Physics Letters,* vol. 89, Dec 18 2006.

[156] S. K. Chen, M. Wei, and J. L. MacManus-Driscoll, "Strong pinning enhancement in MgB_2 using very small Dy_2O_3 additions," *Applied Physics Letters,* vol. 88, May 8 2006.

[157] N. Ojha, G. D. Varma, H. K. Singh, and V. P. S. Awana, "Effect of rare-earth doping on the superconducting properties of MgB_2," *Journal of Applied Physics,* vol. 105, Apr 1 2009.

[158] W. K. Yeoh, X. Y. Cui, B. Gault, K. S. B. De Silva, X. Xu, H. W. Liu, *et al.*, "On the roles of graphene oxide doping for enhanced supercurrent in MgB_2 based superconductors," *Nanoscale,* vol. 6, pp. 6166-6172, Jun 7 2014.

[159] K. S. B. De Silva, S. Gambhir, X. L. Wang, X. Xu, W. X. Li, D. L. Officer, *et al.*, "The effect of reduced graphene oxide addition on the superconductivity of MgB_2," *Journal of Materials Chemistry,* vol. 22, pp. 13941-13946, 2012.

[160] K. S. B. De Silva, X. Xu, X. L. Wang, D. Wexler, D. Attard, F. Xiang, *et al.*, "A significant improvement in the superconducting properties of MgB_2 by co-doping with graphene and nano-SiC," *Scripta Materialia,* vol. 67, pp. 802-805, Nov 2012.

[161] Z. Ma, Y. Liu, L. Yu, and Q. Zhao, "The accelerated formation of MgB_2 phase with high critical current density by Cu and SiC multidoping during the low-temperature sintering process," *Journal of Applied Physics,* vol. 104, Dec 1 2008.

[162] J. S. Hansdah and P. M. Sarun, "Doping effect of nano-Ho_2O_3 and naphthalene in MgB_2 superconductor prepared by powder-in-sealed-tube method," *Journal of Applied Physics,* vol. 117, Mar 21 2015.

[163] C. Martin, M. D. Vannette, R. T. Gordon, R. Prozorov, J. Karpinski, and N. D. Zhigadlo, "Effect of C and Li doping on the rf magnetic susceptibility in MgB_2 single crystals," *Physical Review B,* vol. 78, Oct 2008.

[164] N. Ojha, V. K. Malik, R. Singla, C. Bernhard, and G. D. Varma, "The effect of carbon and rare earth oxide co-doping on the structural and superconducting properties of MgB_2," *Superconductor Science & Technology,* vol. 23, Apr 2010.

[165] X. F. Pan, A. Matsumoto, H. Kumakura, C. H. Cheng, and Y. Zhao, "Cooperative doping effects of Ti and nano-SiC on transport critical current density and grain connectivity of in situ MgB_2 tapes," *Physica C-Superconductivity and Its Applications,* vol. 471, pp. 1128-1132, Nov 2011.

[166] W. Goldacker, S. I. Schlachter, B. Obst, B. Liu, J. Reiner, and S. Zimmer, "Development and performance of thin steel reinforced MgB_2 wires and low-temperature in situ processing for further improvements," *Superconductor Science & Technology,* vol. 17, pp. S363-S368, May 2004.

[167] W. Yao, J. Bascunan, S. Hahn, and Y. Iwasa, "MgB_2 Coils for MRI Applications," *IEEE Transactions on Applied Superconductivity,* vol. 20, pp. 756-759, Jun 2010.

[168] J. Ling, J. Voccio, Y. Kim, S. Hahn, J. Bascunan, D. K. Park, *et al.*, "Monofilament MgB_2 Wire for a Whole-Body MRI Magnet: Superconducting Joints and Test Coils," *IEEE Transactions on Applied Superconductivity,* vol. 23, Jun 2013.

[169] M. Razeti, S. Angius, L. Bertora, D. Damiani, R. Marabotto, M. Modica, *et al.*, "Construction and operation of cryogen free MgB_2 magnets for open MRI systems," *IEEE Transactions on Applied Superconductivity,* vol. 18, pp. 882-886, Jun 2008.

[170] S. A. Cybart, T. J. Wong, E. Y. Cho, J. W. Beeman, C. S. Yung, B. H. Moeckly, *et al.*, "Large scale two-dimensional arrays of magnesium diboride superconducting quantum interference devices," *Applied Physics Letters,* vol. 104, p. 182604, 2014.

[171] D. Mijatovic, A. Brinkman, D. Veldhuis, H. Hilgenkamp, H. Rogalla, G. Rijnders, *et al.*, "SQUID magnetometer operating at 37 K based on nanobridges in epitaxial MgB_2 thin films," *Applied Physics Letters,* vol. 87, Nov 7 2005.

[172] K. Chen, C. G. Zhuang, Q. Li, Y. Zhu, P. M. Voyles, X. Weng, *et al.*, "High-J(c) MgB_2 Josephson junctions with operating temperature up to 40 K," *Applied Physics Letters,* vol. 96, Jan 25 2010.

[173] K. Chen, C. G. Zhuang, Q. Li, X. Weng, J. M. Redwing, Y. Zhu, *et al.*, "MgB_2/MgO/MgB_2 Josephson Junctions for High-Speed Circuits," *IEEE Transactions on Applied Superconductivity,* vol. 21, pp. 115-118, Jun 2011.

[174] T. Tajima, A. Canabal, Y. Zhao, A. Romanenko, B. H. Moeckly, C. D. Nantista, *et al.*, "MgB_2 for application to RF cavities for accelerators," *IEEE Transactions on Applied Superconductivity,* vol. 17, pp. 1330-1333, Jun 2007.

[175] F. He, D.-t. Xie, Q.-r. Feng, and K.-x. Liu, "MgB_2 films fabricated on molybdenum substrate by hybrid physical-chemical vapor deposition for superconducting RF cavity applications," *Superconductor Science & Technology,* vol. 25, Jun 2012.

Chapter 3

Materials and Methods

The work presented in this thesis requires preparation of MgB_2 superconductor in both bulk and wire forms. Since the results in both cases have been organized in separate chapters, the detailed description of the sample preparation is also given in respective chapters/sections. The general technique chosen for sample preparation and the details of the characterizations done are described in this chapter.

3.1 Preparative methods in present study

The various approaches towards preparation of MgB_2 superconductor in different forms have been described in chapter 2. The present study has used the Powder In Sealed Tube (PIST) method [1-3] developed by our group to prepare MgB_2 in bulk form and the well-known Powder In Tube (PIT) method [4-6] to prepare it in wire form. The Mg powder of Goodfellow (< 105 μm, 99.8 % purity) and amorphous Boron of Merck (< 44 μm, 99 % purity) were used as the starting materials for the synthesis of MgB_2 in both PIST and PIT methods.

3.1.1 Preparation of bulk MgB_2 superconductor

For preparation of bulk MgB_2 by PIST method, stainless tube of OD/ID: 10/8 mm was shaped as a ‘container’ of precursors to be heat treated at the reaction temperatures. The high volatility and oxygen affinity of Mg prohibit us to heat treat the pelletized samples directly in contact with air. Therefore, in the PIST method, we have adopted heat treatment of the precursors in sealed condition. The Mg and B powders which were thoroughly hand mixed in an agate mortar were filled tightly in the one-end pressed piece of SS tube. After press-sealing the other end, the container as a whole was again

flattened. The whole pressings were done using a hydraulic press at a pressure of ~ 1 GPa. The ends of the tube were further sealed by welding. The heat treatment of the samples was done in a programmable muffle furnace with Eurotherm temperature controller (Model: 2404). Usually, the bulk samples were heat treated at 850 °C to 900 °C for 2 hour duration. The samples were then let to be furnace cooled to room temperature. To retrieve the bulk MgB_2 formed, the SS sheath was carefully ground and removed using an electric grinder. The dark brown colored, single piece MgB_2 of size about 10 mm x 10 mm x 3 mm was then shaped/powdered/fractured for various characterizations.

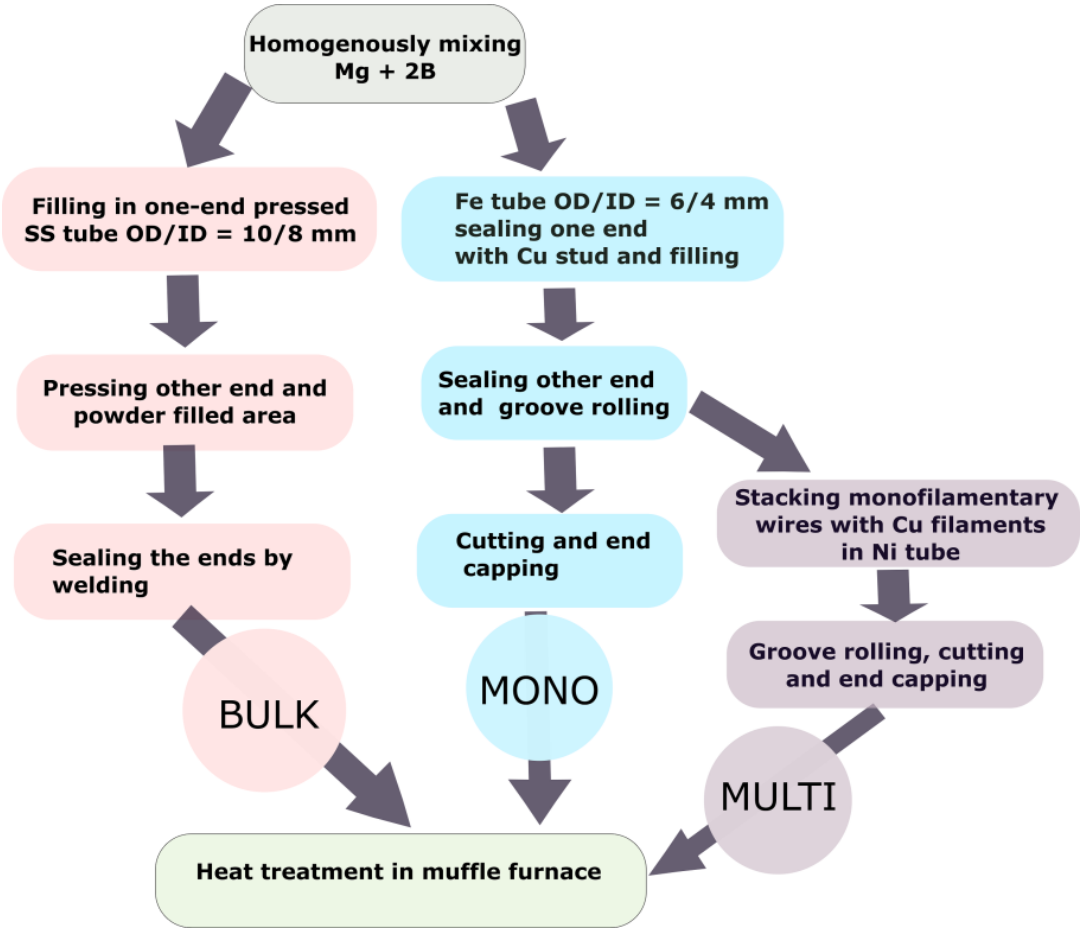

Figure 3.1: Flow chart showing the sequence of processes involved in the preparation of MgB_2 samples in bulk, mono and multi-filamentary forms

3.1.2 Preparation of MgB_2 monofilamentary and multifilamentary wires

In order to make long wires of brittle superconductors, the PIT method was being employed since the beginning of technological exploitation of A15 superconductors [7]. Being a brittle material the *in-situ* PIT method was employed to make MgB_2 wires also. To make monofilamentary wires metallic tubes of OD/ID: 6/4 or 5/3 mm were cut and filled with precursors and tightly compacted mechanically. The ends of the tubes were plugged and sealed using Cu studs. The powder filled tubes were then rolled down through a set of grooves in a groove roller to make fine wires. Typical dimensions of the final wire were 1.4 mm, 1.6 mm and 2.1 mm for various purposes. The ends of the wires were sealed by capping. The final heat treatment makes the precursors to form MgB_2 and thus monofilamentary wires were made. For wires, a lower temperature (600 °C to 750 °C) is required for the heat treatment.

For most of the practical applications, the wires are made into multifilamentary wires for various reasons [8]. For this, a metal tube (nickel was opted in this work) was filled with bundles of unreacted mono filamentary (Mg+2B) wires along with OFHC (Oxygen Free High Conductivity) copper filaments as stabilizer. The groove rolled composite was then subjected to heat treatment. This resulted in very fine filaments of superconducting wires embedded in copper matrix. Figure 3.1 charts the flow of procedures to make bulk and wires of MgB_2.

3.2 Methods used for structural characterization

3.2.1 X-ray diffraction (XRD) analysis

XRD analysis is a non-destructive technique to gather phase assemblage and structural information of crystalline materials. The possibility to analyze properties such as crystalline size, lattice parameters, lattice strain, chemical composition, state of ordering etc. in a convenient way makes XRD technique a fundamental tool in materials science [9].

In the present study, the XRD patterns of powdered samples were taken with Philips X'pert Pro (PW 3040/60) X-ray diffractometer with CuK_α radiation ($\lambda = 1.540566$

Å) employing X'celerator detector and a monochromator at diffracted beam side. The machine has θ-2θ Bragg-Brentano geometry and provision for fully automated operation and data acquisition. The finely powdered samples were filled and pressed into a standard sample holder (volume ~ 150 mm^3) so as to get a smooth and flat surface. A standard zero background holder was used when the volume of the sample was lesser. Most of the samples were scanned with X-ray tube voltage, 40 kV and a current, 30 mA. Programmable slits were used to restrict the X-ray beam into specified sample area. The scans were performed in ambient conditions and the scanning angles were usually from 20° to 85° of 2θ values. The step size of the scan was ~ 0.2° and the total time per sample was ~20 minutes in most cases.

The phase identification from the acquired data was done using X'pert Highscore Plus software loaded with ICDD-PDF-2 database. The peaks of MgB_2 were compared to the standard MgB_2 peaks with reference code: 00-038-1369. Besides the phase detection, the volume percentage of the phases and hence the purity of the MgB_2 were determined using a semi-quantitative phase analysis using the relation,

$$Vol.\%\ of\ phase\ X = \frac{\sum Integrated\ peak\ intencities\ of\ phase\ X}{\sum Integrated\ peak\ intensities\ of\ all\ phases}$$

The d-values of selected peaks were used to calculate lattice parameters. Lattice parameters were calculated for the hexagonal crystal structure of space group p6/mmm, using the equation,

$$\frac{1}{d^2} = \frac{4(h^2 + hk + k^2)}{3a^2} + \frac{l^2}{c^2}$$

The FWHM of the individual peaks in an XRD pattern can be used to determine crystallite size and the presence of lattice distortions (strain) in the crystal [9]. Both are relevant to superconductors since they have a direct influence on flux pinning [10].

3.2.2 Microstructural analysis

The optical microscopy, scanning electron microscopy and high resolution transmission electron microscopy (HRTEM) were used for microstructural analysis of various samples in this work.

Optical microscopy

The measurement of transport critical current density, J_C and engineering current density, J_E requires accurate cross sectional area of the superconducting portion and the wire itself respectively. An optical microscope is very useful for this purpose. A stereo microscope (Leica Model EZ4 HD) with maximum magnification 30x and integrated with 3 megapixel inbuilt camera interfaced to a computer was used in this work for estimating the cross sectional area of the wires. A proprietary software (Leica LAS EZ) enables the live measurement of area and length accurately.

The reaction layers formed between MgB_2 core and sheath metal of the wire samples can also be studied using optical microscope. In multifilamentary wires, the homogeneity and geometry of the filaments and relative areas of core/barrier/stabilizer/sheath were also studied. The short samples of 1-2 cm length were cut, mechanically polished and held in suitable holders to examine the morphology.

Scanning Electron Microscopy (SEM)

Since the resolution of optical microscope is limited by wavelength of visible region, a magnification beyond ~1500x and good depth of focus are unattainable. Therefore, in order to study the microstructural aspects such as grain size, grain boundaries, porosity, inclusions of the superconductor samples; a SEM is used. SEM produces focused high energy electrons and a raster scan is performed over the surface of the sample. The signals generated from electron-sample interaction are used to reveal the sample characteristics [11] .

In the present study, a JEOL JSM 5600 LV Scanning Electron Microscope was used in Secondary Electron Imaging (SEI) mode. The fractured MgB_2 bulk samples were fixed on brass studs using adhesive carbon tapes and loaded in the sample holder of the microscope. Being a fairly good conductor in its normal state, no gold coating was required. Typically, magnifications of 3000x, 5000x, and 10000x were used for analysis. Wire samples cut into very short lengths were also examined.

Transmission Electron Microscopy (TEM)

To get even higher resolution, TEM was used on selected samples. The inter grain and intra grain features and sub-micron and nano-sized inclusions were the main subject of study using TEM in this work. The samples were analyzed using a model HRTEM FEI-Tecnai G^2 30 S-Twin 300 kV. The finely powdered sample was dispersed in acetone (due to its low boiling point), sonicated (to remove agglomerations) and dropped on carbon and polymeric film coated copper grids. The coated samples were kept overnight to evaporate the solvent before analysis.

3.3 Superconducting characterization methods

Transport and magnetic measurements were carried out on various MgB_2 samples to find superconducting properties such as T_C, J_C, $J_C(H)$ and H_{irr}. For transport measurements, a cryogen free cryocooler was used to attain temperatures as low as ~7 K. In-field transport properties were studied in an 8 T LHe vapor cooled superconducting solenoid magnet. The magnetic measurements were done using a VSM or SQUID based PPMS in collaboration with RRCAT, Indore and JNCASR, Bangalore.

3.3.1 Transport characterization

Four probe resistivity method was used for transport measurements (figure 3.2). For self-field measurements, the wire samples of ~ 4 cm of length were cut, thoroughly cleaned and then, current and voltage leads were soldered using phosphoric acid as flux. The sample was mounted on the home made sample holder fixed at the second stage of cryogen free cryocooler. The cryocooler used was a Gifford-Mcmahon cooler made by Sumitomo Heavy Industries Ltd (SRDK-408). The cryocooler was integrated with an indigenously designed cryostat (figure 3.3).

To assess the performance of samples in an external magnetic field, a LHe based 8 T solenoid magnet system manufactured by American magnetics Inc (AMI System Number: 13641) was used. The magnet was immersed in LHe and the sample was cooled by LHe vapor whose flow can be controlled by a throttle valve. The details of components of the magnet system are given in figure 3.4.

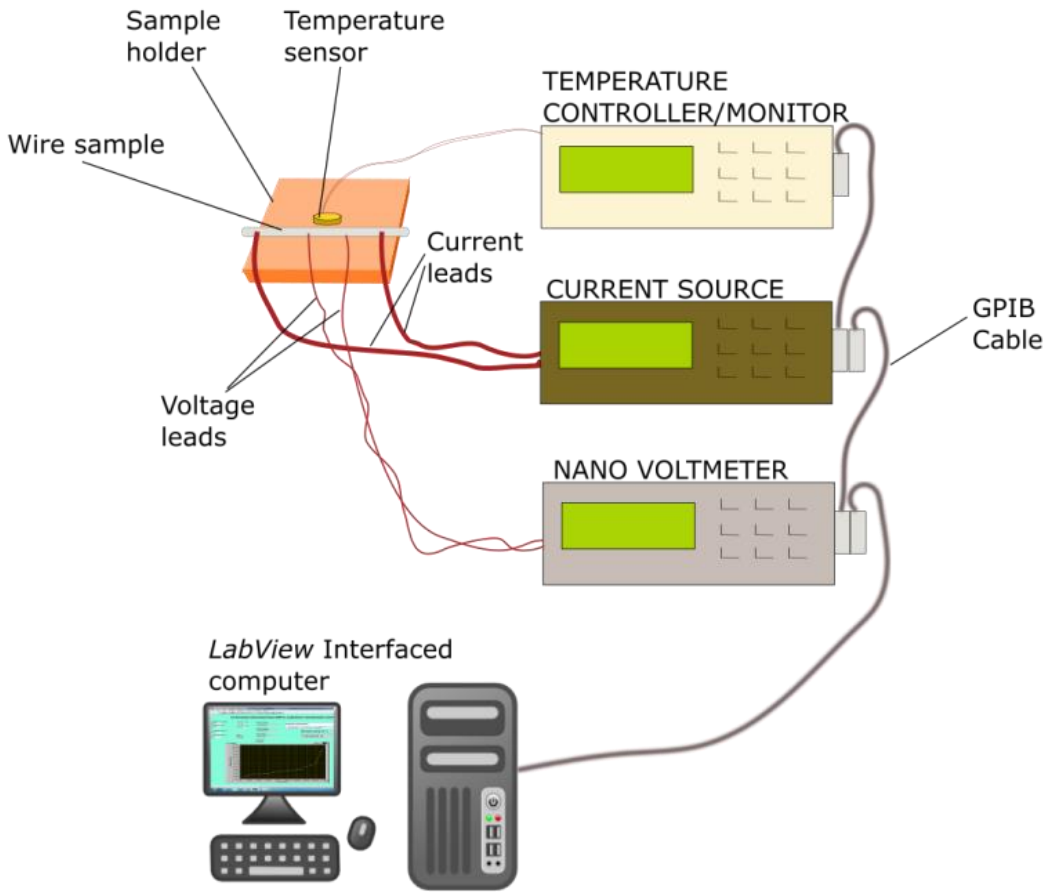

Figure 3.2: The schematic diagram of transport characterization. The sample holder (only bottom plate is shown)is fixed either to the sample stage of the cryocooler or to the uniform magnetic field zone of the 8T magnet system.

For both R-T and I-V measurements, a Keithley nano voltmeter (Model: 2182A) was used. A constant current of 10 mA was passed through the sample from a Keithley milliampere current source (Model: 6220) in R-T measurements. Constant current sources with high ampere ratings from 100 A to 1000 A were used for I-V measurements. These include APLAB (Model: 9711 P) with 30 V, 100 A rating and Sorensen (Model: DHP 5-1000 M1M9D) with 5 V, 1000 A rating.

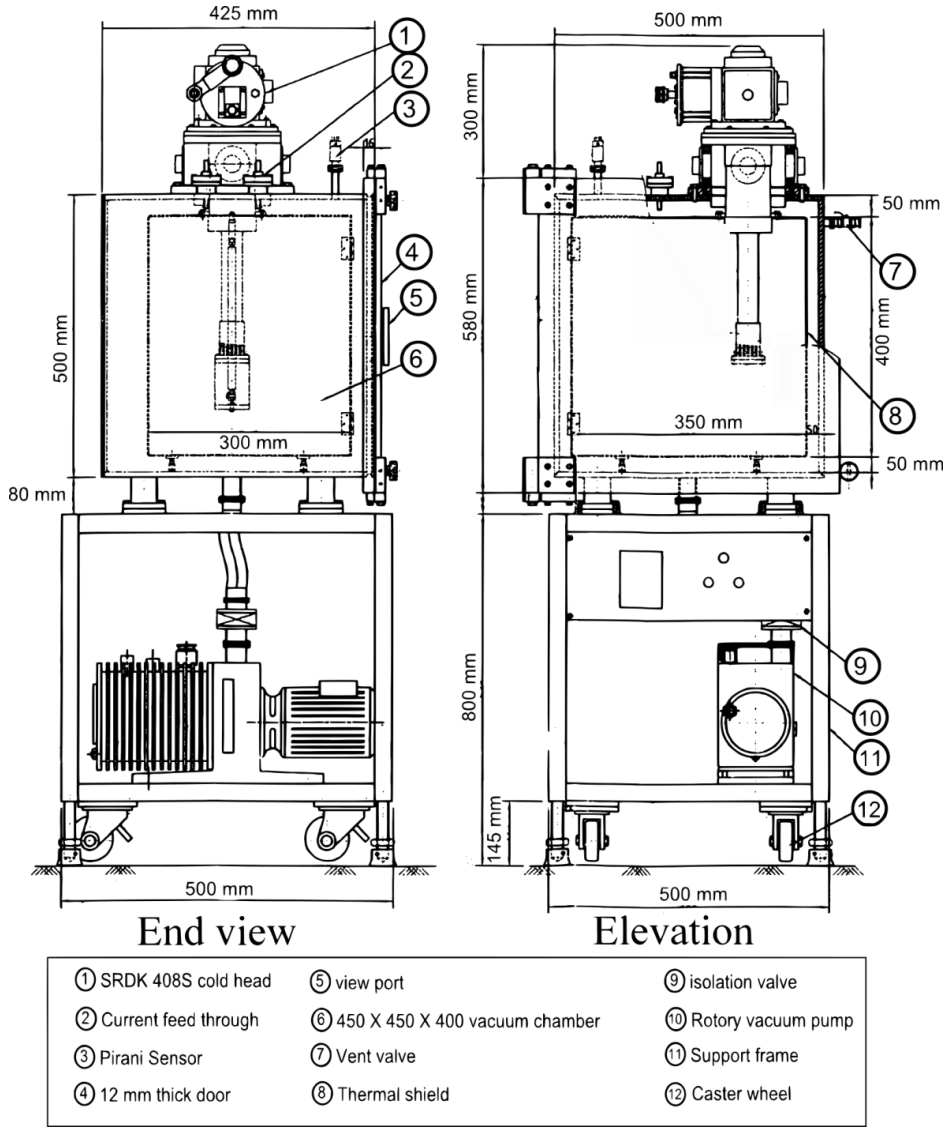

Figure 3.3: Schematic diagram of cryocooler integrated cryostat

The temperature of the sample was measured and controlled using Lakeshore temperature Controllers (Models: L340/L332). For this, a silicon diode based temperature sensors (Model: DT-670B-Cu/470B-Cu) were installed at the sample holder very close to the sample and a heater coil was installed at the second stage of the cryocooler. Cernox (CX-1050-Cu) sensors were used instead of normal DT sensors whenever temperature is measured in presence of a magnetic field. All the instruments were interconnected serially with GPIB cables and the whole measurements were automated with self-coded programs in *LabVIEW*.

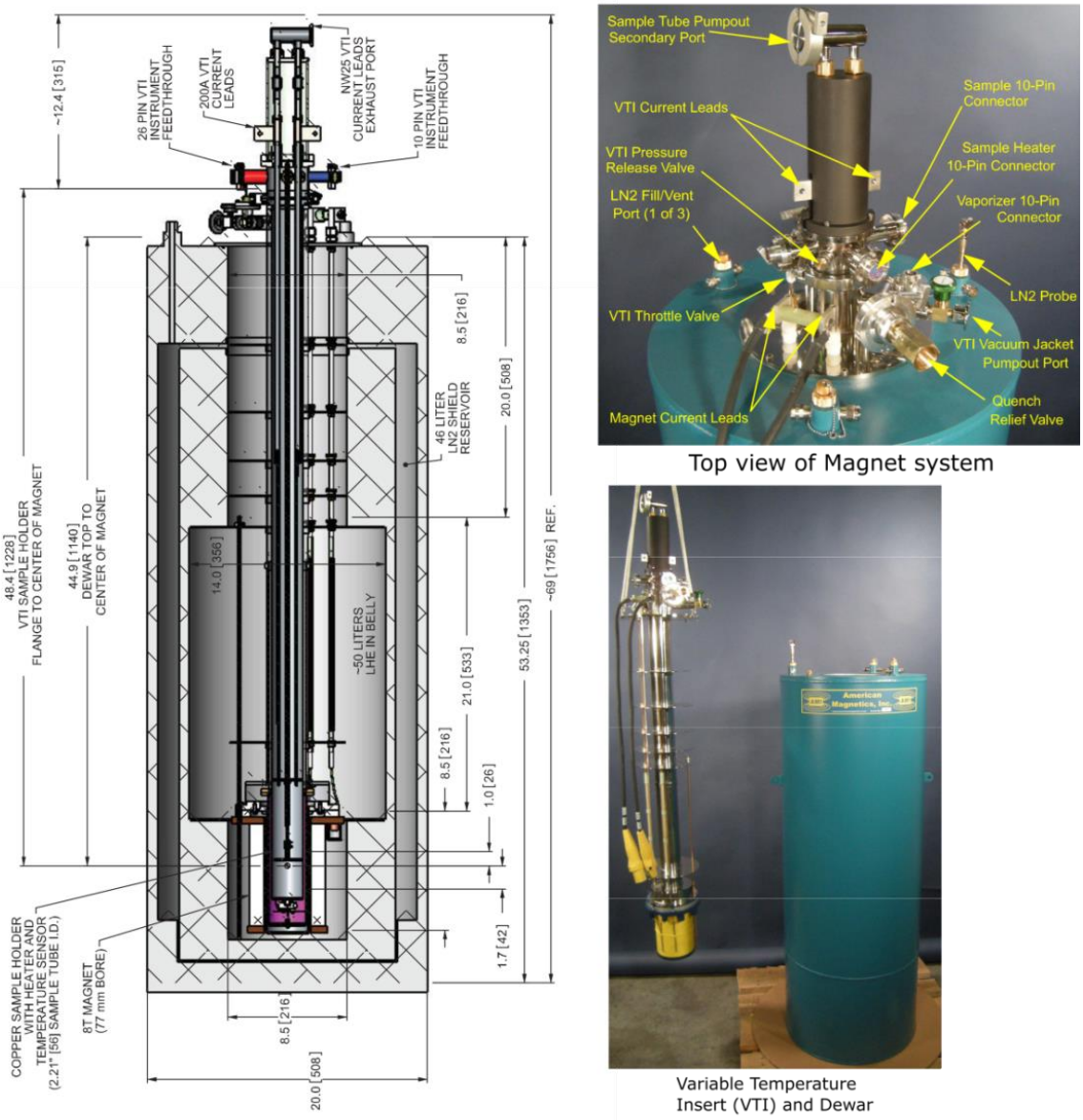

Figure 3.4: Schematic diagram and photographs of 8 T magnet system

The T_C and ΔT_C were measured from R-T characteristics. The temperature at which the resistance of the wire begins to fall sharply was taken as T_C onset. To calculate ΔT_C, the difference between temperatures corresponding to 90 % and 10 % of normal resistance of the wire at 40 K was taken. The I_C is taken as the value of the current in I-V graph, where the voltage begins to rise sharply. The criterion of 1 μV/cm was used for measuring the I_C. To estimate J_C or J_E values, cross sectional area was measured with optical microscope. The whole arrangements are shown schematically in figure 3.2.

3.3.2 Magnetic characterization

Magnetic measurements are non-contact measurements and the characterization includes recording of magnetization in sample by varying the temperature (M-T plot) and by varying the external field (M-H plot). The measurements were done in collaboration with JNCASR, Bangalore and RRCAT, Indore. Bulk MgB_2 samples were shaped into typical dimensions of 3 mm × 3 mm× 2 mm. The magnetic field was applied along the longest dimension of the samples. The M-T measurements were done in Zero Field Cooled (ZFC) condition at 20 Oe field. The M-H measurements were done at 5 K and fields up to 8 T. The T_C and ΔT_C were found from M-T graph. The T_C is taken as the temperature at which magnetization M begins to fall and ΔT_C is taken as the difference between the temperatures corresponding to the 90 % and 10 % of the maximum shielding signal.

The variation of J_C as the function of external field, $J_C(H)$ was estimated based on Bean critical state model by the equation [12],

$$Jc(H) = \frac{20 \times \Delta M}{a\left(1 - \frac{a}{3b}\right)} \qquad Acm^{-2}$$

Where ΔM (emu/cm^3) is the width of the M-H loop, a and b (a < b and both in cm) are dimensions of the sample perpendicular to the field and V is the volume of the sample in cm^3. Variation of flux pinning force F_P with the field can be calculated as $\boldsymbol{F_P = J_C \times \mu_0 H}$. The H_{irr} of the sample may be estimated as the field at which J_C is reduced to 100 Acm^{-2}.

REFERENCES

[1] S. Thomas, S. Rahul, K. M. Devadas, N. Varghese, A. Sundaresan, and U. Syamaprasad, "Co-addition of nano-carbon and nano-silica: An effective method for improving the in-field properties of magnesium diboride superconductor," *Materials Chemistry and Physics*, vol. 148, pp. 190-194, Nov 14 2014.

[2] N. Varghese, K. Vinod, S. Rahul, P. Anees, K. M. Devadas, S. Thomas, *et al.*, "Effect of Carbon Substitution on the Superconducting Properties of Nanocarbon-, Nanodiamond- and Nano-SiC-Doped MgB_2," *Journal of the American Ceramic Society*, vol. 94, pp. 1133-1137, Apr 2011.

[3] R. G. A. Kumar, K. Vinod, R. P. Aloysius, and U. Syamaprasad, "A simple and inexpensive method for rapid synthesis of MgB_2 superconductor," *Materials Letters*, vol. 60, pp. 3328-3331, Dec 2006.

[4] K. M. Devadas, S. Rahul, S. Thomas, N. Varghese, K. Vinod, U. Syamaprasad, *et al.*, "Transport properties of sealed MgB_2/Fe/Ni multifilamentary wires heat treated in air," *Journal of Alloys and Compounds*, vol. 509, pp. 8038-8041, Aug 4 2011.

[5] N. Varghese, K. Vinod, S. Rahul, K. M. Devadas, S. Thomas, S. Pradhan, *et al.*, "Influence of nano-Cu additive on MgB_2 phase formation, processing temperature, and transport properties," *Journal of Applied Physics*, vol. 109, Feb 1 2011.

[6] B. A. Glowacki, M. Majoros, M. Vickers, J. E. Evetts, Y. Shi, and I. McDougall, "Superconductivity of powder-in-tube MgB_2 wires," *Superconductor Science & Technology*, vol. 14, pp. 193-199, Apr 2001.

[7] J. E. Kunzler, E. Buehler, F. S. L. Hsu, and J. H. Wernick, "Superconductivity in Nb_3Sn at high current density in a magnetic field of 88 kgauss," *Phys. Rev. Lett.*, vol. 6, pp. 89-91, 1961.

[8] P. Seidel, Ed., *Applied Superconductivity: Handbook on Devices and Applications*: Wliey, 2015.

[9] S. Suryanarayana and M. Grant Norton, *X-Ray Diffraction: A Practical Approach*: Springer, 1998.

[10] P. J. Lee, *Engineering Superconductivity*: Wiley, 2001.

[11] L. Reimer, *Scanning Electron Microscopy: Physics of Image Formation and Microanalysis*: Springer, 2013.

[12] C. P. Bean, "Magnetization of hard superconductors," *Physical Review Letters*, vol. 8, pp. 250-252, 1962.

Chapter 4

Improvement of in-field critical current density ($J_C(H)$) of MgB_2 by chemical addition

Since the discovery of superconductivity in MgB_2, it has been considered as a material of great interest due to its high critical current density (J_C), low anisotropy, large coherence length, absence of weak links, simple crystal structure and low cost. Its high transition temperature (T_C = 39 K) makes it operable at around 20 K with the aid of cryogen free cryocoolers [1, 2]. Though MgB_2 possesses a self-field J_C of 10^5 - 10^6 A/cm^2 at 4.2 K, it falls rapidly on application of high magnetic fields. The reasons for the degradation of $J_C(H)$ depend on various factors such as phase purity of material, low H_{C2}, poor flux pinning, microstructural properties and lack of grain connectivity [3].

The phase purity of the material can be achieved by using the phase pure reactants, optimizing the reaction temperature and avoiding the exposure to impurities during the time of reaction. The H_{C2} of a superconductor is its intrinsic property. Hence to change the H_{C2} significantly, we have to change the chemical composition of the material itself without adversely affecting its superconducting properties. This can be achieved by doping of other elements to the MgB_2 lattice. But among various elements tried carbon is the only element which is appreciably successful in entering the MgB_2 lattice by replacing the boron atoms and consequently increases the Hc_2 and J_C *(H).*

The poor flux pinning properties of MgB_2 can be remedied by introducing nano-sized and well dispersed impurities in MgB_2 grains so as to trap the flux lines. Since the grain boundaries can also act as good flux pinning centers for MgB_2, the microstructure of the material is also very important. The loss of grain connectivity is possible in formation of doped MgB_2. So that this problem also should be addressed for the better enhancement of $J_C(H)$ especially at lower magnetic fields.

Even though the major applications of a superconductor can be realized by making them in the form of wires, for the basic research its bulk form is ideal due to easiness in making and characterizing when compared to wires. After optimizing the process parameters in bulk MgB_2 it can be translated into wire form depending on the specific application.

4.1 Sample preparation and characterization

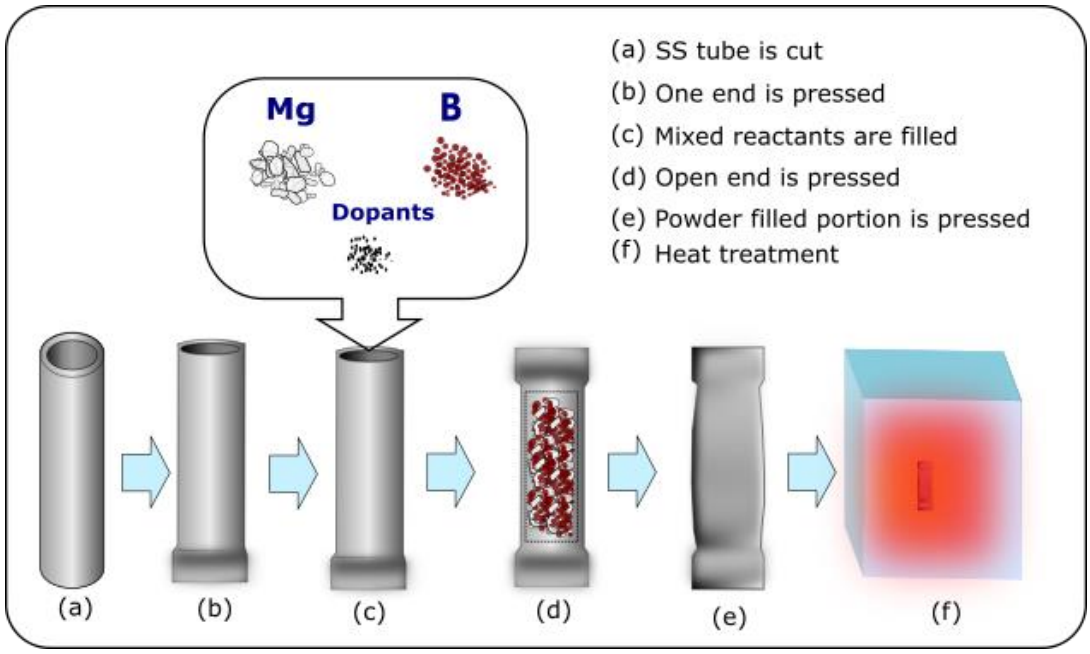

Figure 4.1: Schematic diagram showing the preparation of bulk MgB_2 by PIST method

To prepare the bulk MgB_2 samples, the Powder In Sealed Tube (PIST) method was adopted, in which the sample formation takes place inside a sealed metal tube. A stainless steel (SUS 304) tube of external diameter 10 mm and internal diameter 8 mm was cut for a length about 8 cm which is enough to prepare 1 g of MgB_2. One end of the tube was pressed uniaxially using a hydraulic press with a pressure of about 1 GPa. The Mg powder (< 105 μm, 99.8 % purity), B powder (< 44 μm, 99 % purity) and the dopants, if any, were weighed stoichiometrically using an electronic balance. The powders were then homogeneously mixed by grinding it with agate mortar and pestle. When dopants were present as reactants, the boron powder and the dopants were first mixed well and then the mixture was ground with Mg powder. The total grinding time can be about 1 hour or more depending on the quantity of the reactants and the number and the nature of the dopants present. The final mixture was then filled and tightly packed inside the one end sealed SS tube but leaving a small unfilled

space. The unfilled space was then pressed by applying the same pressure as that for the other end and subsequently the powder filled portion was also pressed and thus a bar shaped specimen was obtained. Figure 4.1 shows a schematic diagram of the procedure of the PIST method. The ends of the pressed tube were weld-sealed to avoid oxidation of the reactants during heat treatment in air. A wet cloth was wound around the specimen to avoid the sample from heating up.

The samples were then subjected to heat treatment in programmable muffle furnace at desired temperatures, usually range from 800 to 900 °C. The heat treatment was done directly in air with a ramp rate of 4˚C/minute and subsequently subjected to furnace cooling. Then the bar shaped samples were taken out and the MgB_2 core formed was retrieved by mechanically grinding and peeling off the SS sheath. The core was cut and lapped into different shapes for various type of characterization.

The phase and structural analysis of the sample were done by powder X-ray diffraction method using X-ray diffractometer. The identification of the phases was carried out using X'pert Highscore Plus software aided with ICDD PDF II database. The microstructural analysis was done by employing an optical microscope, scanning electron microscope and an HRTEM. DC magnetic measurements (M-T and M-H) were carried out by VSM/SQUID on the sample pieces which were cut to 3×3×1.5 mm dimension with the field applied along the longest dimension. The detailed description on the methods of characterizations is given in the chapter 3.

4.2 Carbon substitutional effects on in-field critical current density of MgB_2 from nano-carbon and nano-diamond sources

4.2.1 Introduction

Among the various attempts to enhance the $J_C(H)$ of MgB_2, the most promising one is to dope it with carbon or carbon containing compounds. Because of the comparable ionic radii of carbon and boron, carbon can enter to the MgB_2 lattice and can create lattice defects which can serve as electron scatterer. The scattering reduces the electron mean free path and thereby reduces the coherence length [4]. This leads to an increase in H_{C2} and eventually better $J_C(H)$ of the superconductor. But in order to achieve better results, the source and amount of the carbon to be doped

should be selected and optimized wisely. Accordingly, as a basic step to enhance the $J_C(H)$, carbon from two different sources, the nano-carbon (n-C) and nano-diamond (n-D) were used as dopants. The sample with the best performance shall be considered as a reference composition for further $J_C(H)$ enhancement studies.

$MgB_{1-x}C_x$ samples were prepared where x is 0, 0.1, and 0.2 with n-C (< 50 nm, 99+ % purity) and n-D (< 10 nm, 99+ % purity) as sources of carbon. The heat treatment of the samples was done at 850˚C for duration of 2 hour. The sample codes for various samples are given in the table 4.1.

4.2.2 Results and Discussion

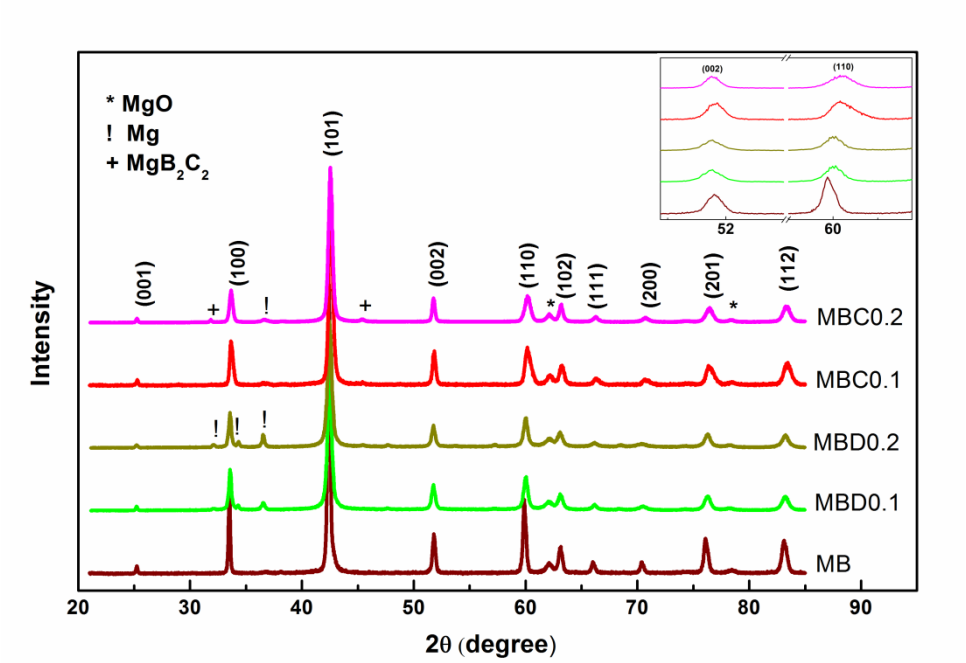

Figure 4.2: XRD patterns of pure and doped MgB_2 samples. The inset shows an expanded view of the (002) and (110) peaks of all samples

The figure 4.2 shows the powder XRD patterns of pure and doped samples of MgB_2. The peaks of MgB_2 are indexed with (hkl) values of the respective planes of reflections. The undoped sample shows very sharp peaks of MgB_2 with a trace of MgO as impurity. The presence of MgO is observable in all samples due to the entrapped air during the precursor filling stage of the sample preparation. The n-D doped samples show presence of considerable amount of unreacted Mg and its presence is found to increase with the increase of doping percentage. The n-C doped

samples generally show a better phase purity than the n-D doped samples but the sample MBC0.2 shows slight amount of MgB_2C_2 as reacted secondary phase.

An enlarged view of (002) and (110) peaks are shown in the inset of figure 4.2. The peak shift occurred for (110) plane indicates that the carbon substitution has been taken place in MgB_2 lattice. The calculation of lattice parameters, shown in table 4.2 confirms the carbon substitution since the *a*-axis length is decreased with the substitution of carbon by replacing the born atoms from the hexagonal structure. But the *c*-axis length is not much affected and hence there is no noticeable peak shift for (002) plane.

Table 4.1: FWHM values of (100), (101), (002), and (110) peaks of samples

Sample details	Sample code	FWHM of selected peaks (degree)			
		100	101	002	110
MgB_2	MB	0.188	0.273	0.318	0.315
$MgB_{1.9}C_{0.1}$ (n-D)	MBD0.1	0.232	0.385	0.352	0.391
$MgB_{1.8}C_{0.2}$ (n-D)	MBD0.2	0.261	0.419	0.322	0.392
$MgB_{1.9}C_{0.1}$ (n-C)	MBC0.1	0.349	0.423	0.340	0.583
$MgB_{1.8}C_{0.2}$ (n-C)	MBC0.2	0.409	0.403	0.312	0.585

The Full Width at Half Maximum (FWHM) values of selected planes of pure and doped samples are shown in table 4.1. The peaks other than (002) peak of the doped samples show significant broadening. The FWHM is a measure of size, crystallinity and strain in the sample. So the carbon doping is found to have significant effect on sintering and grain growth of the samples. Figure 4.3 shows the temperature dependence of zero field cooled magnetization values for the pure and doped samples, where the T_C value is taken as the onset temperature at which samples exhibit diamagnetism. The measured values of T_C are tabulated in table 4.2. The table shows that, the T_C of the doped samples is decreased with level of carbon substitution. The n-C doped samples show lower values for T_C than the n-D doped ones.

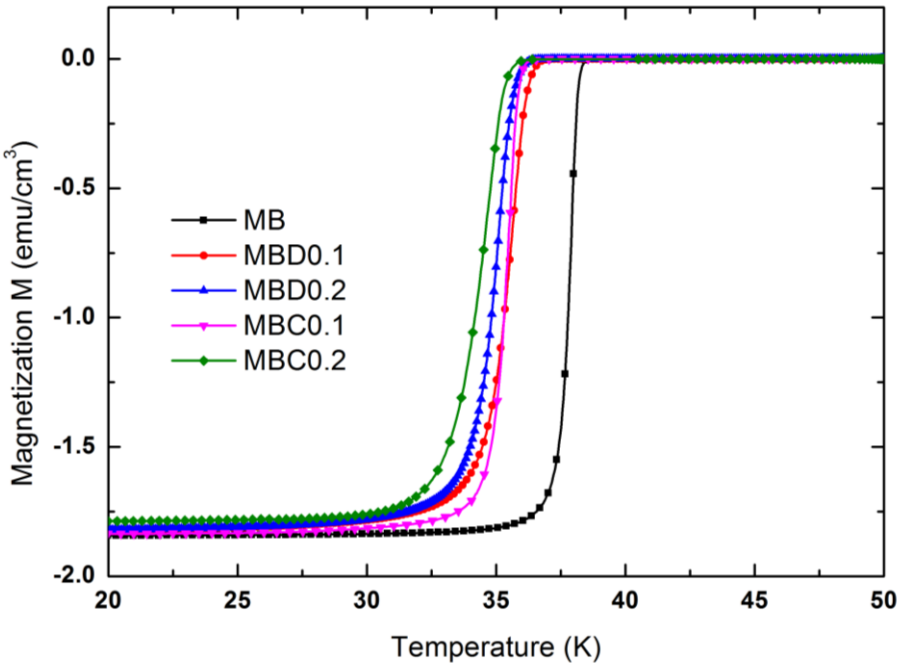

Figure 4.3: Zero field cooled magnetization versus temperature plots of the pure and doped samples taken at 20 Oe

Table 4.2: Structural and superconducting properties of pure and doped samples

Sample	Lattice parameters (Å)		T_C Onset (K)	ΔT_C (K)	J_C at 8 T and 5 K ($\times 10^3$ A/cm^2)
	a-axis	*c*-axis			
MB	3.0878	3.5284	38.4	1.05	0.14
MBD0.1	3.0784	3.5223	36.7	2.21	1.52
MBD0.2	3.0781	3.5252	36.5	2.32	1.62
MBC0.1	3.0749	3.5248	36.3	1.44	5.14
MBC0.2	3.0747	3.5252	36.1	2.53	2.15

The values of transition width ΔT_C are also given in table 4.2. Since ΔT_C is a measure of homogeneity and phase purity of the sample we can infer that the sample MBC0.1 is the most homogenous and phase pure sample among the doped samples. Presence of reacted secondary phases and unreacted Mg and carbon reduces the purity of other doped samples.

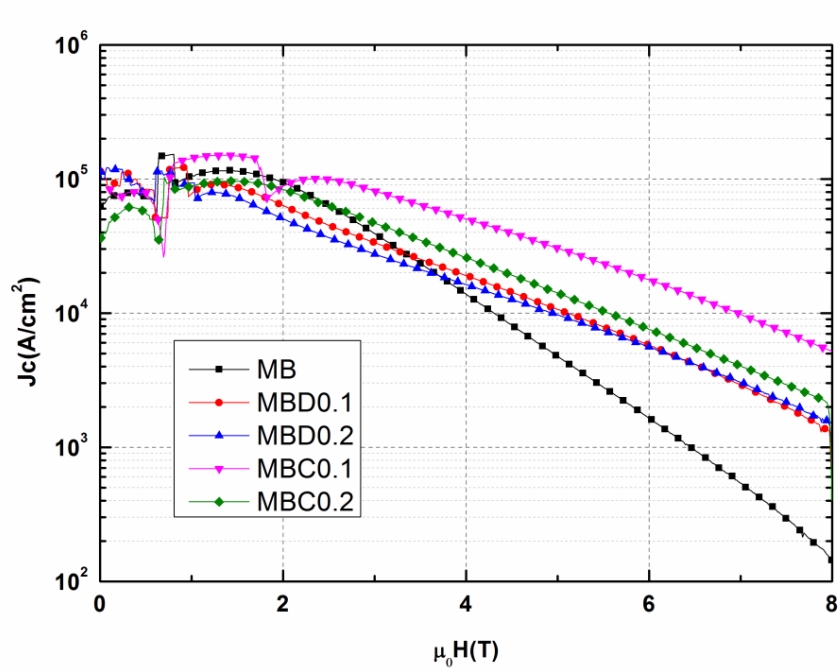

Figure 4.4: Magnetic field dependence of critical current density of pure and doped MgB_2 samples at 5 K

The in-field critical current density $J_C(H)$ of the pure and doped samples deduced from the M-H curves is shown in the figure 4.4. All the doped samples show enhanced $J_C(H)$ compared to the pure sample at higher fields. The sample doped with n-C shows better $J_C(H)$ performance than the n-D doped samples at both lower and higher fields. The better reactivity of n-C makes it more soluble in the MgB_2 lattice and helps carbon substitution more effective. The presence of non-superconducting phases causes the diamond doped samples to show degradation of $J_C(H)$ compared to the pure sample at lower fields, or in these samples the grain to grain connectivity is not as good as that for other samples. When comparing the two samples doped with n-C, the sample MBC0.1 shows better results than MBC0.2. Even though the substitution level of the carbon is comparable in both samples as evident from the values of a-lattice parameters, the presence of secondary phases and unreacted n-C cause to decrease the level of $J_C(H)$ enhancement of MBC0.2 than that of MBC0.1.

The sample MBC0.1 shows the best result among all the samples. It is the most phase pure sample among the doped samples and the level of the carbon substitution is also high in this sample. The lower ΔT_C shows that the substitution is also homogeneous for the sample. MBC0.1 shows better values of $J_C(H)$ even at

lower fields. At 8 T the sample shows around 38 times enhancement in J_C than that of the pure sample. The increased $J_C(H)$ of the carbon doped samples can be related to the increased lattice defects and introduction of electron scatterers in MgB_2 lattice. The H_{C2} of a superconductor is related to its coherence length ξ in such a way that H_{C2} increases with the decrease in ξ. The addition of impurities reduces the electron mean free path and thereby reduces the coherence length and thus increases the in-field performance of the superconductor.

4.2.3 Conclusions

The effect of carbon doping on the structural and in-field J_C of MgB_2 was studied using two different C sources namely, n-C and n-D. The sample with 0.1 at.% of n-C ($MgB_{1.9}C_{0.1}$) was found to have the best superconducting properties. The XRD study showed that carbon was effectively substituted into MgB_2 lattice and the depression in T_C confirmed this. The FWHM of the (hk0) planes of all doped samples widened and which is an indication of increased lattice strains. The $J_C(H)$ of the best sample was enhanced by 38 times that of pure at 8 T and 5 K. The study points to the possibility of further enhancement of $J_C(H)$ of the best sample, $MgB_{1.9}C_{0.1}$ by introducing other methods to increase flux pinning such as introduction of nano-sized secondary impurities. The sample $MgB_{1.9}C_{0.1}$ can be considered as a reference level for further $J_C(H)$ enhancement studies.

4.3 Enhancement of in-field critical current density of MgB_2 by combined addition of nano-carbon and nano-silica

4.3.1 Introduction

To enhance the $J_C(H)$, the carbon doping method mainly intended the substitution of boron atoms by carbon in the MgB_2 lattice and to create lattice defects. Another approach is to create nano/submicron sized inclusions of reacted or unreacted phases within the grains of MgB_2. Both of these methods can improve the H_{C2} and H_{irr}, and hence the $J_C(H)$. Among the various elements and compounds tried so far, carbon and carbon containing compounds such as n-C [5-7], carbon nanotubes [8-10], n-SiC [11-13], B_4C [14], BRH [15], graphene [16], graphene oxide [17, 18] and hydrocarbons [19-23] are found to be effective in enhancing the $J_C(H)$ to a significant

level. While the effectiveness of the substitution of boron atoms by carbon has made n-C a favorable dopant, carbon substitution and distribution of nano-scale reacted secondary phases in MgB_2 grains are the advantages of n-SiC [24, 25]. In addition to the carbon substitution, the size and amount of the additive and the homogeneity in distribution of the secondary phases also should be optimum for achieving enhanced flux pinning and hence improved $J_C(H)$.

In the present work instead of using n-SiC as single dopant, co-doping of n-C and n-SiO_2 is carried out and the results are compared with those of pure and n-C and n-SiC independently doped samples. The doping level of carbon in all doped samples and all the processing parameters were kept identical for a meaningful comparison.

Polycrystalline samples with initial composition: MgB_2, $MgB_{1.9}C_{0.1}$, MgB_2 + 8.7 wt.% n-SiC (8.7 wt.% of SiC is equivalent to 0.1 at.% of C in MgB_2) and $MgB_{1.9}C_{0.1}$ + 2.5 wt.% n-SiO_2 were prepared by in situ Powder-In-Sealed-Tube (PIST) method using Mg (< 105 μm, 99.8%), amorphous B (< 44 μm, 99%), n-C (< 50 nm, 99+%), n-SiC (< 100 nm, 97.5%) and n-SiO_2 (10 nm, 99.5%) as starting powders. The stoichiometry of carbon was decided on the basis of the previous study. The samples were heat treated at 850˚C for 2 hours.

4.3.2 Results and Discussion

Figure 4.5 shows powder XRD patterns of pure and doped samples. The peaks of MgB_2 are indexed with corresponding planes of reflection. The semi quantitative phase analysis of different phases was done using the relation, *Vol.% of phase X = Σ peak intensities of phase X/Σ peak intensities of all phases* and are tabulated in table 4.3. The main phase in all samples is MgB_2, along with traces of MgO. The sample added with nano-C and n-SiO_2 (MBCS), shows higher amount of MgO compared to other samples. This is because besides the entrapped air contained in the precursor filled tubes, n-SiO_2 also acts as an oxygen source. Except MgO, no peaks of any other impurities are observed for pure (MB) and n-C doped (MBC) samples. The sample added with n-SiC (MBS) shows a significant amount of Mg_2Si and minor quantities of unreacted SiC. The dissociation of SiC and reaction of Si with Mg to form Mg_2Si start even at temperatures as below as 600 °C [25, 26].The carbon atoms separated from SiC get substituted into MgB_2 lattice by replacing B atoms. Lower, but an observable amount of Mg_2Si is present in the sample co-doped with n-C and n-SiO_2

(MBCS). Here the formation of Mg_2Si is according to the chemical reaction 4 Mg + SiO_2 → Mg_2Si + 2 MgO. Since the at.% of Si is lower in dopant of MBCS than that in MBS; the vol.% of Mg_2Si is also lower in MBCS.

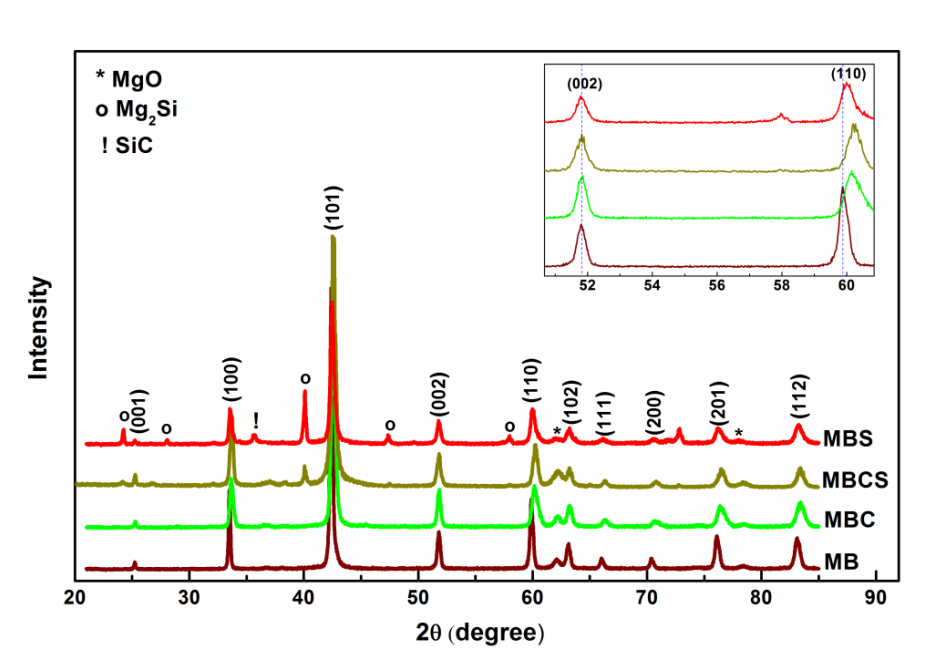

Figure 4.5: XRD patterns of pure, mono-doped and co-doped MgB_2 samples. The inset shows an expanded view of the (002) and (110) peaks of all samples

Table 4.3: Semi-quantitative phase analysis of different phases present in pure and doped samples

Sample	Initial composition	Vol.% of different Phases			
		MgB_2	MgO	Mg_2Si	SiC
MB	MgB_2	98.1	1.9	-	-
MBC	$MgB_{1.9}C_{0.1}$	96.2	3.8	-	-
MBS	MgB_2 +8.7 wt.% n-SiC	72.1	1.1	24.9	1.9
MBCS	$MgB_{1.9}C_{0.1}$ + 2.5 wt.% n-SiO_2	89.5	4.7	5.8	-

Inset of figure 4.5 shows an enlarged view of (002) and (110) peaks. The (110) peaks of all doped samples are shifted towards higher 2θ values, an indication of *a*-axis shrinkage, but (002) peaks do not show appreciable shift from that of pure sample. The lattice parameters '*a*' and '*c*' were calculated and results are tabulated in table 4.3. Among the doped samples, MBCS shows the lowest value of *a*-axis length and MBS the highest. Studies have already revealed that, when carbon atoms replace

boron atoms from MgB_2 lattice, having a hexagonal structure with B atoms forming a graphite like honeycomb network and Mg atoms occupying the pores of these hexagons, due to lower covalent radius of carbon, the in-plane lattice shrinks [27, 28]. All doped samples undergo carbon substitution, of which the sample co-doped with n-SiO_2 shows the best result. Though the sample MBC is also added with same amount of carbon, it shows less carbon substitution than that of MBCS. So it is inferred that the addition of nano-SiO_2 with n-C causes better carbon substitution in MgB_2.

Table 4.4: FWHM values of (100), (101), (002), and (110) peaks of samples

Sample	FWHM of selected peaks (degree)			
	100	101	002	110
MB	0.188	0.273	0.318	0.315
MBC	0.349	0.423	0.340	0.583
MBS	0.285	0.369	0.350	0.482
MBCS	0.308	0.405	0.381	0.503

Table 4.4 shows the FWHM values of (100), (101), (002) and (110) peaks of the XRD patterns of the pure and doped samples of MgB_2. The FWHM of (002) peaks of the doped samples does not show significant variation from that of the pure sample. The broadening of peaks from other (hk0) planes is evident from the table 4.3. Among the doped samples the n-C mono-doped sample (MBC) exhibits the highest peak broadening. The increase in FWHM values can be related to reduced levels of both crystallinity and grain size. Crystallinity is degraded upon carbon doping caused by substitution and inclusion of n-C. The addition of n-SiO_2 with n-C reduces FWHM of sample MBCS. The carbon substitution and dispersion of secondary phases make the n-SiC doped sample also to broaden its peaks, but the broadening is less when compared to other doped samples.

Figure 4.6 shows SEM images of fractured surfaces of the pure and doped samples. The undoped sample (MB) shows randomly oriented hexagonal MgB_2 grains with clear and noticeably sharper grain boundaries. The effect of doping in microstructure is noticeable in other samples. The grain size and crystallinity are

reduced in all doped samples in comparison with undoped sample. The sample doped with n-C (MBC) shows non-uniform sized grains with less clear and sharp boundaries. The sample MBS - the sample added with n-SiC - also shows non-uniformity in grain size but the grain boundaries are sharper and clear than that of MBC. The sample co-doped with n-C and n-SiO_2 (MBCS) shows improvement in crystallinity when compared to MBC. The average grain size is smaller and well packed. The reduced grain size leads to more concentration of grain boundaries in the system and this might have a reasonable role in $J_C(H)$ enhancement by grain boundary pinning.

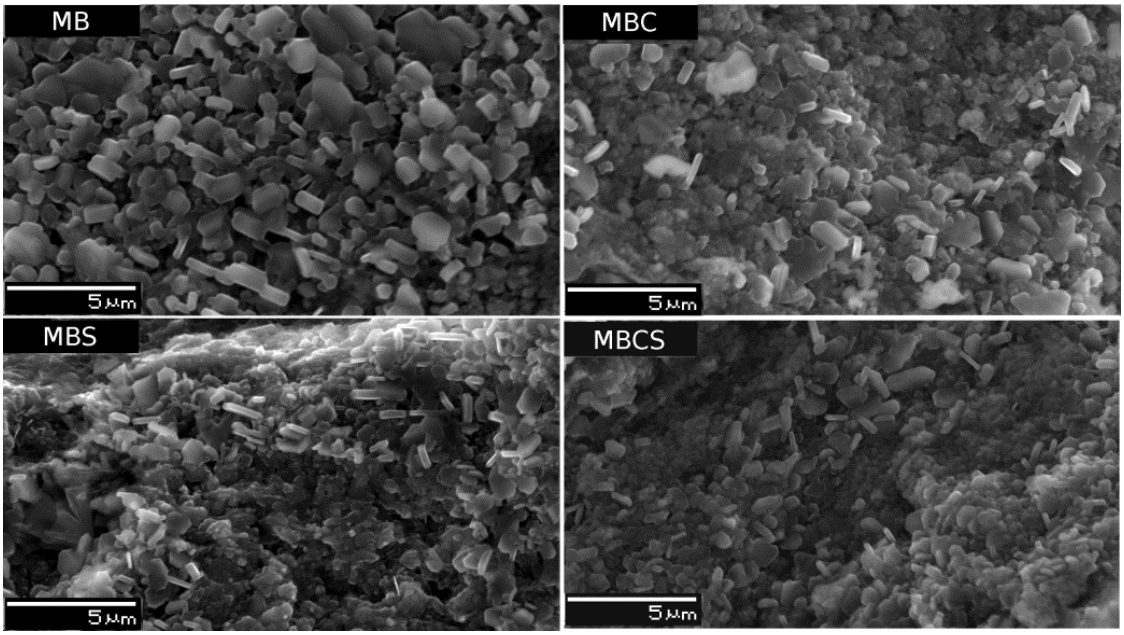

Figure 4.6: SEM images of the fractured surfaces of pure and doped samples

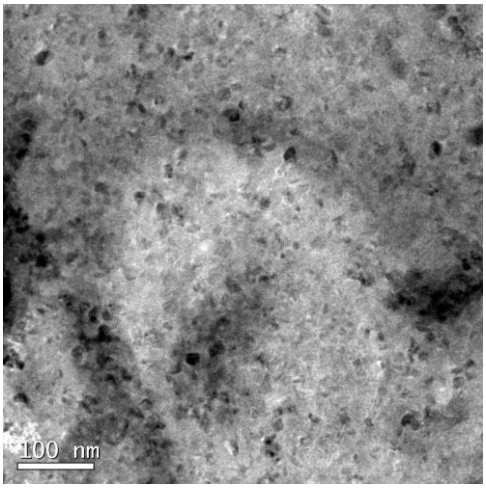

Figure 4.7: TEM image of the sample MBCS showing nano-sized inclusions within the MgB_2 grain

Figure 4.7 shows high resolution TEM image of a typical area within the grain of MBCS. Homogeneously dispersed nano-scale inclusions are clearly visible within the grain. The size of these intragranular inclusions (~ 10 nm) is found to be comparable with the coherence length (~ 5 nm) of MgB_2. Hence these can act as good flux pinners.

Table 4.5: Structural and superconducting properties of pure and doped samples

Sample	Lattice parameters (Å)		T_C Onset (K)	ΔT_C (K)	J_C at 8 T and 5 K ($\times 10^3$ A/cm^2)
	a-axis	*c*-axis			
MB	3.0878	3.5284	38.4	1.05	0.15
MBC	3.0749	3.5248	36.3	1.44	5.14
MBS	3.0764	3.5252	35.8	2.88	4.02
MBCS	3.0723	3.5261	35.4	1.36	9.02

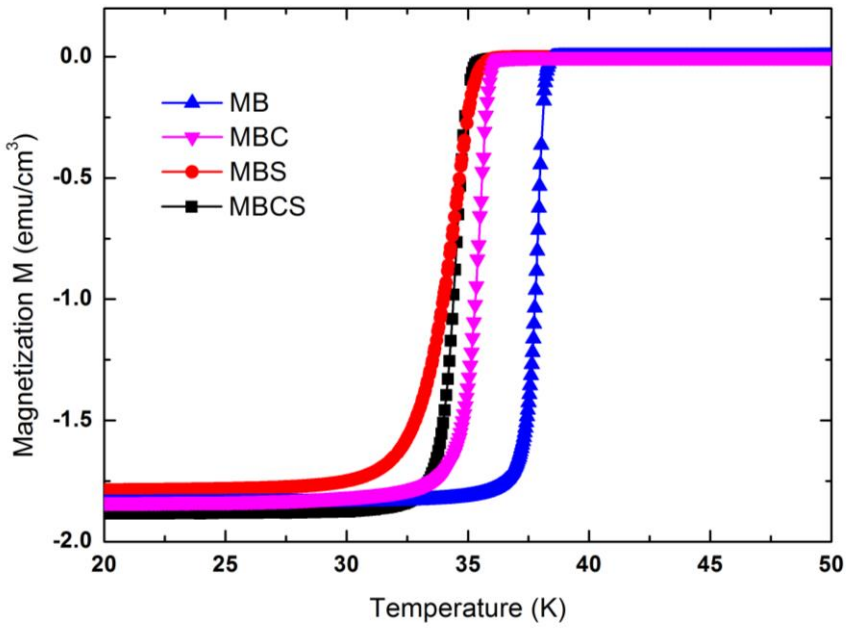

Figure 4.8: Zero field cooled magnetization versus temperature plots of the pure and doped samples measured at 20 Oe

Temperature dependence of zero-field cooled magnetization values for the pure and doped samples are measured in an external field of 20 Oe and are plotted in figure 4.8. T_C is defined as the onset temperature at which the samples start exhibiting diamagnetic properties and the observed values of T_C are tabulated in table 4.5. The

pure sample exhibits the highest T_C (38.4 K) and the lowest T_C is observed in sample MBCS, which is 3 K less than that of the pure sample. The decrease in T_C in doped samples can be related to the amount of carbon substituted and the lattice strains induced by nano-inclusions. The sharpness of the transition is a measure of crystallinity and homogeneity of samples and which is examined by calculating the transition width ΔT_C (defined as the difference in temperatures corresponding to 10% and 90% of the maximum shielding signal). The ΔT_C values of the samples are tabulated in table 4.5. The undoped sample has a ΔT_C of 1.05 K, which is found to be increased upon doping. The co-doped sample (MBCS) has the least ΔT_C (~ 1.36 K) among doped samples and the maximum transition width (~ 2.88 K) is observed in SiC added sample. This is due to the presence of relatively large amount of non-superconducting phases such as Mg_2Si and SiC, reduced crystallinity and inhomogeneity in carbon substitution. The lowest value of T_C onset for the sample MBCS indicates that, the level of carbon substitution is the highest in this sample. The measure of homogeneity is also superior for this sample as it can be inferred from the lowest ΔT_C of the sample.

Figure 4.9 shows magnetic field dependence of J_C ($J_C(H)$) of the pure and doped samples at 5 K deduced from magnetic hysteresis measurements. As severe flux jumps are observed in all samples at lower fields, estimation of J_C is not accurate in the region. The $J_C(H)$ of undoped sample falls rapidly as field increases, while all doped samples show significant enhancement in J_C values particularly at higher fields. Of all the doped samples, MBCS i.e. the sample co-doped with n-C and n-SiO_2 shows the highest J_C values throughout the entire range of fields studied. The J_C values of all samples at 8 T and 5 K are given in table 4.5. The J_C of MBCS (9.02×10^3 A/cm^2) is around 60 times greater than that of the pure sample. When we compare the $J_C(H)$ behavior of other two doped samples, the performance of nano-carbon doped sample (MBC) is marginally higher than the nano-SiC doped sample especially at fields higher than 4 T. Enhancement in J_C (H) of doped samples can be explained in terms of both carbon substitution and flux pinning caused by nano particle inclusions in MgB_2 grains and the grain boundary pinning as a result of reduced grain size by doping. For the sample MBC, enhancement of J_C is mainly due to effective substitution of carbon. For MBS, it is partly due to carbon substitution and partly due

to presence of reacted Mg_2Si as flux pinner. XRD analysis has revealed that, in the sample MBS, carbon substitution is not as effective as in MBC and large quantity of impurities are present in it. The addition of n-SiO_2 with n-C to MgB_2 helps to increase the level and homogeneity carbon substitution, as evident from reduced *a*-lattice length and diminished T_C onset and ΔT_C values. A larger J_C value at lower fields is also observed for this sample and this indicates that the grain to grain connectivity is also improved in the sample. The amount of reacted secondary phase is minimum for MBCS, but when the intragrain distribution of such secondary phases are homogeneous and size of these inclusions are in the range of coherence length of MgB_2, and hence these can serve as good flux pinners.

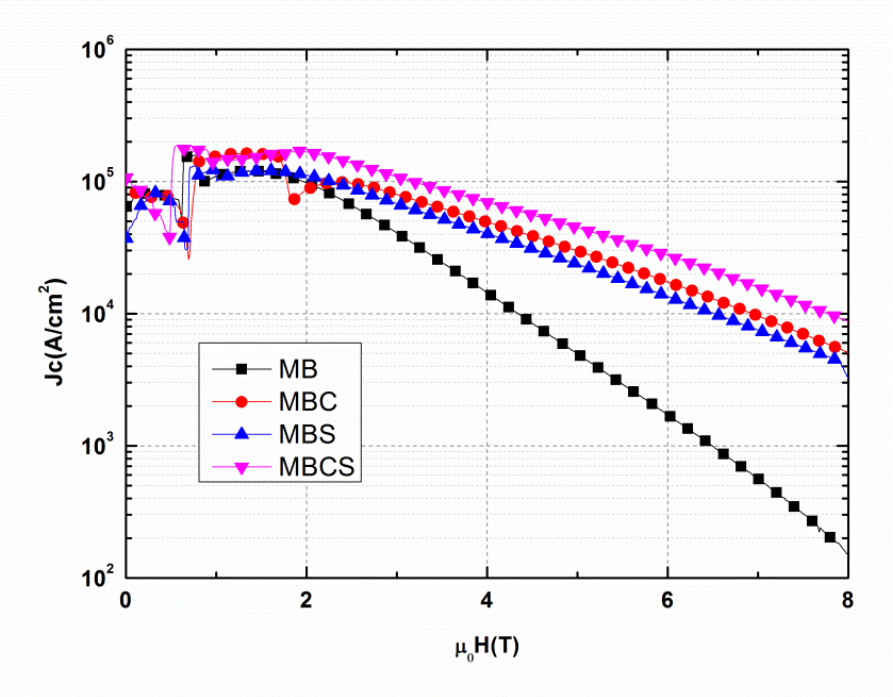

Figure 4.9: Magnetic field dependence of critical current density of pure and doped MgB_2 at 5 K

4.3.3 Conclusions

Co-doping effect of n-C and n-SiO_2 in MgB_2 was studied and the results were compared with pure and mono doped n-C and n-SiC samples. The study showed that the superconducting properties of the co-doped sample distinctly dominated the other samples throughout entire range of magnetic field studied. The shrinkage of *a*-lattice parameter and the reduced critical temperature of the doped samples implied that carbon is getting substituted at boron sites, which results in local strains in the MgB_2

lattice. As seen from XRD and TEM, the co-doped and SiC doped samples showed presence of reacted homogeneously dispersed secondary phase inclusions of Mg_2Si, which act as good flux pinners. Better carbon substitution, improved grain connectivity as observed from SEM and inferred from high J_C values at low fields and homogeneous distribution of flux pinners made the co-doped sample to perform better than the others throughout the entire field range.

4.4 Advantageous effects of nano-copper addition to infield critical current density of MgB_2

4.4.1 Introduction

Several work to improve $J_C(H)$ of MgB_2 has reported that nano-rare earth oxides (REOs) such as Y_2O_3 [29], Dy_2O_3 [30], Ho_2O_3 [31], Tb_4O_7 [32], Eu_2O_3 [33], Nd_2O_3 [34] and PrO_{11} [35] can be introduced into MgB_2 to enhance flux pinning ability. These REOs react with B to form their respective borides without any significant substitution at Mg/B sites. Among various REOs tried, Ho_2O_3 doped MgB_2 has shown the best flux pinning properties. Here the reacted phase (HoB_4) has a strong magnetic moment, and hence this will have stronger interaction with magnetic flux lines and can exert stronger force to trap flux lines in superconducting matrix.

Co-doping of two or more dopants with specific effects on MgB_2 is being employed for further enhancement of $J_C(H)$. Addition of rare earth oxides along with carbon in MgB_2 has been reported earlier [36]. In which E_2O_3 and P_6O_{11} are found to be cooperative with carbon in enhancing $J_C(H)$ at higher fields. But due to the inferior grain connectivity the $J_C(H)$ of these samples are lower than that of pure MgB_2 at low fields. Even carbon mono-doped samples exhibit such lower critical current density than the carbon-free sample at lower fields. Therefore increasing $J_C(H)$ at higher fields without compromising the low field $J_C(H)$ is necessary for doped MgB_2 samples. In this work we use a metallic nano powder, namely nano-copper (n-Cu) as a co-dopant with carbon mono-doped MgB_2 and carbon and nano-Ho_2O_3 co-doped MgB_2. It is found that the added n-Cu helps in accelerating the MgB_2 phase formation, crystallinity and grain connectivity and enhances the J_C both in the low and high field regions.

Pure and doped magnesium boride superconducting samples with starting compositions: MgB_2, $MgB_{1.9}C_{0.1}$, $MgB_{1.9}C_{0.1}$ + 2.5 wt.% n-Cu, $MgB_{1.9}C_{0.1}$ + 2.5 wt.% n-Ho_2O_3 and $MgB_{1.9}C_{0.1}$ + 2.5 wt.% n-Ho_2O_3 + 2.5 wt.% n-Cu were prepared by in situ Powder-In-Sealed-Tube (PIST) method, using Mg (< 105 μm, 99.8%), amorphous B (< 44 μm, 99%), nano-carbon (< 50 nm, 95%) nano-Ho_2O_3 (< 60 nm, 99.5%) and nano-copper (< 100 nm, 99.8%) as starting powders. The samples were sintered at 850˚C for 2 hour.

4.4.2 Results and Discussion

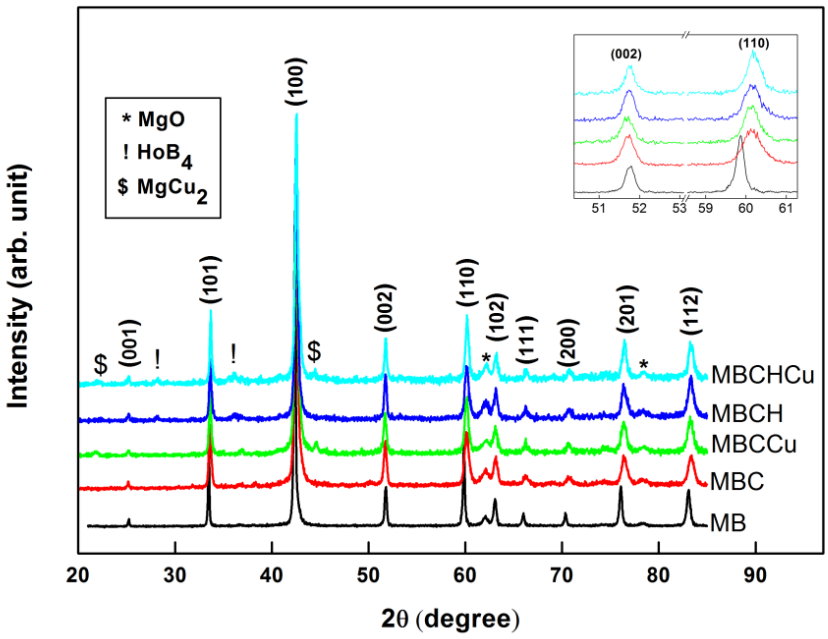

Figure 4.10: XRD patterns of pure and doped samples. The inset shows an expanded view of the (002) and (110) peaks of all samples.

Figure 4.10 shows powder XRD patterns of pure and doped MgB_2 samples. Peaks of MgB_2 phase are indexed with corresponding (hkl) values. All samples contain MgB_2 as major phase with minor quantities of secondary phases such as MgO, HoB_4 and $MgCu_2$, depending on the sample. The entrapped air in the powder filled tube is responsible for the presence of MgO in MB and MBC samples, but in addition to this, presence of oxygen in Ho_2O_3 makes the quantity of MgO little higher in MBCH and MBCHCu. Smaller quantities of HoB_4 are identified in samples added with Ho_2O_3 while $MgCu_2$ is detected in the samples added with Cu. The semi quantitative phase analysis of different phases is done and tabulated in table 4.6.

Table 4.6: Semi-quantitative phase analysis of different phases present in pure and doped samples

Sample	Initial composition	Vol.% of different Phases			
		MgB_2	MgO	HoB_4	$MgCu_2$
MB	MgB_2	98.4	1.6	0	-
MBC	$MgB_{1.9}C_{0.1}$	97.2	2.8	0	-
MBCCu	$MgB_{1.9}C_{0.1}$ + 2.5 wt.% n-Cu	95.0	2.7	-	2.2
MBCH	$MgB_{1.9}C_{0.1}$ + 2.5 wt.% n-Ho_2O_3	94.9	3.7	1.4	-
MCHCu	$MgB_{1.9}C_{0.1}$ + 2.5 wt.% n-Ho_2O_3 + 2.5 wt.% n-Cu	93.9	2.9	1.6	1.4

The Inset of the figure 4.10 shows enlarged view of (002) and (110) peaks. A systematic shift for (110) peaks towards higher angle is observed in doped samples. This arises due to the decrease in *a*-lattice parameter as the result of carbon substitution. But the position of (002) peaks for doped samples doesn't vary considerably, since carbon doping has less effect on *c*-lattice parameter. The variation of the lattice parameter length with respect to the different dopants as seen in table 4.7 makes it clear that minor amount of n-Cu doping is not a hindrance to carbon substitution but promotes it too.

Table 4.7: Structural and superconducting properties of pure and doped samples

Sample	Lattice parameters (Å)		T_C Onset (K)	ΔT_C (K)	J_C at 8 T and 5 K ($\times 10^3$ A/cm^2)
	a-axis	*c*-axis			
MB	3.0873	3.5284	38.4	1.05	0.15
MBC	3.0749	3.5310	36.2	1.44	5.10
MBCCu	3.0740	3.5304	35.7	1.25	6.40
MBCH	3.0734	3.5305	35.3	1.85	4.52
MBCHCu	3.0719	3.5300	35.2	1.11	9.37

The FWHM values of selected XRD peaks of the pure and doped samples are calculated and plotted in figure 4.11. All peaks of the doped samples except that from (002) planes show considerable broadening with respect to that of the pure sample. The peak broadening can occur due to reduced grain size, crystallinity, and increased lattice strain. The carbon substitution at boron sites and distribution of nano-sized secondary phases in the grains are responsible for this. But it is to be noted that, the addition of n-Cu to the n-C mono-doped sample and n-C + n-Ho_2O_3 co-doped sample

leads to a noticeable decrease in FWHM. This is due to the improvement in crystallinity as the result of accelerated phase formation with the addition of n-Cu.

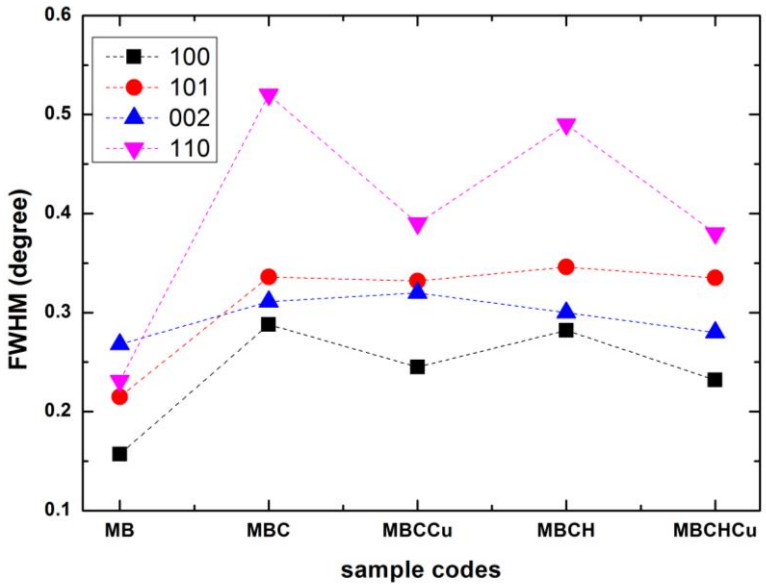

Figure 4.11: FWHM values of (100), (101), (002), and (110) peaks of samples

The SEM images of fractured surfaces of the pure and doped samples are shown in figure 4.12(a) – 4.12(e). The pure sample consists of hexagonal grains with clear grain boundaries, and the average grain size is around 1 μm. It is seen that doping decreases the crystallinity of samples. Hexagonal grains with inhomogeneous size distribution are observed in n-C doped sample. The sample co-doped with n-C and n-Ho_2O_3 shows randomly oriented grains with different size and unclear boundaries. But the distinctive effect of n-Cu addition is observable from SEM. It is observed that the co-addition of n-Cu increases the crystallinity and packing. The sample MBCCu shows tightly packed hexagonal grains with well-defined boundaries but average size is less than that of pure sample. A similar characteristic is observed in sample MBCHCu too. This sample shows tightly packed hexagonal grains with well-defined boundaries but average size is very much less than that of pure sample.

Figure 4.12(f) shows a high resolution TEM image of a typical grain of the sample MBCHCu. The nano-sized impurities distributed within the grains are clearly visible. Since the size of these nano inclusions (< 10 nm) is in range of the coherence length of MgB_2, these can act as strong flux pinners to improve in-field critical current density.

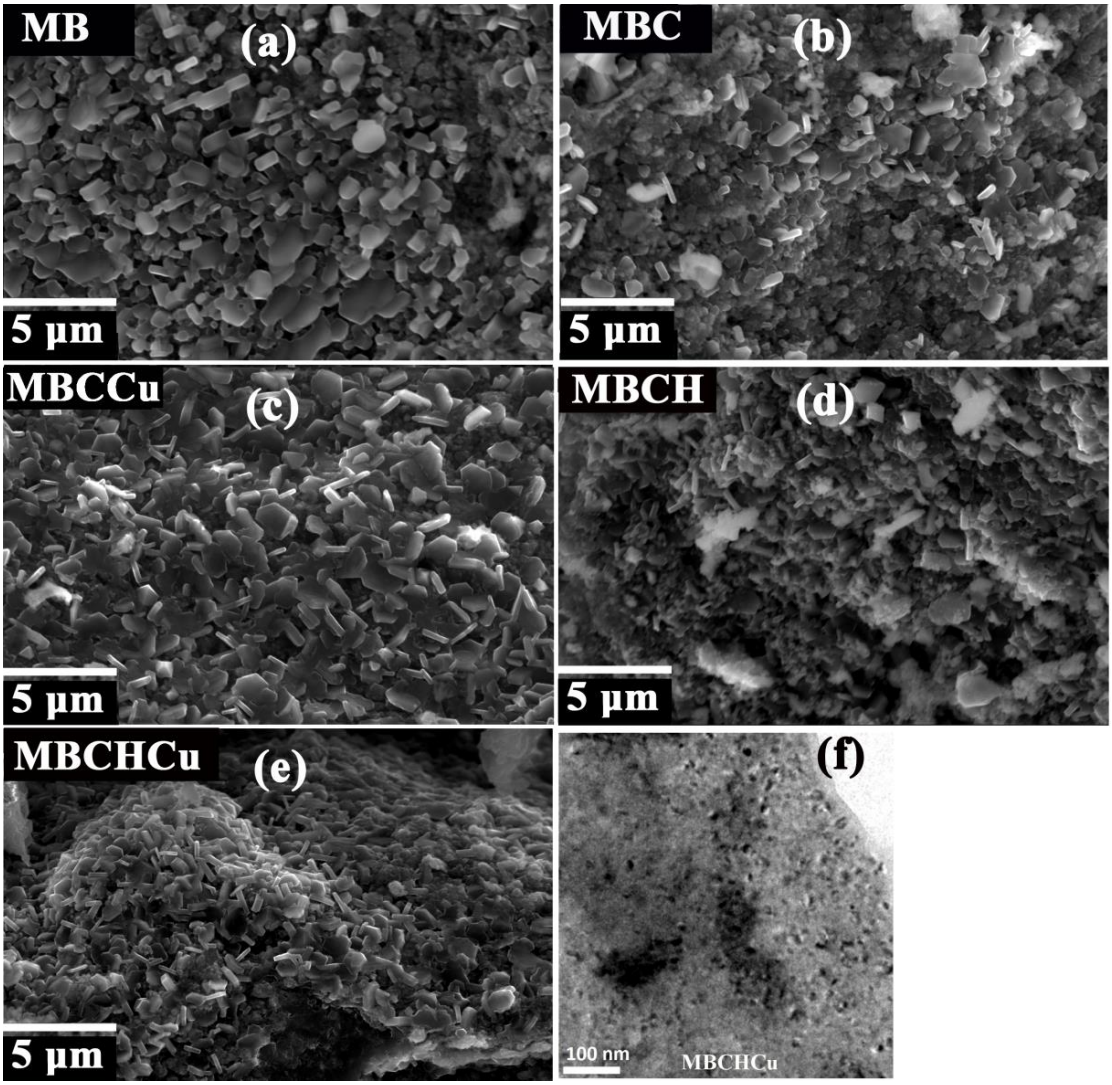

Figure 4.12 (a) – 4.12(e): SEM images of the fractured surfaces of pure and doped samples. 4.12 (f): TEM image of a typical grain of the sample MBCHCu

The variation of zero field cooled (ZFC) magnetization of the samples with temperature is measured at 20 Oe and the results are plotted in figure 4.13. The T_C and the width of transition (ΔT_C, defined as the difference in temperatures corresponding to 10% and 90% of the maximum shielding signal) are tabulated in table 4.8. The undoped sample shows the highest T_C of 38.4 K. Due to the carbon substitution and lattice strain caused by nano-sized inclusions, all doped samples exhibit lower T_C. As it is evident from XRD analysis (figure 4.10), the sample MBCHCu with the lowest *a* axis length shows the lowest T_C. The ΔT_C is the minimum for the undoped sample. The higher values of ΔT_C are observed in samples MBCH and MBC due to inhomogeneities in carbon substitution in these samples. The effect of n-Cu doping in increasing the chemical homogeneity of the samples can be easily inferred from the

lower values of ΔT_C of the samples MBCCu and MBCHCu from that of MBC and MBCH.

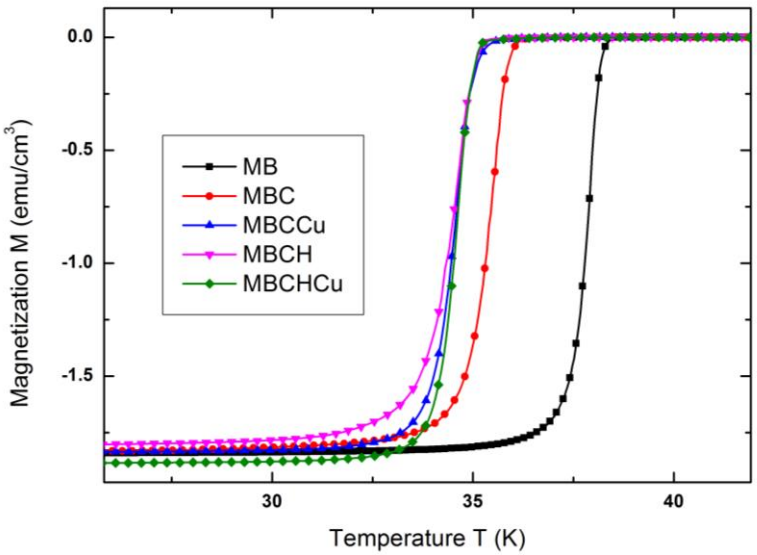

Figure 4.13: Zero field cooled M-T plots of the pure and doped samples measured at 20 Oe.

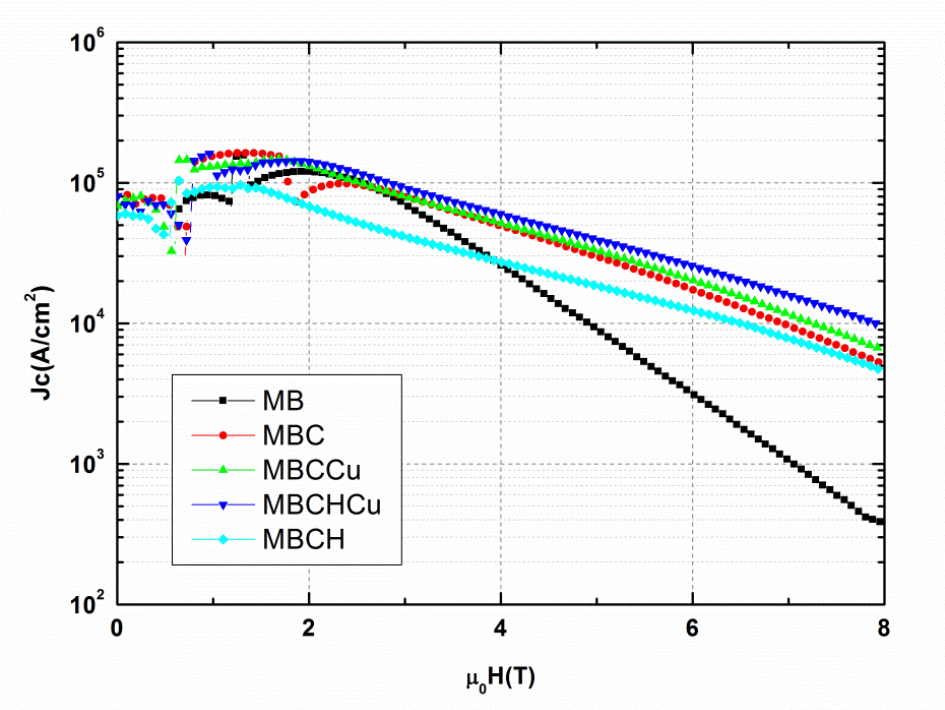

Figure 4.14: $J_C(H)$ curves of pure and doped MgB_2 samples at 5 K

Figure 4.14 shows the magnetic field dependence of the critical current density ($J_C(H)$) from 0 to 8 T at 5 K deduced from magnetic hysteresis (M-H) measurements. At lower fields the estimation of $J_C(H)$ is not accurate due to flux jumps. The rate of

deterioration in J_C of undoped sample with increase in applied field is very high when compared to the doped samples while the carbon doped samples and other co-doped samples show less degradation in J_C with the increase in magnetic field. The sample doped with n-C shows significant enhancement of $J_C(H)$ at all fields without any unbearable reduction in lower magnetic fields. But the sample MBCH has poor J_C values at lower magnetic fields which is lower than that of the pure sample up to about 4 T. This result implies that the co-doping of n-C and n-Ho_2O_3 in MgB_2 is not co-operative at lower range of fields as they affect adversely on grain connectivity and hence reduces effective cross sectional area for supercurrents. Deterioration of J_C at lower fields in samples co-doped with rare earth oxides and carbon has been reported earlier [36].

The advantage of n-Cu doping is explicit from the $J_C(H)$ curves. The J_C of n-Cu doped samples overtakes its n-Cu deficit variants. For the sample MBCCu the J_C improvement becomes noticeable at higher fields and though the improvement is not so high, it tends to be significant at higher fields. The negative effects caused by co-doping of n-C and n-Ho_2O_3 in the sample MBCH is rectified by the co-doping with n-Cu. At 2 T the sample MBCHCu exhibits about 2 times J_C than that of MBCH and maintain this 2 fold increment even up to 8 T, the highest field used. So that, although the value of $J_C(H)$ is lower for the sample MBCH, rate of degradation of the J_C with the magnetic field is comparable with the n-Cu added sample MBCHCu. This means that, the sample MBCH also has good flux pinning ability which prevents the sudden drop of its J_C with increase in field; but the absolute value of J_C in this sample is limited by poor grain connectivity caused by co-doping and which is apparent from the value of J_C at field 0 T itself. For a better understanding of the flux pinning ability of the samples, the normalized flux pinning force $F_P(H)/F_P^{max}$, where $F_P(H) = J_C \times \mu_0 H(T)$, of the samples are plotted against applied magnetic field in figure 4.15. The curve depicts the flux pinning ability of all samples with external field. As expected, beyond 3 T, the undoped sample is not able to effectively pin flux lines in place. The addition of n-Cu with n-C increases the flux pinning ability due to increased carbon substitution. The samples MBCH and MBCHCu shows similar flux pinning abilities even though they differ in their J_C values. Since the nano-carbon is a common dopant in all doped samples, the effects of carbon substitution – the creation of lattice defects

and the increment of H_{C2} by increased scattering in pi-band – are common for the doped samples.

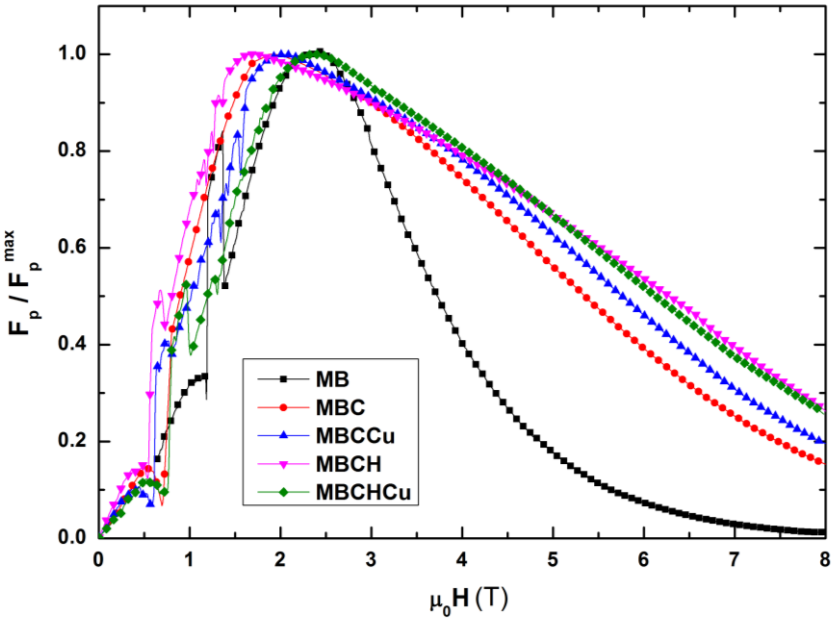

Figure 4.15: $F_P(H)/F_P^{max}$ versus applied field at 5 K of pure and doped MgB_2 samples.

From XRD analysis (figure 4.11) it is clear that, for the samples MBC and MBCH the FWHM of the (110) peaks are highly broadened and hence the crystallinity is also lesser for these two samples when compared to the other samples. This can leads to increased grain boundary pinning and hence higher H_{irr} [37]. Other than the carbon substitution and grain boundary pinning effect, the intragrain dispersion of nano-sized secondary phase HoB_4 which can act as a good flux pinner also contributes towards the flux pinning and prevents of sudden degradation of J_C at higher fields. Distinct effects of the n-Cu doping can be observed by comparing the n-Cu doped sample with their n-Cu deficit variants. The n-Cu addition causes enhanced carbon substitution as observed from the reduced *a*-lattice parameter and drop in T_C onset. The addition of n-Cu increases the crystallinity, grain connectivity and the homogeneity of the sample which can be observed from the FWHM, SEM and ΔT_C of these samples. Apart from these effects, the n-Cu addition causes distribution of nano-sized $MgCu_2$ particles in MgB_2 grains which contributes towards the point pinning of the flux lines. Hence, the carbon substitution, improved connectivity and intragrain distribution of secondary phases like HoB_4 and $MgCu_2$ which effectively trap flux lines, make the sample MBCHCu to perform the best among all samples throughout

the entire range of fields. At 8 T and 5 K a J_C of 9.5×10^3 A/cm^2, which is 65 times the J_C of the undoped sample, is obtained in MBCHCu.

4.4.3 Conclusions

The scope of further improvement of $J_C(H)$ of doped MgB_2 superconductor by using nano-copper as a co-dopant was investigated systematically. The co-doped samples showed larger *a*-lattice shrinkage than the carbon mono-doped sample. The sample co-doped with carbon and Ho_2O_3 showed deterioration in crystallinity as evident from XRD and SEM, and its J_C becomes closer to that of carbon doped sample as the applied field increases. . The J_C of n-Cu doped samples exhibited better $J_C(H)$ values than corresponding their n-Cu deficit samples. For the sample MBCCu the J_C improvement became noticeable at higher fields. The sample co-doped with n-C, n-Ho_2O_3 and n-Cu showed the best J_C performance in the entire field range studied. The variation in *a*-lattice parameter showed that carbon has been more effectively substituted in this sample. The depression in T_C also confirmed this. The FWHM and SEM results and the reduced transition width indicated that the sample MBCHCu has greatly improved its homogeneity, crystallinity and grain connectivity. A J_C, 65 times higher than that of the pure sample and about 2 times that of other doped samples was obtained for this sample at 8 T. The carbon substitution at boron site and intragrain distribution of nano-sized particles like HoB_4 and $MgCu_2$ with good flux pinning ability are responsible for this enhancement.

4.5 Summary

The enhancement of $J_C(H)$ by chemical doping was studied. The carbon was found to be suitable dopant to increase the $J_C(H)$ by its substitutional effects. Among the two different carbon sources-n-D and n-C-tried, n-C was found to be the best. To further enhance the $J_C(H)$ of MgB_2 co-doping the MgB_2 with 2 or more dopants was adopted. Instead of doping MgB_2 with nano-SiC, the co-doping with n-C and n-SiO_2 was found to be more effective. In this co-doping, apart from carbon substitution, intragrain distribution of Mg_2Si also helped to enhance the $J_C(H)$ by pinning the flux lines. In another co-doping study, nano-sized Cu and Ho_2O_3 were used as dopants. The presence of n-Cu as a co-dopant showed better carbon substitution and grain connectivity in doped samples. With its ability to distribute nano-sized HoB_4 in the

MgB_2 grain, n-Ho_2O_3 was also found to be an effective dopant. The best results of chemical doping study are compiled in figure 4.16.

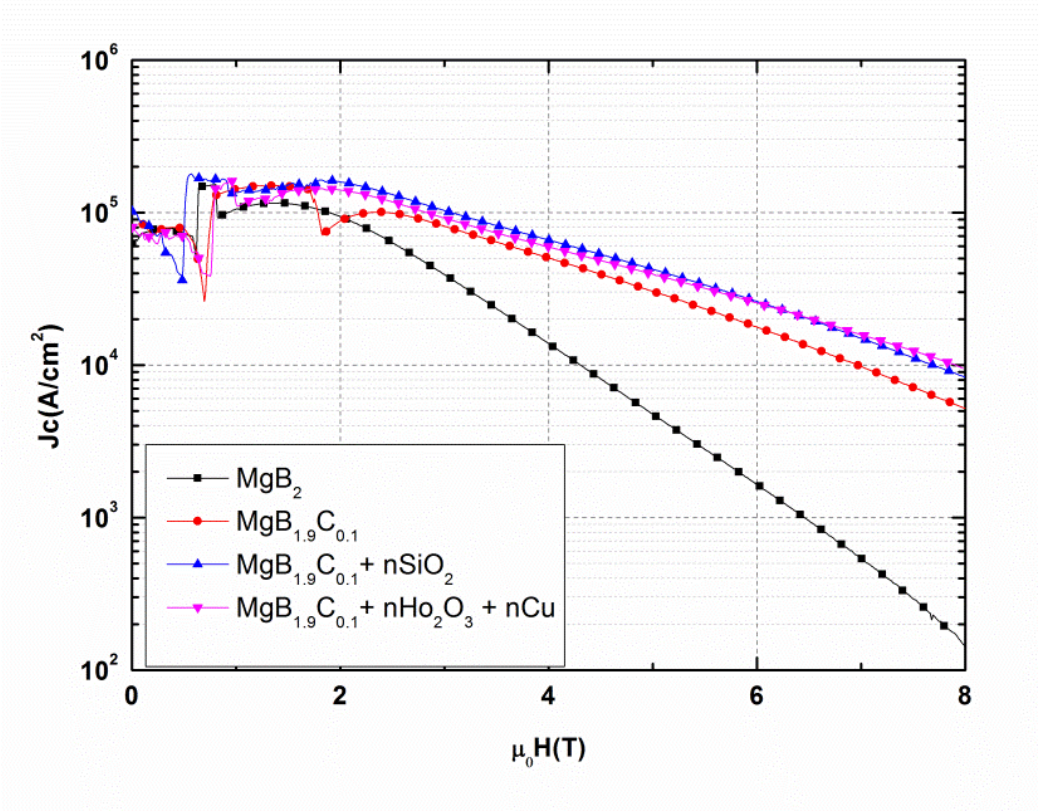

Figure 4.16: Summary of chemical addition study to enhance $J_C(H)$ of MgB_2 bulk superconductor

REFERENCES

[1] C. Buzea and T. Yamashita, "Review of the superconducting properties of MgB_2," *Superconductor Science & Technology,* vol. 14, pp. R115-R146, Nov 2001.

[2] D. Larbalestier, A. Gurevich, D. M. Feldmann, and A. Polyanskii, "High-T-c superconducting materials for electric power applications," *Nature,* vol. 414, pp. 368-377, Nov 15 2001.

[3] K. Vinod, R. G. A. Kumar, and U. Syamaprasad, "Prospects for MgB_2 superconductors for magnet application," *Superconductor Science & Technology,* vol. 20, pp. R1-R13, Jan 2007.

[4] A. Gurevich, S. Patnaik, V. Braccini, K. H. Kim, C. Mielke, X. Song, *et al.*, "Very high upper critical fields in MgB_2 produced by selective tuning of impurity scattering," *Superconductor Science & Technology,* vol. 17, pp. 278-286, Feb 2004.

[5] S. C. Yan, G. Yan, L. Zhou, Y. Jia, H. H. Wen, and Y. F. Lu, "Enhancement of the upper critical field in sub-micron carbon-doped MgB_2 by two-step reaction method," *Superconductor Science & Technology,* vol. 20, pp. 377-380, Apr 2007.

[6] W. K. Yeoh, J. H. Kim, J. Horvat, X. Xu, and S. X. Dou, "Enhancement of critical current density and irreversibility field by nano-carbon substitution in MgB_2," *Physica C-Superconductivity and Its Applications,* vol. 460, pp. 568-569, Sep 1 2007.

[7] J. L. Wang, R. Zeng, J. H. Kim, L. Lu, and S. X. Dou, "Effects of C substitution on the pinning mechanism of MgB_2," *Physical Review B,* vol. 77, May 2008.

[8] W. K. Yeoh, J. Horvat, J. H. Kim, X. Xu, and S. X. Dou, "Effect of carbon substitution on the superconducting properties of MgB_2 doped with multi-walled carbon nanotubes and nano carbon," *IEEE Transactions on Applied Superconductivity,* vol. 17, pp. 2929-2932, Jun 2007.

[9] S. X. Dou, W. K. Yeoh, J. Horvat, and M. Ionescu, "Effect of carbon nanotube doping on critical current density of MgB_2 superconductor," *Applied Physics Letters,* vol. 83, pp. 4996-4998, Dec 15 2003.

[10] A. Serquis, G. Serrano, S. M. Moreno, L. Civale, B. Maiorov, F. Balakirev, *et al.*, "Correlated enhancement of H_{C2} and J(c) in carbon nanotube doped MgB_2," *Superconductor Science & Technology*, vol. 20, pp. L12-L15, Apr 2007.

[11] A. Yamamoto, J. I. Shimoyama, S. Ueda, Y. Katsura, S. Horii, and K. Kishio, "Doping effects on critical current properties of MgB_2 bulks synthesized by modified powder-in-tube method," *IEEE Transactions on Applied Superconductivity*, vol. 15, pp. 3292-3295, Jun 2005.

[12] S. X. Dou, S. Soltanian, J. Horvat, X. L. Wang, S. H. Zhou, M. Ionescu, *et al.*, "Enhancement of the critical current density and flux pinning of MgB_2 superconductor by nanoparticle SiC doping," *Applied Physics Letters*, vol. 81, pp. 3419-3421, Oct 28 2002.

[13] S. Soltanian, X. L. Wang, J. Horvat, S. X. Dou, M. D. Sumption, M. Bhatia, *et al.*, "High transport critical current density and large H_{C2} and H_{irr} in nanoscale SiC doped MgB_2 wires sintered at low temperature," *Superconductor Science & Technology*, vol. 18, pp. 658-666, May 2005.

[14] A. Yamamoto, J. Shimoyama, S. Ueda, I. Iwayama, S. Horii, and K. Kishio, "Effects of B_4C doping on critical current properties of MgB_2 superconductor," *Superconductor Science & Technology*, vol. 18, pp. 1323-1328, Oct 2005.

[15] N. Varghese, K. Vinod, Shipra, A. Sundaresan, and U. Syamaprasad, "Burned Rice Husk: An Effective Additive for Enhancing the Electromagnetic Properties of MgB_2 Superconductor," *Journal of the American Ceramic Society*, vol. 93, pp. 732-736, Mar 2010.

[16] X. Xu, S. X. Dou, X. L. Wang, J. H. Kim, J. A. Stride, M. Choucair, *et al.*, "Graphene doping to enhance the flux pinning and supercurrent carrying ability of a magnesium diboride superconductor," *Superconductor Science & Technology*, vol. 23, Aug 2010.

[17] W. K. Yeoh, X. Y. Cui, B. Gault, K. S. B. De Silva, X. Xu, H. W. Liu, *et al.*, "On the roles of graphene oxide doping for enhanced supercurrent in MgB_2 based superconductors," *Nanoscale*, vol. 6, pp. 6166-6172, Jun 7 2014.

[18] K. S. B. De Silva, S. Gambhir, X. L. Wang, X. Xu, W. X. Li, D. L. Officer, *et al.*, "The effect of reduced graphene oxide addition on the superconductivity

of MgB_2," *Journal of Materials Chemistry,* vol. 22, pp. 13941-13946, 2012 2012.

[19] J. H. Kim, S. Zhou, M. S. A. Hossain, A. V. Pan, and S. X. Dou, "Carbohydrate doping to enhance electromagnetic properties of MgB2 superconductors," *Applied Physics Letters,* vol. 89, Oct 2 2006.

[20] J. H. Kim, X. Xu, M. S. A. Hossain, D. Q. Shi, Y. Zhao, X. L. Wang, *et al.*, "Influence of disorder on the in-field J_C of MgB_2 wires using highly active pyrene," *Applied Physics Letters,* vol. 92, Jan 28 2008.

[21] C. H. Jiang, S. X. Dou, Z. X. Cheng, and X. L. Wang, "Light carbon doping by oxygen-free paraffin wax to enhance the current density of MgB_2 in the entire field regime," *Superconductor Science & Technology,* vol. 21, Jun 2008.

[22] H. Agil, O. Cicek, E. Ertekin, A. Motaman, M. S. A. Hossain, S. X. Dou, *et al.*, "Effects of MgO on the Electronic and Superconducting Properties in Succinic Acid ($C_4H_6O_4$) Doped MgB_2 Bulks," *Journal of Superconductivity and Novel Magnetism,* vol. 26, pp. 1525-1529, May 2013.

[23] A. Motaman, M. S. A. Hossain, X. Xu, K. W. See, K. C. Chung, and S. X. Dou, "A comprehensive study of the pinning mechanisms of MgB_2 wires treated with malic acid and their relationships with lattice defects," *Superconductor Science & Technology,* vol. 26, Aug 2013.

[24] Z. Ma, Y. Liu, Q. Zhao, Z. Dong, and L. Yu, "Mechanism analysis for the enhanced electromagnetic properties in nano-SiC-doped MgB2 based on the discussion of the sintering process," *Superconductor Science & Technology,* vol. 22, Aug 2009.

[25] S. X. Dou, O. Shcherbakova, W. K. Yoeh, J. H. Kim, S. Soltanian, X. L. Wang, *et al.*, "Mechanism of enhancement in electromagnetic properties of MgB_2 by nano SiC doping," *Physical Review Letters,* vol. 98, Mar 2 2007.

[26] A. Yamamoto, J.-i. Shimoyama, S. Ueda, S. Horii, and K. Kishio, "Reactivity of carbides in synthesis of MgB_2 bulks," *Physica C-Superconductivity and Its Applications,* vol. 445, pp. 801-805, Oct 1 2006.

[27] S. M. Kazakov, R. Puzniak, K. Rogacki, A. V. Mironov, N. D. Zhigadlo, J. Jun, *et al.*, "Carbon substitution in MgB_2 single crystals: Structural and superconducting properties," *Physical Review B,* vol. 71, Jan 2005.

[28] Z. H. Cheng, B. G. Shen, J. Zhang, S. Y. Zhang, T. Y. Zhao, and H. W. Zhao, "Superconductivity of $Mg(B_{1-x}C_x)_2$ ternary compounds," *Journal of Applied Physics,* vol. 91, pp. 7125-7127, May 15 2002.

[29] J. Wang, Y. Bugoslavsky, A. Berenov, L. Cowey, A. D. Caplin, L. F. Cohen, *et al.*, "High critical current density and improved irreversibility field in bulk MgB_2 made by a scaleable, nanoparticle addition route," *Applied Physics Letters,* vol. 81, pp. 2026-2028, Sep 9 2002.

[30] S. K. Chen, M. Wei, and J. L. MacManus-Driscoll, "Strong pinning enhancement in MgB_2 using very small Dy_2O_3 additions," *Applied Physics Letters,* vol. 88, May 8 2006.

[31] C. Cheng and Y. Zhao, "Enhancement of critical current density of MgB_2 by doping Ho_2O_3," *Applied Physics Letters,* vol. 89, Dec 18 2006.

[32] K. Vinod, N. Varghese, U. Syamaprasad, Shipra, and A. Sundaresan, "Structural and superconducting properties of bulk MgB_2 with added nano Tb_4O_7," *Superconductor Science & Technology,* vol. 21, Feb 2008.

[33] N. Ojha, G. D. Varma, H. K. Singh, and V. P. S. Awana, "Effect of rare-earth doping on the superconducting properties of MgB_2," *Journal of Applied Physics,* vol. 105, Apr 1 2009.

[34] C. Yao, X. Zhang, D. Wang, Z. Gao, L. Wang, Y. Qi, *et al.*, "Doping effects of Nd_2O_3 on the superconducting properties of powder-in-tube MgB_2 tapes," *Superconductor Science & Technology,* vol. 24, May 2011.

[35] X. F. Pan, T. M. Shen, G. Li, C. H. Cheng, and Y. Zhao, "Doping effect of Pr6O11 on superconductivity and flux pinning of MgB2 bulk," *Physica Status Solidi a-Applications and Materials Science,* vol. 204, pp. 1555-1560, May 2007.

[36] N. Ojha, V. K. Malik, R. Singla, C. Bernhard, and G. D. Varma, "The effect of carbon and rare earth oxide co-doping on the structural and superconducting properties of MgB_2," *Superconductor Science & Technology,* vol. 23, Apr 2010.

[37] A. Yamamoto, J. Shimoyama, S. Ueda, Y. Katsura, I. Iwayama, S. Horii, *et al.*, "Universal relationship between crystallinity and irreversibility field of MgB_2," *Applied Physics Letters,* vol. 86, May 23 2005.

Chapter 5

Preparation and Characterization of MgB_2 Superconducting Wires with Improved $J_C(H)$

5.1 Introduction

Since the discovery of superconductivity in MgB_2, worldwide efforts have been going on to make use of it for practical applications. For most of the practical applications the superconductor is to be made into long length wires. The possibility of operability at 20 - 30 K temperatures with cryogen free cryocoolers makes MgB_2 superconducting wires highly competitive with NbTi and Nb_3Sn superconductors [1], which are normally operated at 4.2 K in liquid helium. The low anisotropy and lower material cost make it an inexpensive alternative to HTS tapes, and thus adaptable and economically viable for superconducting devices like magnets, generators, motors, transformers and current leads at temperatures above 20 K.

Since MgB_2 is brittle, it cannot be easily drawn into wires. But the flow of supercurrent in MgB_2 is not prohibited by grain boundaries significantly due to the relatively large coherence length and this property lead to the quick development of MgB_2 wires and tapes by a number of research groups [2-10]. Although a number of methods have been tried for the fabrication of MgB_2 conductors, the most successful and easier one is the Powder In Tube (PIT) method. Both *ex situ* PIT [3-6] and *in situ* PIT [7-10] methods have been tried for the conductor fabrication. The lower reaction temperature, easiness for doping and high grain to grain coupling are the main advantages of *in situ* process, while less porosity and ability to control the phase purity are the main advantages of the *ex situ* process.

The selection of sheath material and reaction temperature has significant effect on the superconducting properties of wires made by PIT techniques. In addition to the

high J_C values, the conductor should have good thermal stability. Therefore when fabricate multifilamentary conductors; stabilizing materials also should be incorporated to the matrix to prohibit the burnout of the conductor when a quench occurs and for better heat transfer.

This chapter mainly deals with preparation and characterization of MgB_2 superconducting wires with improved transport $J_C(H)$. The work includes identification of suitable sheath material, optimization of processing temperature, comparative study of the *in situ* and *ex situ* processes in terms of self-field transport critical current density and development of multifilamentary wires with the incorporation copper stabilizer. Later, efforts are made to to enhance the $J_C(H)$ of superconducting wires through chemical doping by translating the results of the studies on bulk MgB_2 as described in chapter 4.

5.2 Method of MgB_2 monofilamentary wire preparation

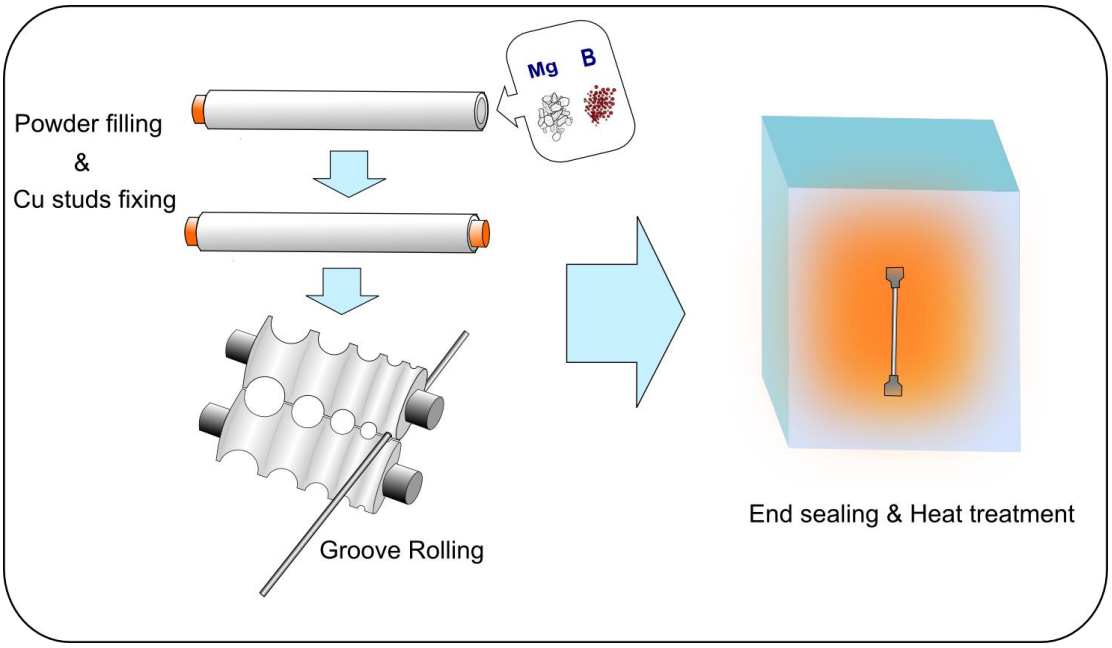

Figure 5.1: Schematic diagram of preparation of monofilamentary MgB_2 wires

The sheath metal in the form of tube with OD/ID: 6/4 mm was cut into pieces of desired length, typically 6 to 10 cm. The one end of the tube is tightly closed with a copper stud. Stoichiometrically weighed and homogeneously mixed Mg and B powders were filled in the tube and tightly packed mechanically. After the powder filling, the other end was also closed using copper stud. The tube was then subjected

to groove rolling, and reduced the diameter to 2.1 mm / 1.8 mm / 1.6 mm / 1.4 mm according to the requirement. The groove rolled wire was then cut for sufficient length and ends were sealed by a capping technique; in which the ends of the wire were inserted into Fe tube of suitable diameter and of length about 1 cm length. The tube is then pressed using a hydraulic press such that the ends of the wire was pressed inside the tube and perfectly sealed from the outside atmosphere. The wire was then heat treated directly in the air i.e. without any vacuum or inert atmosphere, inside a programmable muffle furnace at temperatures as required with a ramp rate of 5 °C / min. The sample was then furnace cooled. After cleaning the thin surface oxidation layer, the sample was subjected to various characterizations.

5.3 Selection of sheath material and reaction temperature

5.3.1 Introduction

Various efforts have been made to make MgB_2 superconducting wires to use it for practical applications by adopting PIT method of wire making. To make the superconducting wire of a brittle superconductor, an appropriate sheath material is to be selected. The sheath material should be chemically non-reactive to Mg and B powder. It should have good mechanical strength to support brittle MgB_2 core formed inside. The sheath material should not be permeable to gases like oxygen as we have opted to do heat treatment directly in the air. Apart from these, the electrical and thermal conductivities of sheath also have key roles in the stable operation of the superconductor device especially when operated with cryogen free cryocoolers. Various attempts have been reported for fabrication of MgB_2 wires with various sheath materials like Fe, Ni, Cu, Ag, SS, Nb, and Ta [11-17], which include *in situ* and *ex situ* methods.

Other than the sheath material, the properties of MgB_2 such as phase purity, density, microstructure, and critical current density are highly dependent on the formation temperature. Various groups have reported that for *in situ* method of wire making, heat treatment in the temperature range 650 - 800 °C is appropriate [18-20]. Even though for the preparation of bulk MgB_2 800 – 850 °C is found to be necessary, the same temperature cannot be applied to wire preparation since the processing environment is different and the reactivity of sheath material also should be considered.

Therefore, in order to select appropriate sheath material and reaction temperature for the preparation of pure MgB_2 superconducting wires, four commonly available and relatively inexpensive metals namely, Fe, Cu, SS, and Ni were chosen and prepared monofilamentary wires. The wires were heat treated at temperatures 625, 650, 675 and 700 °C for 2 hours. The core formed inside the sheath was recovered by peeling off the sheath and phase analysis was done by using XRD. The R-T and I-V measurements were done by four probe method by using a cryostat interfaced with a heavy duty cryocooler.

5.3.2 Results and discussion

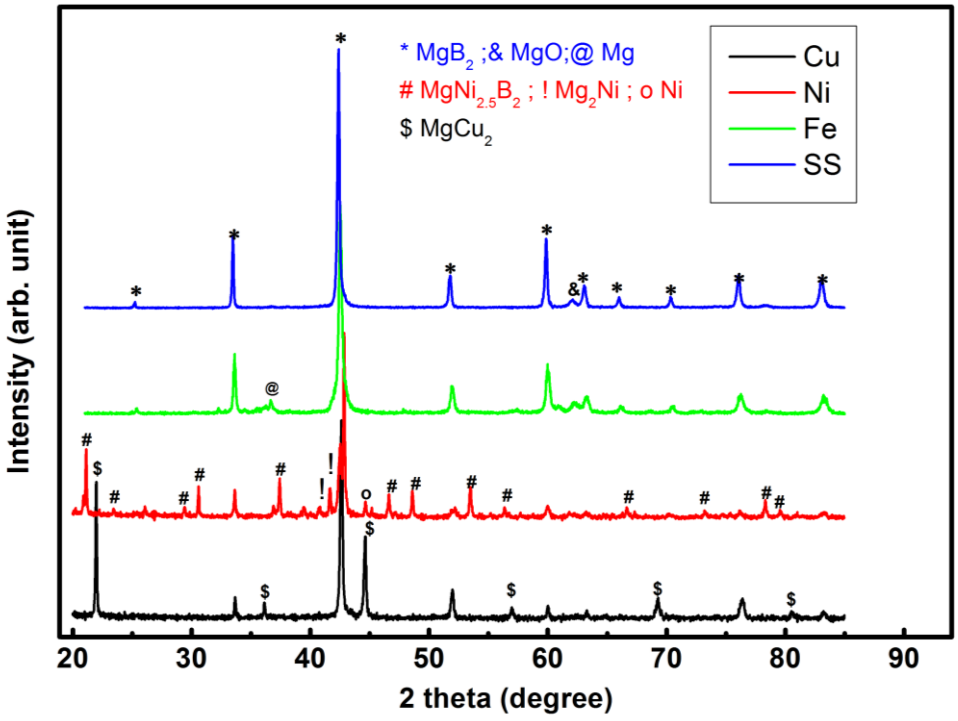

Figure 5.2: XRD patterns of the wire samples heat treated at 650 °C

A semi quantitative phase analysis using the XRD patterns of samples retrieved from the wires was done using the relation, *Vol.% of phase X = Σ Peak intensities of phase X/Σ Peak intensities of all phases*. Figure 5.2 shows the XRD patterns of the samples retrieved from the wires after the heat treatment at 650 °C. Figure 5.3 shows the bar plots showing the relative volume percentage of MgB_2 phase with respect to the impurity phases at various reaction temperatures for all the four sheaths used. The impurity phases include different compounds depending on the nature of sheath material and reaction temperature.

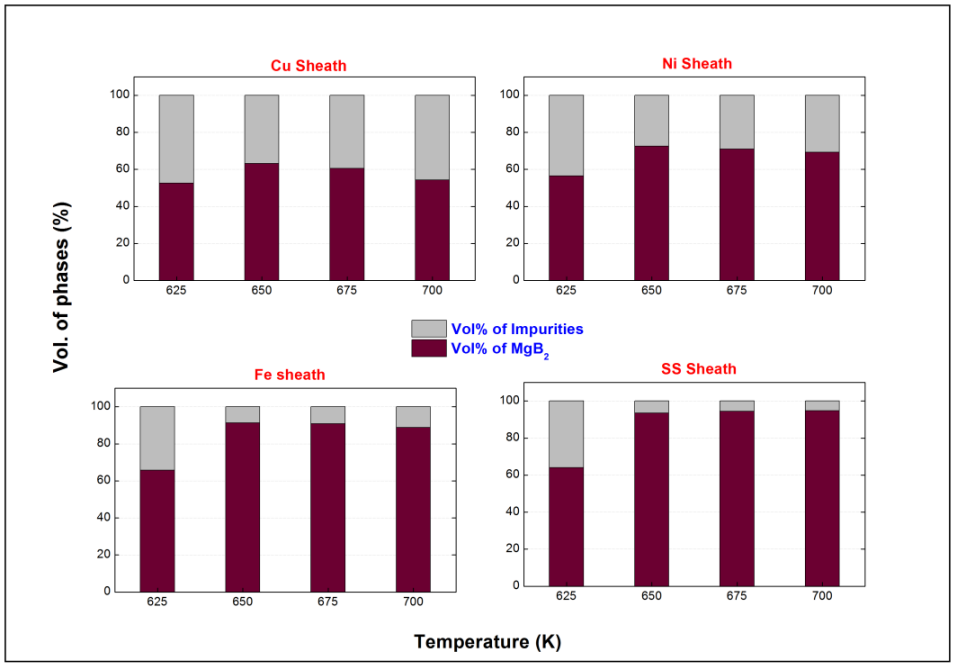

Figure 5.3: Relative vol.% of MgB_2 to impurities

As it can be seen from the figure 5.3, at 625 °C for all sheaths, the formation of MgB_2 is not complete and shows a low volume percentage of MgB_2. For Fe and SS sheaths, the impurity phases are the Mg and slight amount of MgO but for Cu and Ni sheaths, the reacted phase includes Mg_2Cu, MgNi, and $MgNi_{2.5}B_2$. When the reaction temperature is raised to 650 ˚C, the presence of unreacted Mg is decreased. As it can be seen from the figure 5.2, due to the large amount of reacted secondary phases in Cu and Ni sheaths, one can presume that they are not chemically compatible for wire making. For Cu and Ni sheaths the vol.% of MgB_2 phase is the maximum at 650 °C. As the sintering temperature rises, the reacted secondary phases also tend to increase largely for these sheath metals. For Fe sheath, the vol.% of MgB_2 is more than 90 at 650 °C and further increase in temperature causes a minor increase at 675 °C and at 700 °C it slightly decreases due to the presence of small amount of impurity phase Fe_2B. In SS sheathed sample, no impurities other than MgO is observed. The vol.% of MgB_2 maintains almost same level at 675 °C and 700 °C.

Figure 5.4 shows cross sectional views of MgB_2 wires made of different sheaths and heat treated at 650 ˚C. The reacted interface layer is clearly visible in the case of Cu and Ni sheaths, and no reaction layer is seen in Fe and SS sheaths. But on a closer examination, one can find that the core-sheath boundary of Fe is not as well

defined as in the case of SS sheath. This is because of the very low reactivity of SS with Mg when compared to that of Fe.

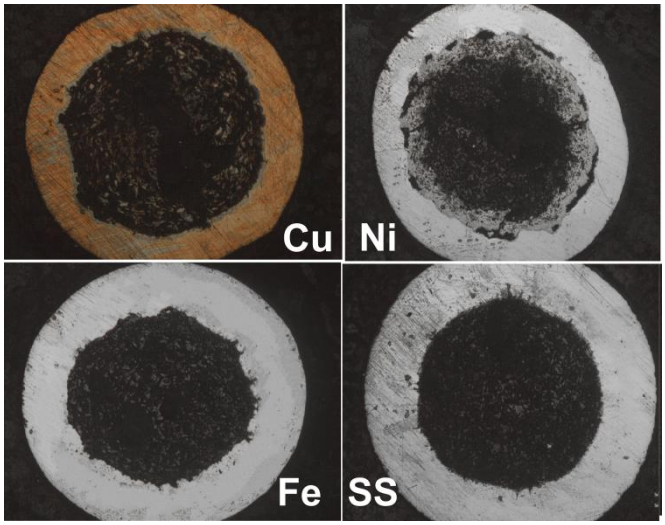

Figure 5.4: Optical image of cross sections of wires heat treated at 650 °C

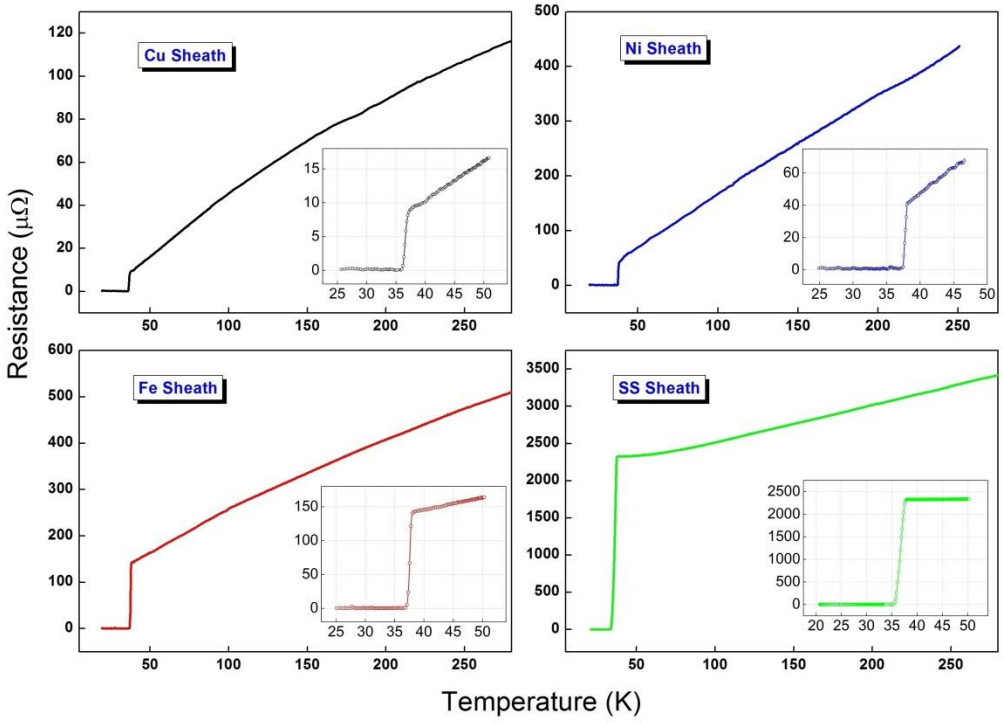

Figure 5.5: R-T plots of the wire samples with different sheath materials, heat treated at 650 °C. Inset shows enlarged view of transition region

The R-T plots of all wires with different sheath materials heat treated at 650 °C are shown in figure 5.5. The resistance values were measured with same cooling rate for all the samples. Above the superconducting transition temperature, the plots

give the values of the resistivity of each sheath-core combination from room temperature down to about 39 K. The very high resistivity of SS sheathed wire is to be noted in the scenario of cryocooler based measurements/applications since it can generate very high and sudden heat flux which may cause the sample to transit abruptly from superconducting to normal state.

Table 5.1: Superconducting properties of the MgB_2 wires with different sheaths heat treated at 650 °C

Sheath metal	T_C (K)	ΔT_C (K)	J_C at 30 K ($\times 10^3$ A/cm^2)
Cu	37.2	1.3	6.6
Ni	37.8	1.0	3.8
Fe	37.9	0.9	12.1
SS	37.3	2.1	8.4

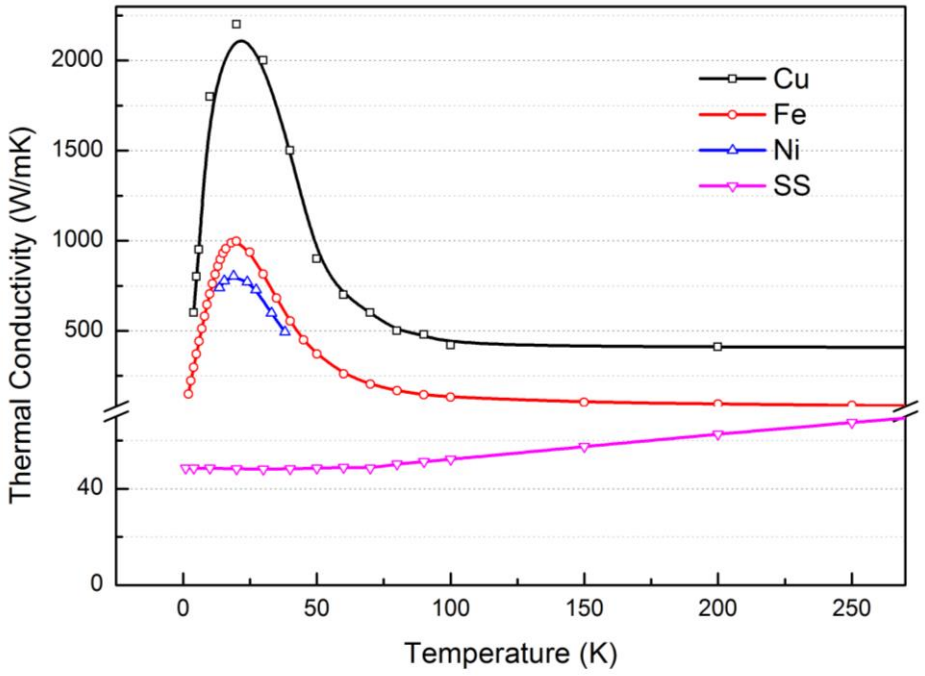

Figure 5.6: Variation of thermal conductivities of different sheath materials with temperature

The T_C and ΔT_C of all the four wire samples are obtained and tabulated in the table 5.1. The presence of impurity phases may lead to increase in transition width. The increased ΔT_C of Ni and Cu sheathed samples with respect to that of Fe sheathed

sample is due to this reason. Other reasons which can influence the measurement of transition width of the wire samples in cryocooler based measurement are the cooling rate of the sample and the thermal conductivity of the sheath material. Since the thermal conductivities of the sheath materials are different, by keeping the same cooling rate for all wire samples, the transition width will be higher for the superconducting wire which has a sheath of lesser thermal conductivity. Figure 5.6 shows the plots of variation of thermal conductivity of the four sheath materials used with respect to temperature [21]. Unlike other sheath materials, the thermal conductivity of SS is very low at room temperature and also it decreases with decreasing the temperature even up to very low temperatures. At 30 K, the thermal conductivity of Fe and Ni is about 15 times of that of SS and for Cu the ratio is about 40. The high electrical resistivity (as given in figure 5.5) and low thermal conductivity of SS can cause thermal instabilities for SS sheathed superconducting wires.

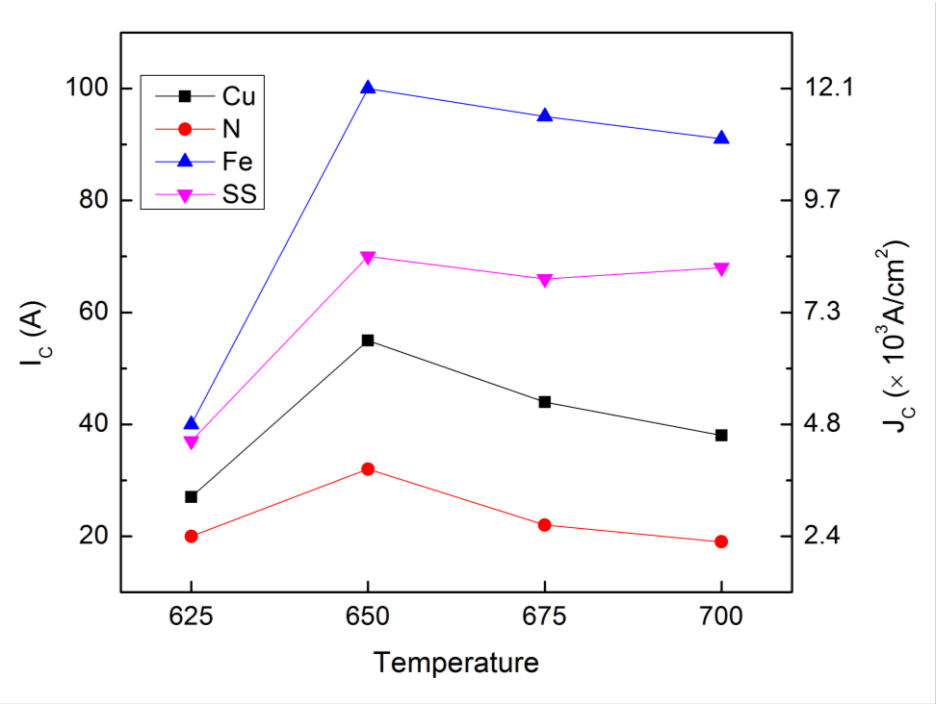

Figure 5.7: Transport I_C and J_C (at 30 K) of superconducting wires with different sheath materials heat treated at various temperatures

Figure 5.7 shows the transport I_C and J_C values of the wires at 30 K with different metal sheaths and heat treated at different temperatures. At 625 °C, the formation of MgB_2 is far below the completion in 2 hour heat treatment and hence the J_C is lower for all the samples. When the heat treatment temperature is raised, the vol.% of MgB_2 formed is also increased as it can be seen from figure 5.3. For Cu and

Ni sheathed wires, the vol.% of MgB_2 formed is the maximum at 650 ^oC and so is the J_C too. Though the vol.% of MgB_2 is marginally higher at 675 ^oC for Fe sheathed wires, the measurements show that Fe sheathed wire has better J_C at 650 °C. This shows that the presence of slight amount of unreacted Mg does not have adverse effect on J_C, but increases the J_C, possibly due to increase in grain connectivity. Similar result has been reported earlier [22, 23]. The J_C of SS sheathed wire is not as high as that of Fe sheathed wire as expected. This can be related to its lower thermal stability which arises due to low thermal conductivity and a current transfer length (CTL) of high resistivity.

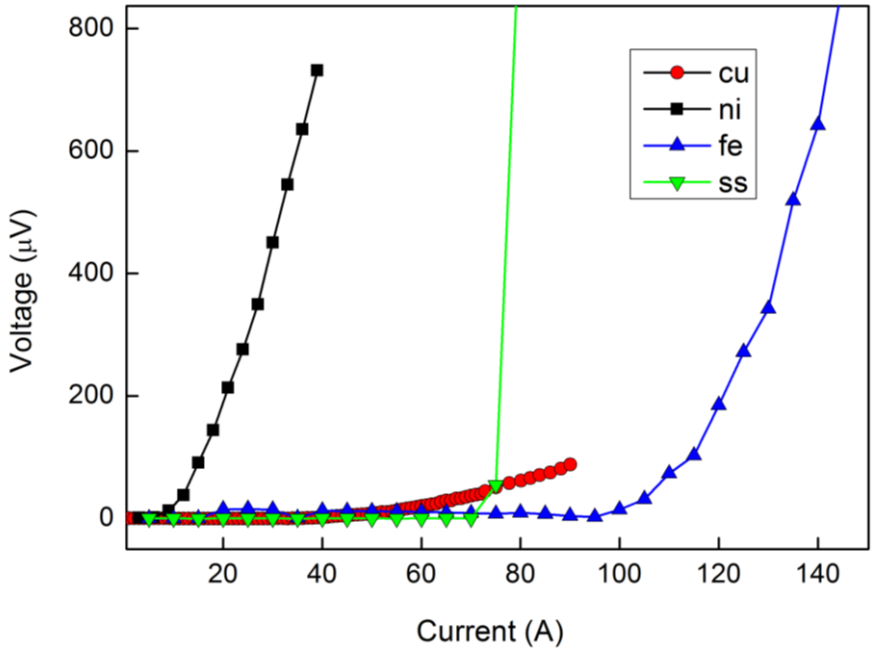

Figure 5.8: I -V plots (at 30 K) of the wire samples heat treated at 650 °C

The current transfer length is the distance travelled by the applied current through the sheath of a superconducting wire before it reaches the superconducting core [24]. The CTL depends on the thickness and resistivity of the sheath metal [25]. Figure 5.8 shows the I-V plots of the samples heat treated at 650 °C and measured at 30 K. The abrupt transition from superconducting to normal state for SS sheathed wire shows its lower stability. Therefore, cryocooler based measurement of short length SS sample can generate high heat flux due to CTL and high resistivity of the SS sheath. Since this is an instantaneous process, the sample can transit to normal state if the passing current is high enough.

When comparing the results of characterizations done over the samples with different sheath materials and sintering temperatures, one can select Fe sheathed wire heat treated at 650 ^oC as the best sample. The reactivity of the Cu and Ni sheaths with Mg doesn't qualify them to be good sheath material for MgB_2 superconducting wire making. The lower thermal stability and lower malleability are the disadvantages of SS sheath. It is observed that the hardening of the SS leads to cracks in monofilamentary wires when it is rolled into lower wire diameters. But the reactivity with Mg is the least for SS sheath. Fe sheath is not reactive with Mg at 650 °C. Even at 700 °C, only traces of reacted phases are observed. It has got good thermal conductivity and lower resistivity when compared to SS. Also Fe is malleable enough and easy to roll into long wires. Measurements show that Fe sheathed wire has the best J_C values and the width of the transition from normal to superconducting state is also narrow. Apart from these Fe tubes are cheaper and commonly available at desired outer/inner diameters.

5.3.3 Conclusions

From the comparative study of the properties of the superconducting wires sheathed with four commonly available and cheaper sheath materials, namely Cu, Ni, Fe and SS, and heat treated at various temperatures, it was found that the Fe sheath is most suitable for the practical applications. A sintering temperature of 650 ^oC was found to be optimal for pure MgB_2 wires with Fe sheath. The study was carried out on the basis of applications of the wires using cryogen free cryocoolers. All the superconducting characteristics were also done in a cryocooler based set up without the use of any cryogen. On the basis of this experimental study, Fe is chosen as the sheath material for the sample preparation for the further studies on MgB_2 superconducting wires in this thesis.

5.4 Comparison of *in situ* and *ex situ* methods of wire preparation

Though the *in situ* PIT method is easier and widely used technique for MgB_2 wire preparation, it has some disadvantages. The theoretical density of Mg + 2B mixture is considerably lower than that of the MgB_2 compound. So, after the heat treatment there will be porosities in superconducting core and this can decrease the effective cross sectional area to the passage of super current. But in *ex situ* PIT technique, where reacted and ground MgB_2 powder is filled and rolled into wires, the

porosity can be reduced significantly. The possibility of reaction between MgB_2 and sheath is also lower in *ex situ* wires. Preparation and properties of *ex situ* MgB_2 wires have been reported shortly after the discovery of its superconductivity [3-6]. But since the melting point of MgB_2 is high, it is difficult to form a bulk monolithic structure with very good connectivity on heat treatment. Considering these facts, to compare the self-field current carrying capacities of *in situ* and *ex situ* wires, we prepared *ex situ* wires also from preformed MgB_2 powder. Fe was chosen as the sheath material for *ex situ* wires too.

Preformed MgB_2 powder with a phase purity of ~ 97% was used for the wire preparation. The powder was filled in Fe tubes of OD/ID: 6 mm/4 mm. The rolled wires were cut, end sealed and heat treated at 800 °C, 850 °C and 900 °C for two hours. The superconducting properties were measured using a cryocooler interfaced cryostat. The *in situ* wire heat treated at 650 °C for 2 hours was used to compare the properties with *ex situ* wires.

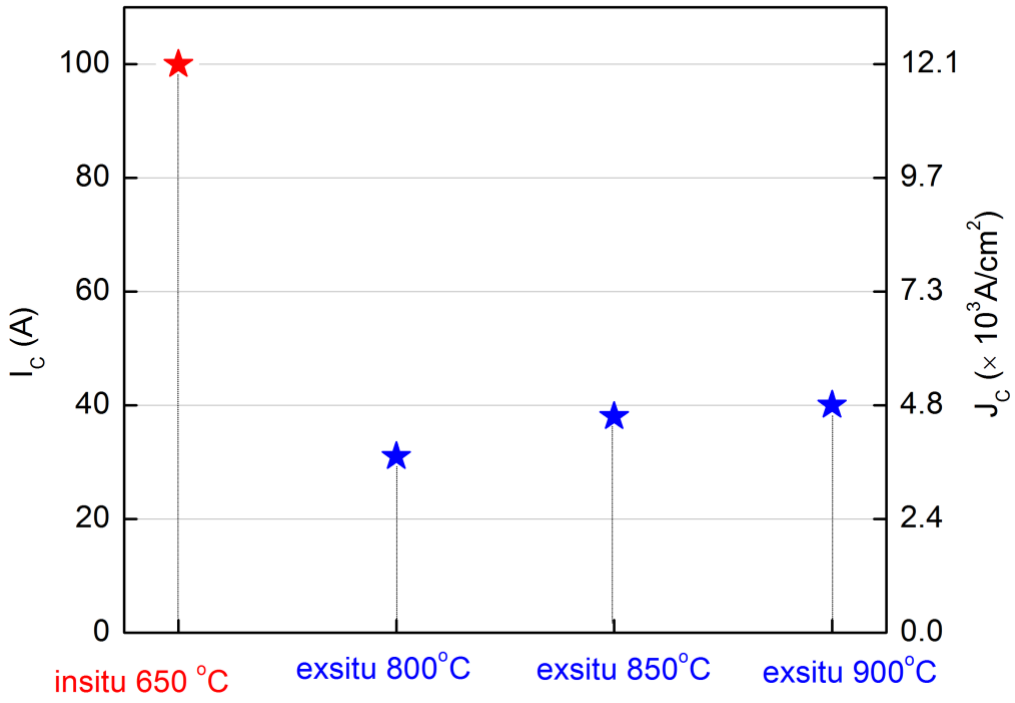

Figure 5.9: The transport I_C and J_C of *ex situ* and in situ wires measured at 30 K

Figure 5.9 shows the measured transport I_C and J_C values for the *ex situ* samples and the values are compared with that of best *in situ* wire sample. It is clear

that the J_C values for the *ex situ* wires are significantly lower than that of the *in situ* wire. Among the *ex situ* samples, the wire which was heat treated at 900 ^oC shows marginally higher J_C values than that of the sample heat treated at 850 °C. The J_C is still lower for the sample heat treated at 800 °C. The increased J_C with increase in heat treatment temperature is due to the increased intergrain connectivity in the superconducting core. Since the J_C of all the *ex situ* samples is lower than that of the *in situ* sample, we can assume that the effective cross sectional area of the former is also lower than that of the latter. Or in *ex situ* samples the supercurrent fails to find path between the superconducting grains of MgB_2 due to poor sinterability at these temperatures.

In short, when we compare both the above methods, the *in situ* method of wire making has a clear edge over *ex situ* method. Other than achieving higher self-field J_C, the easiness to dope impurity atoms, lower heat treatment temperature and fewer processing steps make *in situ* method more acceptable. Therefore throughout this thesis we have chosen *in situ* method of wire preparation for rest of our investigations.

5.5 Preparation and characterization of multifilamentary MgB_2 wires

For most of the practical applications, the MgB_2 is to be made in the form of multifilamentary wires as in the case of any other superconductors. The multifilamentary composite conductor has many advantages over monofilamentary form, when comes to applications. During the operation, the operating point of a superconductor may go out of the critical surface due to various reasons like accidental passage of over current, failure of the cooling system, fluctuation in current density at high currents etc. These can lead to formation of a normal or non-superconducting zone inside the material and which propagates throughout the entire material due to joule heating. Generally, at normal state, superconductors are of very high resistivity and hence passage of high current can cause severe damage to the device. Therefore, it is necessary to have an alternate low resistance path parallel to the superconductor to flow the current in such critical situations. Usually this is done by incorporating low resistive Oxygen Free High Conductivity (OFHC) Copper in superconducting wire itself. But since the reactivity of Cu with Mg is high, it is not preferred to make Cu sheathed wire by *in situ* method as seen from the section 5.3. Also the mechanical strength of the Cu is not adequate to protect the superconducting

core. Hence in order to make multifilamentay MgB_2 wire, Fe sheathed monofilamentary wires are bundled along with OFHC copper wires in Nickel tube. Here Fe acts as barrier material and OFHC copper acts as stabilizing material and Ni, the outer sheath. The multifilamentary wires also possess better strain tolerance and high critical current density due to densified core. Another important advantage of multifilamentary wire is its reduced ac losses. When a superconducting wire has to be used to pass ac current or in a time varying field, ac losses will occur due to the motion of flux lines and eddy current losses of the conductor and sheaths [26]. This can be reduced by minimizing the cross sectional area of the superconducting core [27].

This section discusses the fabrication of MgB_2 multifilamentary wires and their characterization. Both self-field and in-field J_C was studied for the prepared wires.

5.5.1 Making of multifilamentary wires

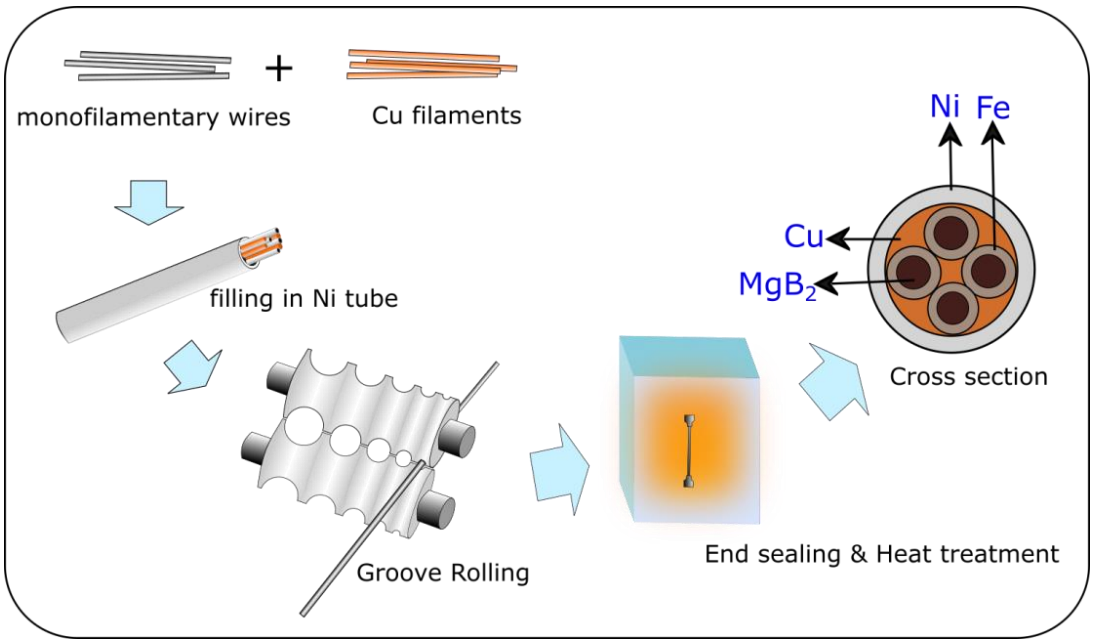

Figure 5.10: Schematic diagram of MgB_2 multi-filamentary wire making

Figure 5.10 shows a schematic diagram of preparation of multifilamentary wires. Fe sheathed mono filamentary wires of 2.1 mm diameter are obtained by groove rolling of powder filled Fe tubes as described in the section 5.2. The as rolled mono wires are packed in Ni tube of OD/ID – 8/6 mm and of desired length (typically 6 to 10 mm). The number of filaments is decided by the number of mono wires

packed inside the Ni tube. OFHC copper wires of diameter 0.75 mm are cut and bundled along with the mono wires inside the Ni tube.

The figure 5.11 (a) shows the composite tube bundled with monowires and Cu filaments before groove rolling. This is groove rolled into 1.67 mm diameter wires, cut into desired length and end sealed by capping technique. The sealed wires are then subjected to heat treatment at 650 °C for 2 hours in a muffle furnace without any inert or vacuum atmosphere. After furnace cooling, the sample is surface cleaned and characterized.

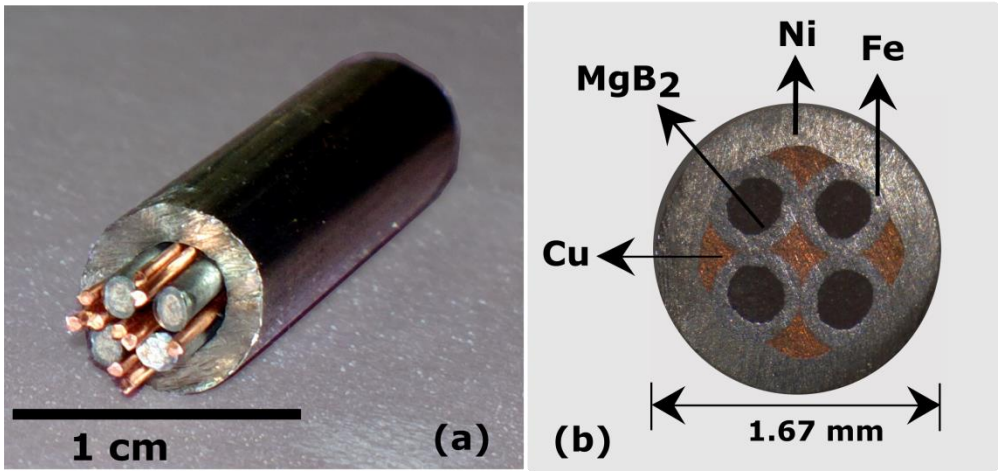

Figure 5.11 (a): Ni tube filled with mono wires and Cu filaments. (b): Cross section of 4 filamentary wire after groove rolling and heat treatment

5.5.2 Results and discussions

The figure 5.11 (b) shows optical micrograph of the cross section of the multifilamentary wire. The different parts, MgB_2, Fe, Cu and Ni are well distinct and separated by clear boundaries. The percentage of area fractions of each phase can be measured by measurement option in the image capturing software. A typical 4 filamentary wire has about 55% of Ni, 8 % of Cu, 27 % of Fe and 10 % of MgB_2.

Figure 5.12 shows the R-T plot of the multifilamentary wire prepared where R is normalized with respect to room temperature resistance of the wire. A sharp normal to superconducting transition was observed with a T_C onset at 38.5 K. The width of the transition is narrow and less than 1 K as it can be seen from inset of the figure. The low value of ΔT_C indicates that the sample has good crystallinity, phase purity and thermal stability.

The transport I_C of the sample was measured at various temperatures from 6 K to 35 K and the J_C was estimated. The voltage taps were kept 1 cm apart and I_C was measured at 1 μV/cm criterion. The results are shown in the figure 5.13. The wire has an I_C of 264 A at 6 K and 41 A at 35 K with corresponding J_C of 1.58×10^5 A/cm^2 and 0.25×10^5 A/cm^2, respectively.

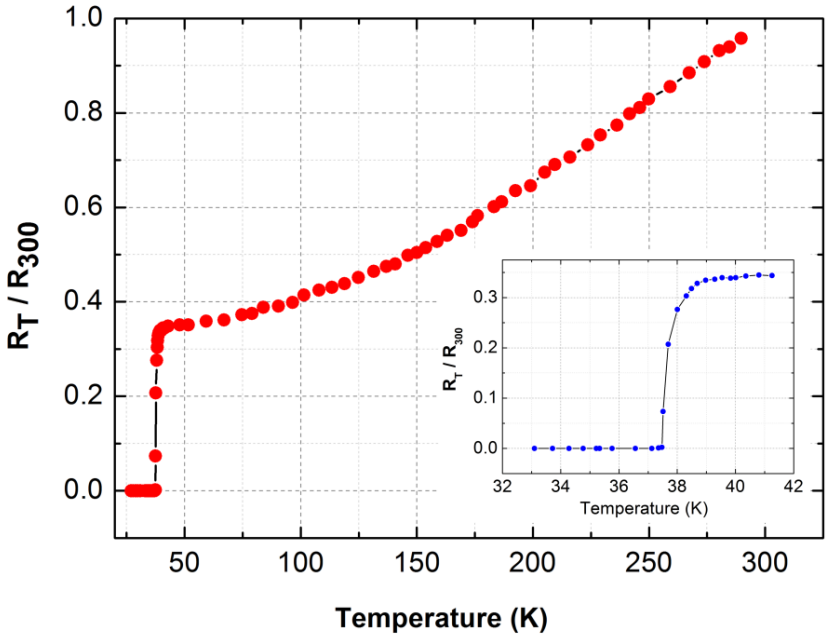

Figure 5.12: R-T plot of the multifilamentary wire. Inset shows enlarged view of superconducting transition region

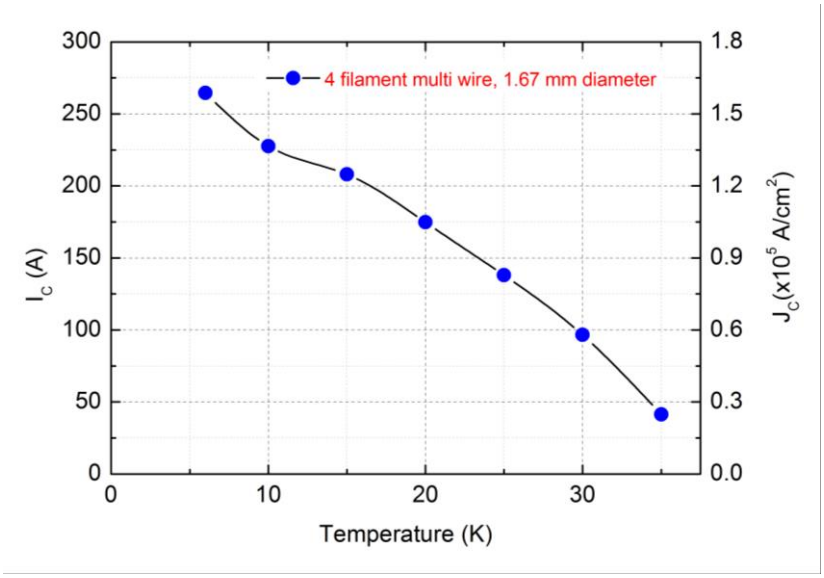

Figure 5.13: The transport I_C & J_C of the multifilamentary wire at various temperatures

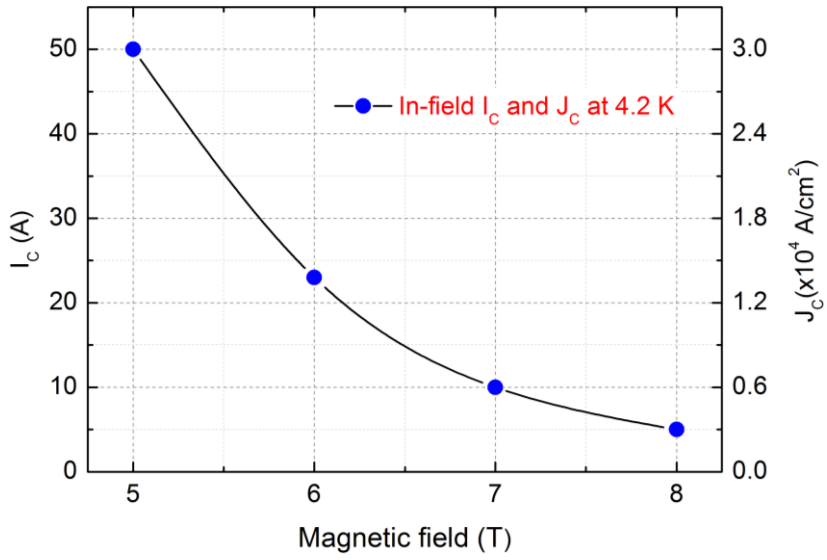

Figure 5.14: Variation of transport I_C & J_C of the multifilamentary wire at different magnetic fields. The measurements were done at 4.2 K

The in-field critical current densities of the wires were measured at LHe temperature 4.2 K. The values obtained in fields of 5 T to 8 T are shown in figure 5.14. Since the wire is made of pure MgB_2 without any dopants, the J_C of 3×10^4 A/cm^2 obtained at 5 T was degraded to 0.3×10^4 A/cm^2 at 8 T. Though, these wires possess higher self-field J_C than that of monofilamentary wires for corresponding measuring temperature (figures 5.7 and 5.9).

5.6 Improvement of transport $J_C(H)$ of Fe sheathed MgB_2 monofilamentary wires by nano-carbon doping

5.6.1 Introduction

For engineering applications where high ambient magnetic field is present, the transport J_C of MgB_2 wire should not degrade sharply with increase in field. Therefore, it is necessary to improve the transport $J_C(H)$ behavior of this superconducting wire. The chapter 4 has already presented various efforts to improve $J_C(H)$ behavior of MgB_2, but the studies were on samples with bulk geometry. From an engineer's point of view; these results have to be translated into the samples of mono or multifilamentary architecture. But in wire form, the preparative conditions are no longer the same as that in bulk sample preparation. In wire preparation there is variation in the sheath material and the reactants are more densified into a small

volume by groove rolling and hence there will be increased vapor pressure during heat treatment. This can vary the microstructure, doping levels and impurity percentage from that of bulk sample if both were heat treated at the same temperature. Therefore, in order to get best results via doping for MgB_2 wires one has to optimize the reaction temperature also.

Many researchers have reported the results of doping of carbon/carbon based compounds on the superconducting properties of MgB_2 wire/tape forms. The dopants include CNT [28], hydrocarbons [29-31], SiC [32, 33], amorphous carbon [34], nano-carbon [35, 36]. The sheath, wire geometry and processing route are different for different work. The $J_C(H)$ characterization also differs in various work. Some groups have done magnetic characterization based on Bean's model by removing the sheath of wire/tape, and many have reported transport characterization where a current source is used to pass current directly through the superconductor. The transport characterization is more meaningful because for the actual application the wires have to carry the transport current. This section describes preparation and characterization of nano-carbon doped MgB_2/Fe monofilamentary wires processed at different temperatures. The results of study on the structural properties and the transport $J_C(H)$ behavior of the doped samples are compared with those of the undoped MgB_2/Fe wire samples.

On the basis of the study on the bulk MgB_2 (section 4.2), 0.1 atomic percentage of the nano-carbon was selected as dopant level. The reactants were weighed and mixed for the stoichiometric formula $MgB_{1.9}C_{0.1}$. The wires were rolled (as described in section 5.2) and heat treatment was done at 700 °C, 750 °C and 800 °C for 2 hours in a muffle furnace. Structural characterization was done on the sample recovered from the wires. The transport $J_C(H)$ behavior was studied at magnetic fields varying from 0 to 8 T in helium vapor at temperature 4.2 K. The results were compared with those of pure wire sample heat treated at 650 °C.

5.6.2 Results and discussions

Figure 5.15 shows the XRD patterns of the samples retrieved from the wires after the heat treatment. The pure sample shows slight amount of unreacted Mg apart from the impurity MgO which is present in all samples. The nano-carbon doped samples show presence of Fe_2B which is able to block the flow of supercurrent by

being at grain boundaries. Presence of Fe_2B increases with increase in sintering temperature. The deficiency in B has created the excess Mg and because of this the vol.% of the superconducting phase decreases. The inset of the figure shows the enlarged view of the (002) and (110) peaks. The shift in (110) peak is due to the substitution of the carbon at lattice by replacing the boron atoms. Unlike the pure sample, the broadening of the peaks is observed for doped samples. This is due to loss of crystallinity and increased strain as a result of carbon substitution. The FWHM of selected peaks are shown in the table 5.2. It can be observed that for the sample heat treated at 800 °C, the peak broadening is lower than that of other two samples. This is due to the increase in crystalinity.

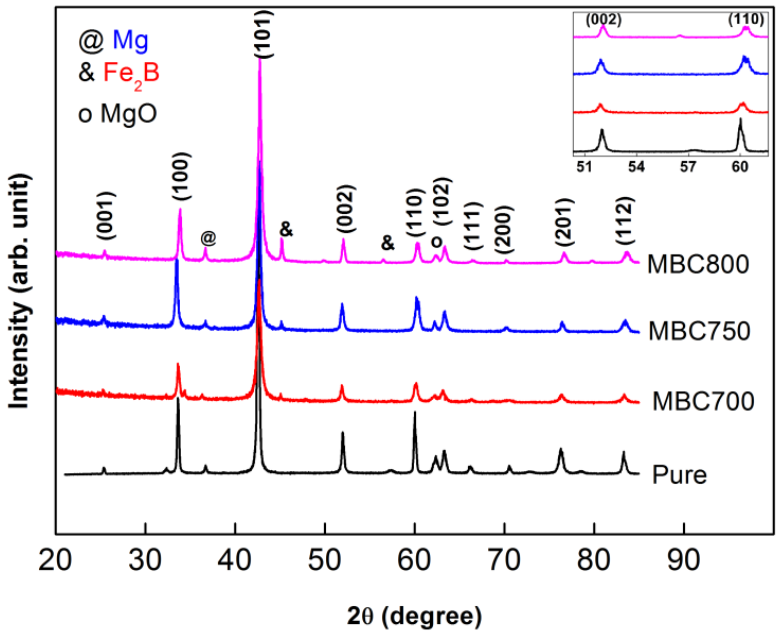

Figure 5.15: XRD patterns of pure and nano-carbon doped wire samples heat treated at various temperatures. Inset shows enlarged view of the (002) and (110) peaks

The lattice parameters *a* and *c* were calculated and plotted in figure 5.16. The *a*-axis shrinkage is as expected from the peak shift of doped samples. Similarly the negligible variations in *c*-axis is also evident because there was no clear shift for the (002) peak in XRD pattern. The increase in heat treatment temperature in general causes more substitution of carbon, though there is only a small difference between the samples heat treated at 750 °C and 800 °C.

Table 5.2: FWHM of the selected peaks of the pure and nano-carbon doped samples

Sample details	FWHM of selected peaks (degree)			
	100	101	002	110
Pure	0.214	0.206	0.210	0.212
MBC700	0.313	0.442	0.353	0.481
MBC750	0.313	0.392	0.372	0.503
MBC800	0.287	0.430	0.361	0.433

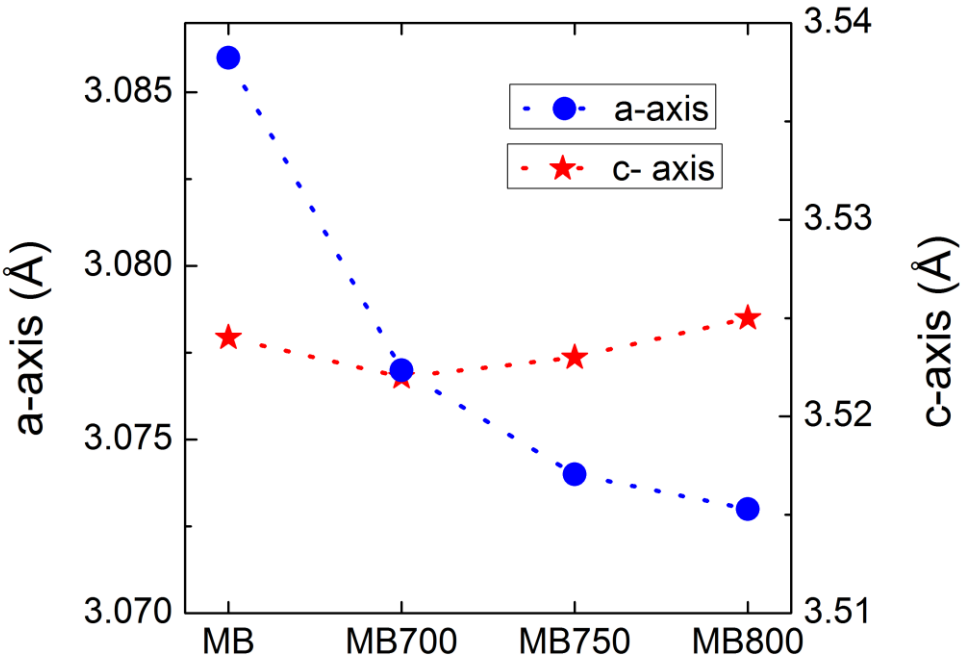

Figure 5.16: Variation of *a* and *c* lattice parameters of pure and nano-carbon doped samples

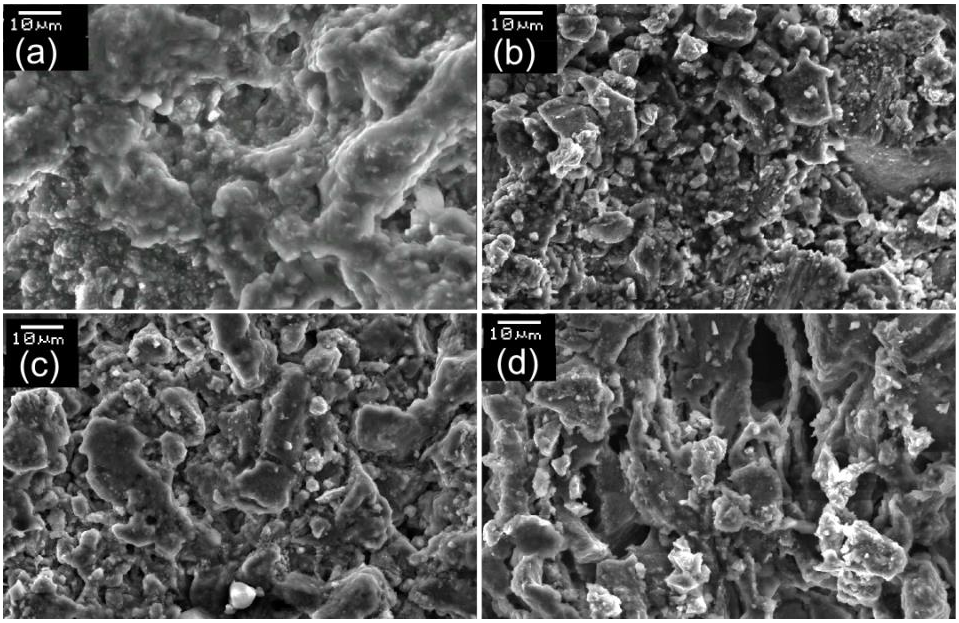

Figure 5.17: SEM images of (a) pure, (b) MBC700, (c) MBC750 and (d) MBC800. The imaging was done on the fractured surfaces of the sample

Figure 5.17 shows the SEM images of the fractured surfaces of the samples. The pure sample shows larger grains formed by liquid-solid reaction. The doping and variation in heat treatment temperature have clear influence on the grain morphology. The sample MBC700 has smaller average grain size when compared to the other samples as an effect of carbon doping. But as the heat treatment temperature is increased there is a trend to form larger grain sizes. The sample MBC800 shows the grain formation with the largest size among doped samples. The increased granular size with increase in heat treatment temperature in both pure and doped sample has been reported earlier [37, 38]. The low grain sized samples has an advantage for application in high magnetic fields because at higher fields grain boundaries have also a significant role in flux pinning [39-41].

The transport I_C of all samples was measured in magnetic fields from 0 to 8 T at 4.2 K. The J_C was estimated for each sample by measuring the MgB_2 core area and the results are plotted in figure 5.18. At 0 T and up to 4 T, the pure sample marginally dominates over other samples in respect of J_C. This is because of the better purity and connectivity of the sample. But beyond 4 T the J_C of the pure sample begins to degrade faster as in the case of bulk sample because of the lack of pinning agents like lattice strains and nano-inclusions. Due to lower density of grain boundaries, the flux pinning caused by grain boundaries is also inferior for the pure sample.

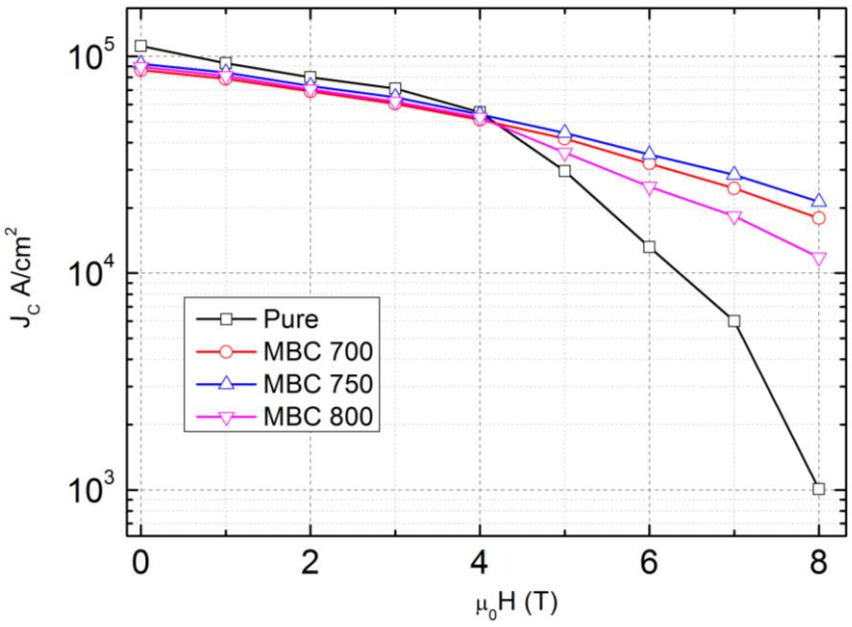

Figure 5.18: Transport $J_C(H)$ characteristics of pure and carbon doped samples measured at 4.2 K

However, in carbon doped samples the substitution of carbon at boron site increases the H_{C2} by modifying the σ and π band scattering and the result is enhancement of $J_C(H)$. Along with this the substitution creates lattice defects and strains which can act as flux pinners. Another positive effect of carbon doping is the modification in grain size. As the grain size reduces the pinning at boundaries increases. Among the doped samples, the best $J_C(H)$ characteristics is shown by the sample heat treated at 750 °C. Though the carbon substitution is higher in the sample MBC800 which was heat treated at 800 °C, the presence of impurities like Fe_2B which can block supercurrent, and the higher granular size make the $J_C(H)$ performance of the sample inferior to other doped samples. Despite of the lower substitution level, the lower grain size and fewer impurities have helped the sample MBC700 to retain its J_C at higher fields as good as or better than MBC800.

5.6.3 Conclusions

Based on the studies on carbon doping in bulk MgB_2, 0.1 at.% of nano-carbon was selected to dope in the wires. Since the reaction environment is different, the doped samples were heat treated at three different temperatures. The carbon

substitution was assessed by lattice parameter calculations, and microstructural changes were studied by SEM analysis. The transport $J_C(H)$ measurements done up to 8 T at 4.2 K have shown that the sample which was heat treated at 750 °C has greater values of J_C than other samples at high magnetic fields. The enhanced H_{C2}, lattice strains and defects created by carbon substitution and the grain boundary pinning are found to be the reasons. With this optimized heat treatment temperature further co-doping studies were taken up.

5.7 Effect of co-doping on the transport $J_C(H)$ of MgB_2/Fe monofilamentary wires

The co-doping of suitable dopants with nano-carbon can create additional pinning agents mainly by formation and intragrain distribution of nano-sized inclusions. The studies on bulk MgB_2 in this work have revealed that the co-doping can enhance the carbon substitution level also. Depending on the nature of the dopants there are specific effects on the microstructure too.

This section reports the translation of the best results of the co-doping studies conducted in bulk MgB_2 (Chapter 4) to Fe sheathed monofilamentary wires. Along with the undoped and carbon doped samples, two co-doped samples were prepared and compared their transport $J_C(H)$ performance. The co-doped samples are with the initial stoichiometry $MgB_{1.9}C_{0.1}$ + 2.5 wt.% n-SiO_2 (sample is coded as MBCS) and $MB_{1.9}C_{0.1}$ + 2.5 wt.% n-Ho_2O_3 + 2.5 wt.% n-Cu (sample is coded as MBCHCu). The samples were made into monofilamentary wires and heat treated at 750 °C. After the surface cleaning, the wires were cut into ~ 4 cm length and the voltage and current leads were soldered. The separation between the voltage leads were kept 1 cm apart. The transport $J_C(H)$ characteristics were studied in 8 T magnet system at 4.2 K temperature.

Figure 5.19 shows the $J_C(H)$ plots of the co-doped samples along with pure and carbon doped samples. The $J_C(H)$ behavior of the co-doped samples followed more or less the same behavior as in the bulk form. At higher fields both are very close as in the case of bulk. The sample MBCHCu has exhibited the maximum J_C ~ 1.8×10^4 A/cm^2 at 8 T. The sample stoichiometry and possible mechanisms behind the improvement of $J_C(H)$ are given in the table 5.3.

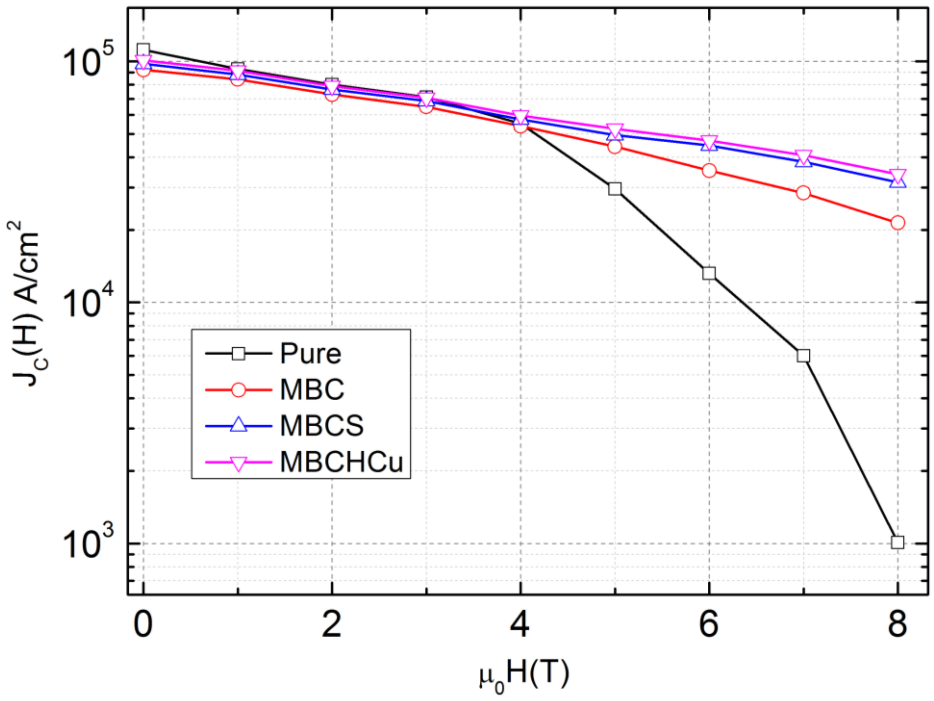

Figure 5.19: Transport $J_C(H)$ characteristics of pure, carbon doped, and co-doped samples measured at 4.2 K

Table 5.3: J_C at 8 T and the mechanisms behind improvement of $J_C(H)$ of doped samples

Sample stoichiometry	**J_C at 8 T and 4.2 K ($\times 10^4$ A/cm^2)**	**Mechanism behind $J_C(H)$ enhancement**
MgB_2	0.08	---
$MgB_{1.9}C_{0.1}$	1.06	• Carbon substitution • pinning by defects and grain boundaries
$MgB_{1.9}C_{0.1}$ + 2.5 wt.% n-SiO_2	1.61	• Carbon substitution • Pinning by defects and grain boundaries • Point pinning by Mg_2Si
$MgB_{1.9}C_{0.1}$ + 2.5 wt.% n-Ho_2O_3 + 2.5wt.% n-Cu	1.80	• Carbon substitution • Pinning by defects and grain boundaries • Point pinning by HoB_4, Mg_2Cu • Increased connectivity

5.8 Summary

MgB_2 superconducting wires both in mono and multifilamentary forms were prepared and characterized. To prepare the monofilamentary wires Fe was chosen as the most acceptable sheath material among the commonly used sheath materials namely, Fe, Cu, Ni and SS by comparing their properties such as reactivity with Mg and B, malleability, electrical and thermal conductivity and cost. Comparison was also done by considering the self-field performance of the wires made, using the above sheaths in a cryogen free cryocooler based measurement setup. To prepare the multifilamentary wires, Ni was selected as the outer sheath and Fe as the barrier material. OFHC copper was used as the stabilizer material for thermal stability, which has got very significant role when considering the application of the wires in cryogen free magnets.

The enhancement of the $J_C(H)$ of the MgB_2 wires was also done on the basis of the studies on the bulk form of the superconductor as described in chapter 4. For this, the reaction temperature was optimized to obtain the best results in respect of 0.1 at.% nano-carbon substituted MgB_2. It was found that the sample heat treated at 750 °C yielded the best results. Having achieved these results efforts to further improve the in-field J_C was done by adopting the co-dopant combinations used in chapter 4. The results of co-doping study in wires were almost the same as in the case of bulk. The results achieved in this work are at par with the international results and the wires in long length multifilamentary form can be used for practical applications.

REFERENCES

[1] K. Vinod, R. G. A. Kumar, and U. Syamaprasad, "Prospects for MgB_2 superconductors for magnet application," *Superconductor Science & Technology,* vol. 20, pp. R1-R13, Jan 2007.

[2] P. C. Canfield, D. K. Finnemore, S. L. Bud'ko, J. E. Ostenson, G. Lapertot, C. E. Cunningham, *et al.*, "Superconductivity in dense MgB_2 wires," *Physical Review Letters,* vol. 86, pp. 2423-2426, Mar 12 2001.

[3] H. Kumakura, A. Matsumoto, H. Fujii, and K. Togano, "High transport critical current density obtained for powder-in-tube-processed MgB_2 tapes and wires using stainless steel and Cu–Ni tubes," *Applied Physics Letters,* vol. 79, p. 2435, 2001.

[4] W. Pachla, A. Presz, R. Diduszko, P. Kovac, and I. Husek, "Structural inhomogeneity of superconducting ex situ MgB_2/Cu wires made by the powder-in-tube technique," *Superconductor Science & Technology,* vol. 15, pp. 1281-1287, Sep 2002.

[5] P. Kovac, M. Dhalle, T. Melisek, H. J. N. van Eck, W. A. J. Wessel, B. ten Haken, *et al.*, "Dependence of the critical current in ex situ multi- and mono-filamentary MgB_2/Fe wires on axial tension and compression," *Superconductor Science & Technology,* vol. 16, pp. 600-607, May 2003.

[6] K. Yamamoto, K. Osamura, S. Balamurugan, T. Nakamura, T. Hoshino, and I. Muta, "Mechanical and superconducting properties of PIT-processed MgB_2 wire after heat treatment," *Superconductor Science & Technology,* vol. 16, pp. 1052-1058, Sep 2003.

[7] A. K. Pradhan, Y. Feng, Y. Zhao, N. Koshizuka, L. Zhou, P. X. Zhang, *et al.*, "Transport behavior and critical current densities in MgB_2 wires," *Applied Physics Letters,* vol. 79, pp. 1649-1651, Sep 10 2001.

[8] E. Martinez, L. A. Angurel, and R. Navarro, "Study of Ag and Cu/MgB_2 powder-in-tube composite wires fabricated by in situ reaction at low temperatures," *Superconductor Science & Technology,* vol. 15, pp. 1043-1047, Jul 2002.

[9] W. Goldacker, S. I. Schlachter, B. Obst, and M. Eisterer, "In situ MgB_2 round wires with improved properties," *Superconductor Science & Technology,* vol. 17, pp. S490-S495, Sep 2004.

[10] H. Yamada, M. Hirakawa, H. Kumakura, A. Matsumoto, and H. Kitaguchi, "Critical current densities of powder-in-tube MgB_2 tapes fabricated with nanometer-size Mg powder," *Applied Physics Letters,* vol. 84, pp. 1728-1730, Mar 2004.

[11] X. L. Wang, S. Soltanian, J. Horvat, A. H. Liu, M. J. Qin, H. K. Liu, *et al.*, "Very fast formation of superconducting MgB_2/Fe wires with high J_C," *Physica C,* vol. 361, pp. 149-155, Sep 15 2001.

[12] P. Kovac, I. Husek, and T. Melisek, "Transport currents of two-axially rolled and post-annealed MgB_2/Fe wires at 4.2 K," *Superconductor Science & Technology,* vol. 15, pp. 1340-1344, Sep 2002.

[13] A. Malagoli, V. Braccini, N. Scati, S. Roncallo, A. S. Siri, and G. Grasso, "Fabrication and superconducting properties of powder-in-tube processed MgB_2 tapes," *Physica C-Superconductivity and Its Applications,* vol. 372, pp. 1245-1247, Aug 1 2002.

[14] M. Eisterer, B. A. Glowacki, H. W. Weber, L. R. Greenwood, and M. Majoros, "Enhanced transport currents in Cu-sheathed MgB_2 wires," *Superconductor Science & Technology,* vol. 15, pp. 1088-1091, Jul 2002.

[15] S. Soltanian, X. L. Wang, J. Horvat, A. H. Li, H. K. Liu, and S. X. Dou, "Improvement of critical current density in the Cu/MgB_2 and Ag/MgB_2 superconducting wires using the fast formation method," *Physica C-Superconductivity and Its Applications,* vol. 382, pp. 187-193, Nov 1 2002.

[16] W. Goldacker, S. I. Schlachter, S. Zimmer, and H. Reiner, "High transport currents in mechanically reinforced MgB_2 wires," *Superconductor Science & Technology,* vol. 14, pp. 787-793, Sep 2001.

[17] P. Kovac, I. Husek, T. Melisek, M. Kulich, and V. Strbik, "MgB_2 composite wires with Fe, Nb and Ta sheaths," *Superconductor Science & Technology,* vol. 19, pp. 600-605, Jun 2006.

[18] H. Fang, S. Padmanabhan, Y. X. Zhou, and K. Salama, "High critical current density in iron-clad MgB_2 tapes," *Applied Physics Letters,* vol. 82, pp. 4113-4115, Jun 9 2003.

[19] P. Kovac, I. Husek, C. Grovenor, and C. Salter, "Properties of as-deformed and post-annealed MgB_2/Fe(Fe-alloy) composite wires," *Superconductor Science & Technology,* vol. 16, pp. 292-296, Feb 2003.

[20] G. Yan, B. Q. Fu, Y. Feng, C. F. Liu, P. Ji, X. Z. Wu, *et al.*, "Preparation and transport J_C(B) properties of Fe-clad MgB_2 wires," *Physica C-Superconductivity and Its Applications,* vol. 386, pp. 607-610, Apr 15 2003.

[21] R. J. Davis, *Metals Handbook Desk Edition* 2ed.: ASM International. Handbook Committee, 1998.

[22] A. Serquis, L. Civale, D. L. Hammon, J. Y. Coulter, X. Z. Liao, Y. T. Zhu, *et al.*, "Microstructure and high critical current of powder-in-tube MgB_2," *Applied Physics Letters,* vol. 82, pp. 1754-1756, Mar 17 2003.

[23] H. Fang, P. Gijavanekar, Y. X. Zhou, G. Liang, P. T. Putman, and K. Salama, "High critical current of Cu-sheathed MgB_2 wire at 20 K," *IEEE Transactions on Applied Superconductivity,* vol. 15, pp. 3215-3218, Jun 2005.

[24] T. Holubek, M. Dhalle, and P. Kovac, "Current transfer in MgB_2 wires with different sheath materials," *Superconductor Science & Technology,* vol. 20, pp. 123-128, Mar 2007.

[25] K. Vinod, N. Varghese, S. Rahul, K. M. Devadas, S. Thomas, P. Gurusamy, *et al.*, "On the current transfer length and current sharing in short length MgB_2 wires," *Superconductor Science & Technology,* vol. 23, Oct 2010.

[26] Y. Wang, *Fundamental Elements of Applied Superconductivity in Electrical Engineering*: Wiley, 2013.

[27] A. V. Narlikar, *High Temperature Superconductivity 1: Materials*: Springer 2004.

[28] J. H. Kim, W. K. Yeoh, M. J. Qin, X. Xu, and S. X. Dou, "The doping effect of multiwall carbon nanotube on MgB_2/Fe superconductor wire," *Journal of Applied Physics,* vol. 100, Jul 1 2006.

[29] M. S. A. Hossain, C. Senatore, R. Fluekiger, M. A. Rindfleisch, M. J. Tomsic, J. H. Kim, *et al.*, "The enhanced J_C and B_{irr} of in situ MgB_2 wires and tapes alloyed with $C4H_6O_5$ (malic acid) after cold high pressure densification," *Superconductor Science & Technology,* vol. 22, Sep 2009.

[30] C. M. Lee, S. M. Lee, G. C. Park, J. Joo, J. H. Lim, W. N. Kang, *et al.*, "Investigation of lauric acid dopant as a novel carbon source in MgB_2 wire," *Physica C-Superconductivity and Its Applications,* vol. 470, pp. 1438-1441, Nov 1 2010.

[31] S. M. Lee, S. M. Hwang, C. M. Lee, W. Kim, J. Joo, J. H. Lim, *et al.*, "Enhancement in the Critical Current Density of C-Doped MgB_2 Wire Using a Polyacrylic Acid Dopant," *Journal of Nanoscience and Nanotechnology,* vol. 12, pp. 1406-1410, Feb 2012.

[32] S. X. Dou, J. Horvat, S. Soltanian, X. L. Wang, M. J. Qin, S. H. Zhou, *et al.*, "Transport critical current density in Fe-sheathed nano-SiC doped MgB_2 wires," *IEEE Transactions on Applied Superconductivity,* vol. 13, pp. 3199-3202, Jun 2003.

[33] S. Soltanian, X. L. Wang, J. Horvat, S. X. Dou, M. D. Sumption, M. Bhatia, *et al.*, "High transport critical current density and large H_{C2} and H_{irr} in nanoscale SiC doped MgB_2 wires sintered at low temperature," *Superconductor Science & Technology,* vol. 18, pp. 658-666, May 2005.

[34] Q. Wang, G. Yan, A. Sulpice, E. Mossang, X. Xiong, G. Liu, *et al.*, "Influence of Amorphous Carbon Doping on Superconductivity of MgB_2/Nb/Cu Wires," *Rare Metal Materials and Engineering,* vol. 41, pp. 1709-1712, Oct 2012.

[35] S. M. Hwang, J. H. Choi, E. C. Park, J. H. Lim, J. Joo, W. N. Kang, *et al.*, "Development of carbon-doped ex situ MgB_2 wire by mechanical alloying," *Physica C-Superconductivity and Its Applications,* vol. 469, pp. 1523-1526, Aug-Oct 2009.

[36] Y. W. Ma, X. P. Zhang, G. Nishijima, K. Watanabe, S. Awaji, and X. D. Bai, "Significantly enhanced critical current densities in MgB_2 tapes made by a scaleable nanocarbon addition route," *Applied Physics Letters*, vol. 88, Feb 13 2006.

[37] S. K. Chen, K. S. Tan, B. A. Glowacki, W. K. Yeoh, S. Soltanian, J. Horvat, *et al.*, "Effect of heating rates on superconducting properties of pure MgB_2, carbon nanotube- and nano-SiC-doped in situ MgB_2/Fe wires," *Applied Physics Letters*, vol. 87, Oct 31 2005.

[38] A. Yamamoto, J. Shimoyama, S. Ueda, Y. Katsura, I. Iwayama, S. Horii, *et al.*, "Effects of sintering conditions on critical current properties and microstructures of MgB_2 bulks," *Physica C-Superconductivity and Its Applications*, vol. 426, pp. 1220-1224, Oct 1 2005.

[39] D. C. Larbalestier, L. D. Cooley, M. O. Rikel, A. A. Polyanskii, J. Jiang, S. Patnaik, *et al.*, "Strongly linked current flow in polycrystalline forms of the superconductor MgB_2," *Nature*, vol. 410, pp. 186-189, Mar 8 2001.

[40] H. Kitaguchi, A. Matsumoto, H. Kumakura, T. Doi, H. Yamamoto, K. Saitoh, *et al.*, "MgB_2 films with very high critical current densities due to strong grain boundary pinning," *Applied Physics Letters*, vol. 85, pp. 2842-2844, Oct 4 2004.

[41] A. Yamamoto, J. Shimoyama, S. Ueda, Y. Katsura, I. Iwayama, S. Horii, *et al.*, "Universal relationship between crystallinity and irreversibility field of MgB_2," *Applied Physics Letters*, vol. 86, May 23 2005.

Chapter 6

Improving the electromechanical properties of MgB_2 superconducting wires

6.1 Introduction

When a superconducting device is fabricated or when the device is operated, the superconducting wires are subjected to various mechanical stress. Hence these wires have to be made in such a way that the stress and strain developed should not deteriorate its superconducting properties beyond an acceptable limit. During the fabrication, if the wires are to be wound into coil, the winding process creates tensile stress as well as bending stress on the wires. While in operation of the devices, during the cooling process mechanical stress can be developed due to varied thermal expansion coefficients of the materials in the composite wire. Another major source of stress the device subjected to is, the stress due to the Lorentz force during the operation [1]. Therefore the electrical properties of the superconducting wire under various mechanical stress or the electromechanical properties of the wires should be evaluated and improved before transfer them for applications.

When comparing the electromechanical properties of conventional LTS materials like NbTi and Nb_3Al with MgB_2 and other HTS materials, the former do well since they are metallic alloys with least anisotropy. But the intermetallic MgB_2 and the oxide ceramic HTS are brittle in nature and have poor mechanical properties. Their current carrying properties are degraded fast when tensile and bending stress exceeds a certain limit [2]. Moreover, the MgB_2 wires prepared by *in situ* PIT method are porous in nature and this again reduces its mechanical strength. This problem has to be addressed seriously while developing MgB_2 wires suitable for applications in superconducting cables, magnets, fault current limiters etc. This chapter presents the evaluation and the

efforts to improve the electromechanical properties of MgB_2 wires prepared via *in situ* route.

6.1.1 'React & Wind' (R&W) and 'Wind & React' (W&R) approaches

For winding coils with superconductor wires, two approaches are often chosen by designers, the react & wind (R&W) method and the wind & react (W&R) method. In former case, the reactants filled and rolled wires are subjected to heat treatment at required temperature in linear geometry or loosely wrapped geometry. These wires are then insulated with an epoxy and wound to the coils of required diameter. In most of the cases, the magnet designing with LTS superconductors follow this R&W approach since they are metallic in nature. But this approach becomes less efficient when we use brittle type superconductors for coil fabrication. The bending stress beyond a threshold level can severely damage the electrical properties of the superconducting wires and thus reduces the current carrying capacity. But, to wind the coils with large diameter this method is efficient for brittle type superconductors too, since the bending strain experienced by the coil is inversely proportional to the bending diameter.

Another method of magnetic coil winding is the W&R method. In this method, the winding is done with the green or unreacted wire. Since there is no unwinding involved, the winding has to be done around a mandrel of required final shape of the coil. After the winding process the system is heat treated at suitable temperature to form the superconducting phase. But a major inconvenience associated with this method is the process of insulation of strands in the coil. Each strand should be electrically insulated from other and the insulation must be able to withstand large electric fields without breakdown and at the same time the insulation layer should be as thinner as possible to increase the winding density. So that high temperature withstanding insulation coating should be applied before the heat treatment. After the heat treatment it should be ensured that the insulation is not damaged at any point. Some designers impregnate the insulation after the heat treatment. Epoxy impregnation is usually used for dry superconductor windings in order to prevent displacement and to form a solid assembly. This also removes as much air as possible and gives better dielectric strength. However voids are unavoidable and overall insulation performance is quite limited. Another problem that

may arise in W&R method is the difference in the thermal expansion of the coil, mandrel insulation etc. and this can cause serious damage to the system under heat treatment. Since the mandrel also must withstand the high sintering temperature, there will be limitations on the selection of material of mandrel. But W&R method is suitable for brittle type superconductors when, either the required coil radius is small or the coil has to be wound in complex shape or with tight bending as in saddle coil, dipole magnets etc.

6.1.2 Calculation of tensile and bending strain

Solids undergo deformation in shape when they are subjected to various stresses such as tensile stress, compressive stress and shear stress. The tensile stress tends to stretch or elongate the object and acts normal to the stressed area. Strain is defined as the deformation of the solid under the stress, or mathematically, it is the ratio of the extension to the original length.

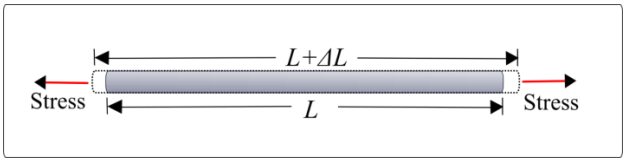

Figure 6.1: Tensile stress on a wire and the associated strain/deformation

So, the tensile strain,

$$\varepsilon = \frac{\Delta L}{L}$$

Where,

ΔL = change in the length

L = original length

It is usual to express the strain ε in %.

Unlike the tensile stress, the stress due to bending causes more complex patterns in the object. During the bending the stress on the object varies in magnitude and direction at different parts. Figure 6.2 shows the schematic diagram of the bending of a

wire of diameter *d* and the wire is bent around a mandrel of diameter *D*. During the process of bending the portion above the neutral axis undergoes tensile stress and elongation in length as depicted in figure 6.2. While the portion below the neutral axis undergoes compressive stress and the length is less than that of the neutral axis. The neutral axis/plane retains the original length of the wire and doesn't experience any stress. So the bending strain can be defined as the ratio of the maximum change in length to the original length. Let θ be the angle subjected by the arc of bent wire at center of the mandrel.

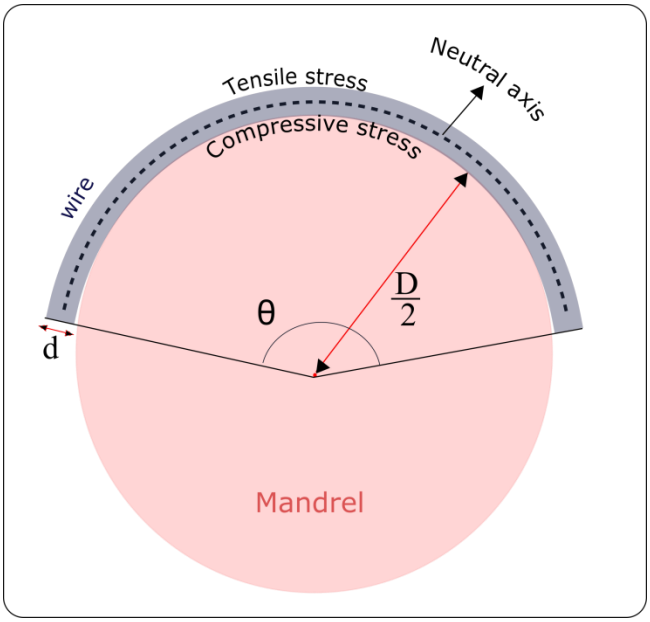

Figure 6.2: Schematic diagram showing the bending of a wire around a mandrel

So the original length or the length of the neutral axis,

$$L = (\frac{D}{2} + \frac{d}{2})\theta$$

The length of the outer arc,

$$L_{out} = (\frac{D}{2} + d)\theta$$

Therefore the change in length,

$$\Delta L = L_{out} - L = \frac{d}{2}\theta$$

So the bending strain is given by,

$$\zeta = \frac{\Delta L}{L} = \frac{d}{d+D}$$

Hence the bending strain is inversely proportional to the bent diameter. The young's modulus (*E*) of a material, which is the measure of stiffness of the material, can be measured by calculating the slope of the stress-strain curve within the elastic limit. As the value of *E* is higher, the stress need to elongate the material also increases. In this work the object under consideration is the superconducting wire which is not a homogeneous object. It includes MgB_2 superconducting core and sheath/barrier/stabilizing materials depending on the monofilamentary or multifilamentary geometry. Since MgB_2 is a brittle material, any elongation beyond the elastic limit causes it to develop crack or to break and hence the current carrying property will be drastically decreased. By the mixing rule, the Young's modulus of a composite is given by,

$$E = \sum_i V_i E_i$$

where V_i is the volume and the E_i is the Young's modulus of the i^{th} material. Therefore to increase the tolerance to the tensile stress of the MgB_2 wire, one can select the sheath with good mechanical strength and adjust the volume ratios between different compositions of materials in wire [3-5]. But since the effect of bending stress is more complex and more relevant in coil winding, it requires a careful study. This chapter focuses mainly on the electrical properties of MgB_2 superconducting wires of various geometry under bending stress and the ways to improve it.

6.2 Effect of bending strain on the J_C of mono-filamentary MgB_2 wires

6.2.1 Introduction

Realizing the potential for applications in cryogen free low cost magnets and other devices, researchers have done some noticeable studies on behavior of MgB_2 conductors under mechanical stress too. Some groups have opted *ex situ* preparation route and have reported the electromechanical properties [6-8]. The results were reported in

tapes and wire geometries. Stress-strain effect of MgB_2 wires with square geometry prepared via *in situ* route has also been reported [4, 9]. In this section, a systematic study on the effect of bending strain on the superconducting behavior of mono filamentary MgB_2/Fe round wires prepared via *in situ* PIT method is presented. A comparison of the results obtained on react & bend (R&B) and bend and react (B&R) approaches is also presented.

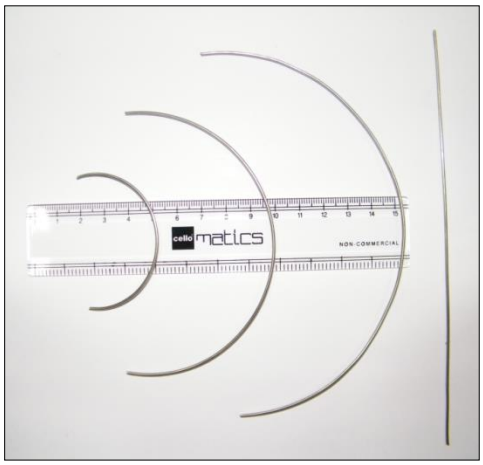

Figure 6.3: Photograph of wires bent at different diameters

The wires were prepared via PIT method (section 5.2). To obtain more workability and hence densification of core, tubes of 5mm/3mm of OD/ID were used for this study. After rolling down to the diameter of 1.67 mm, one set of wires was bent around mandrels of 10, 5 and 2.5 cm diameters. These wires were end sealed and heat treated at 650 °C for 2 hours along with a straight wire and this set was labeled as B&R. To prepare R&B set, heat treated straight wires were cut and bent to different diameters as in B&R set. The phase purity of the polycrystalline MgB_2 was initially assessed by Powder X-ray diffraction done on the MgB_2 powder retrieved from annealed monofilamentary wires. It was found that both B&R and R&B wires consisted of about 97.5% MgB_2. The superconducting characterizations were done in the cryogen-free-cryocooler system using specially fabricated sample holders to hold the bent wires. The I-V characterization was done at 20 K. SEM imaging was done on the cross section of the reacted and bent wires bent at 2.5 cm diameter to study the effect of stress on the microstructure of MgB_2 core.

6.2.2 Results and discussion

Figure 6.4 shows the microstructure of the cross section of the reacted and bent (R&B) wire sample bent at 2.5 cm diameter. As stated earlier, the bending causes to develop both tensile and compressive stress in a material. From the less magnified SEM image itself, the effect of bending on microstructure is clear. For better clarity, two areas - one above and one below from the neutral axis – are selected and their enlarged view is shown as insets of figure 6.4.

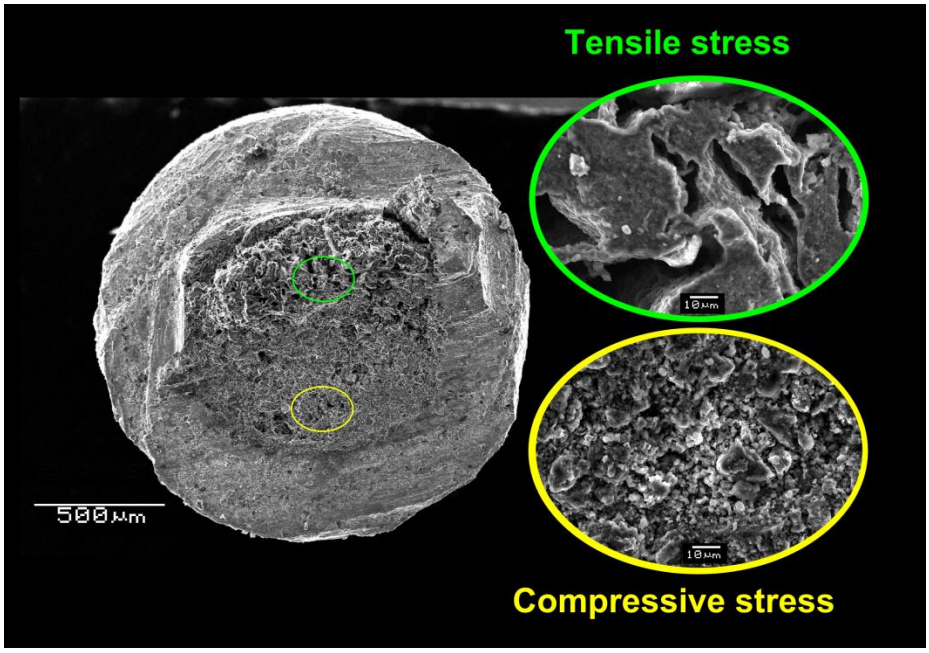

Figure 6.4: SEM image of the cross section of R&B wire of diameter 2.5 cm. The insets show the enlarged views of the area under the tensile and compressive stress

The grains from the area under tensile stress seem to be stretched and separated with large gaps between them. While the grains form the area under the compressive stress appear to be smaller and compacted as they are crushed due to compression. In both cases the connectivity between the grains is severely affected due to bending.

The R-T plots of the R&B set of samples are shown in figure 6.5. An upward shift in the normal state resistance is observed for all the bend samples and the shift increases with increase in bending strain or decrease in bending diameter. This is due strain effect on the sheath metal and increased resistance due to reduced grain connectivity. The T_C

onset and the ΔT_C are estimated and tabulated in table 6.1. As the bending strain increases the T_C onset decreases and ΔT_C increases. This is due to the loss in connectivity as seen from the SEM image. For the bending radius of 10 cm, the shift in T_C is small and width of transition is not large. But as the bending radius is reduced the changes in both T_C and ΔT_C become more significant and noticeable.

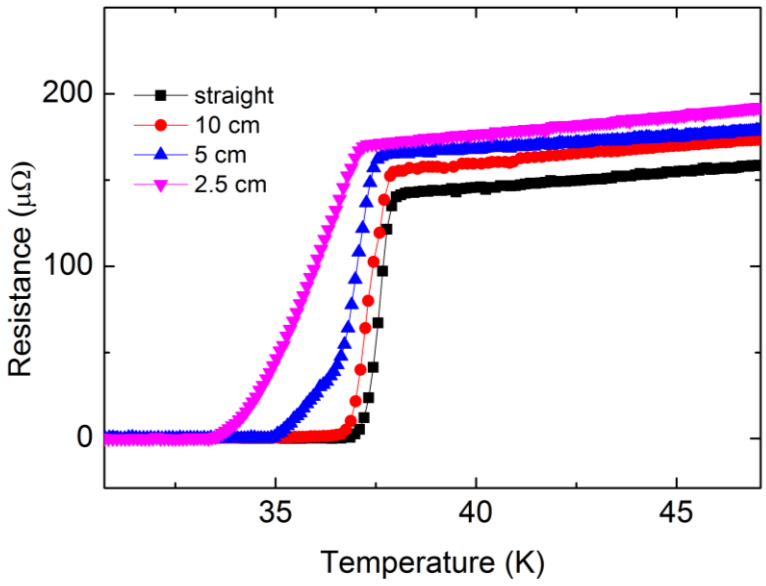

Figure 6.5: R-T plots of the R&B wires and the straight wire

Table 6.1: Bending parameters and corresponding superconducting properties of R&B wires

Bend Diameter (cm)	Bending Strain (%)	T_C (K)	ΔT_C (K)	J_C at 20 K ($\times 10^4$A/cm^2)	% of $J_{C,max}$
Straight	0	38.02	1.0	2.2	100
10	1.64	37.86	1.2	1.5	68
5	3.23	37.55	2.5	0.6	27
2.5	6.01	37.11	3.7	0.4	18

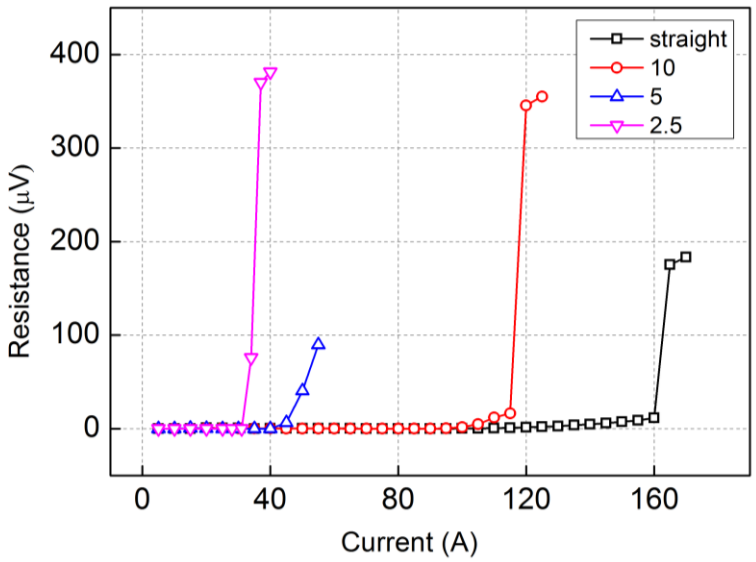

Figure 6.6: I-V plots of the R&B wires along with straight wire measured at 20 K

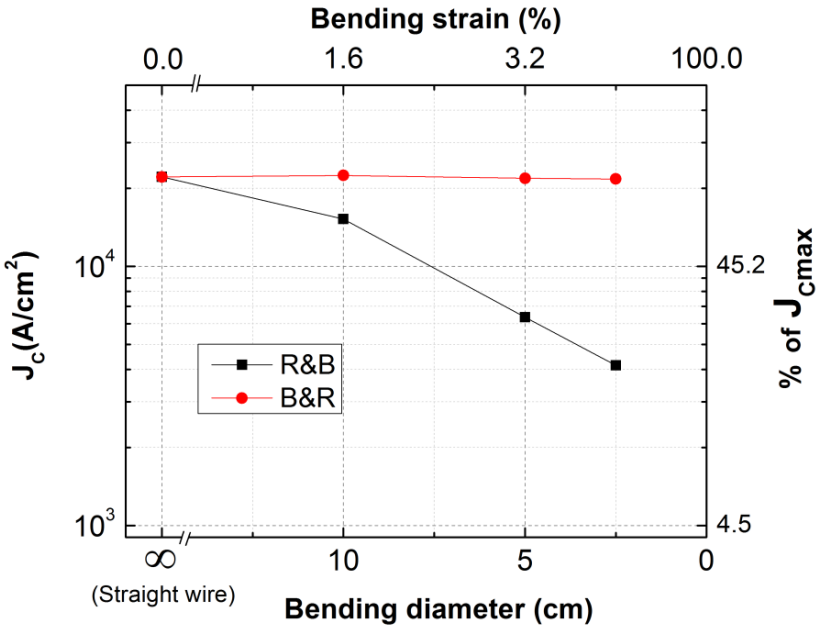

Figure 6.7: Comparison of the J_C of R&B and B&R set of wires with bending strains measured at 20 K

The I-V measurements were done at the temperature of 20 K and the obtained plots for R&B wires are shown in figure 6.6. The corresponding J_C values are estimated and tabulated in the table 6.1. As expected the degradation in J_C with bending can be

observed. At the bending diameter of 10 cm (ζ ~ 1.64 %) the J_C is reduced to ~ 68% of the straight wire and at D = 5 cm, the J_C retained is only 27% of the straight wire.

Figure 6.7 shows a comparison of transport J_C values obtained for both R&B and B&R set of wires measured at 20 K at different bending diameters/strains. The wires which were heat treated after bending (B&R) do not show any significant variations in the J_C from that of the straight wire. This shows the advantage of W&R method of coil making in the aspect of preservation of current carrying capacity. Based on the results obtained, one can conclude that, the reacted monofilamentary wires are less suitable for the fabrication of devices where the bending strain is inevitable.

6.3 Enhanced bending strain tolerance in MgB_2 multifilamentary wires

The multifilamentary wires are most suitable for the magnet applications due to high thermal stability and low ac losses. Another advantage is its increased bending strain tolerance in comparison to monofilamentary wires. There are reports on stress/strain effect on multifilamentary MgB_2 wires with barrirer/sheath combinations such as MgB_2/Ti/Cu/SS and MgB_2/Ta/Cu and MgB_2/Nb/Cu [3, 5, 8, 10] . The aim of this work is to analyze the effect of the bending stress/strain on the current carrying property of the multifilamentary MgB_2/Fe/Ni superconducting wires, prepared via *in situ* route with varying the number of filaments. The R&B and B&R sets of wires were prepared and compared in this study also.

The multifilamentary wires were prepared as depicted in section 5.5.1. But since wires with increased number of filaments were necessary for this study, Ni sheaths of ID/OD ratio 6/8 and 8/10 were also used to make 8 and 16 filamentary wires respectively. The composites were groove rolled down to an OD of 1.67 mm. The wires were cut into sufficient length and number of pieces to make B&R and R&B sets. The bending diameters selected for the study were 15, 10 and 5 cm. The heat treatment was done at the optimized temperature of 650 °C for 2 hours. To assure the phase purity, a monofilamentary wire was also heat treated along with the sample set for retrieving the sample.

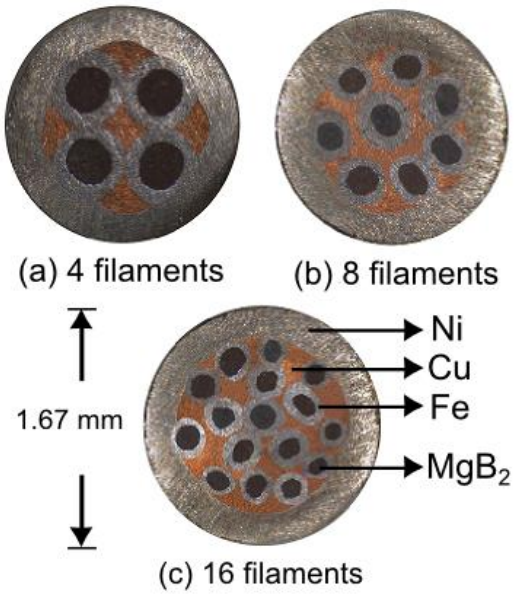

Figure 6.8: Optical images of cross sections of 4, 8 and 16 filamentary wires

Table 6.2: Bending parameters and critical current densities of 4, 8, and 16 filamentary R&B wires

Bending Diameter (cm)	Bending Strain(ζ) (%)	Filament number					
		4		8		16	
		J_C ($\times 10^5$ A/cm^2)	% of $J_{C,max}$	J_C ($\times 10^5$ A/cm^2)	% of $J_{C,max}$	J_C ($\times 10^5$ A/cm^2)	% of $J_{C,max}$
straight	0	2.60	100	2.61	100	2.62	100
15	1.1	1.85	71	2.1	80	2.24	86
10	1.6	1.61	62	1.85	71	2.1	80
5	3.2	0.86	33	1.43	55	1.67	63

The phase purity of the polycrystalline MgB_2 was initially assessed by Powder X-ray diffraction done on the MgB_2 powder retrieved from the annealed monofilamentary wires and found to be consisted of about 97.5% MgB_2. Figure 6.8 shows the optical image of the cross sections of the 4, 8 and 16 filamentary wires after the heat treatment. The image shows the distinct MgB_2 core from Fe barrier without any reaction layer formation. The filaments are intact without any cracks and distributed in the Cu stabilizer

matrix and protected by the Ni outer sheath. There is no significant diffusion of Cu into the barrier or sheath metal is observed. The average filament diameters are found to be 0.30 mm, 0.18 mm and 0.12 mm for 4, 8 and 16 filamentary wires respectively. The bending strain (ζ) on multiwires with respect to the bending diameters is tabulated in Table 6.2.The bending strain becomes higher as the bending diameter decreases.

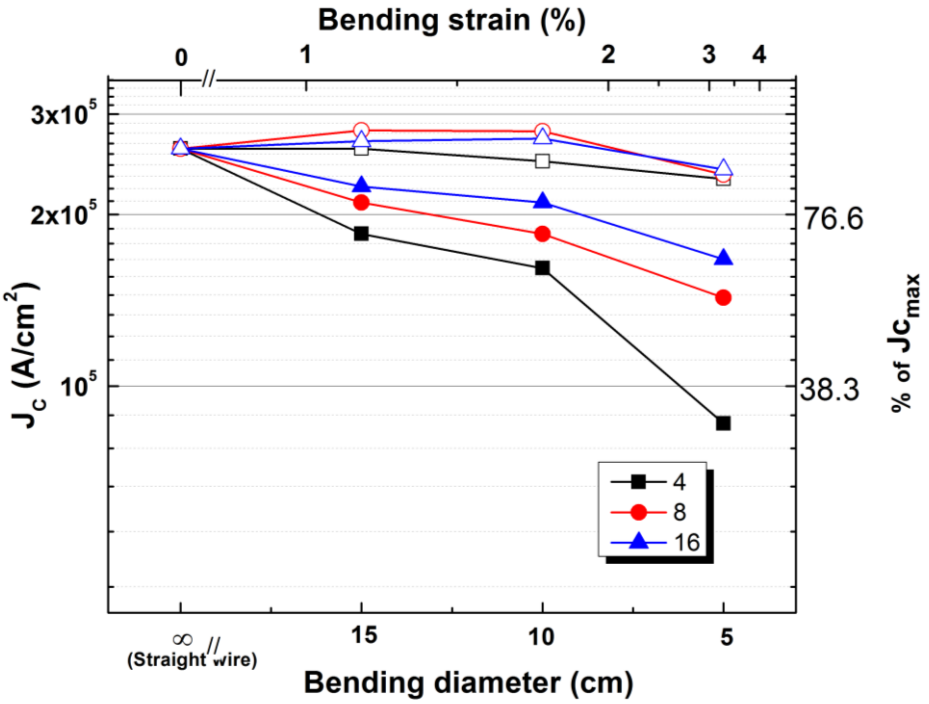

Figure 6.9: Variation of J_C with bending diameters and strain in 4, 8, and 16 filamentary MgB_2 multiwires for both B&R (open) and R&B (closed) sets at 4.2 K

Multiwire samples of 5 cm in length, cut from the middle of each of the wires were used for measurement of superconducting properties. The critical current density of the all wires was measured at 4.2 K in a liquid Helium cryostat at 1 μV/cm criterion. Fig. 6.9 shows the plots of self-field transport J_C as a function of bending diameter and strain for 4, 8 and 16 filamentary MgB_2 multiwires for both B&R and R&B sets at 4.2 K. A J_C about 2.61×10^5 A/cm^2 is obtained for all straight wire samples. The filamentation of MgB_2 wire into 4, 8 and 16 filament geometry has negligible impact on the transport J_C of B&R wires down to the bent diameter of 5 cm, while for R&B wires degradation of J_C is found to be lesser for wires with higher filament numbers. Also on comparing the B&R

and R&B sets, the degradation in J_C with decrease in bending diameter is rapid for the latter, i.e. the wires that are bent after the heat treatment; while the for the former, i.e. the wires that are heat treated after bending, the degradation in J_C is not so significant. The R&B 4-filamentary wire shows a 29% J_C reduction at the bending diameter 15 cm itself and at 5 cm of bending diameter, the J_C retained is only 33% of the initial value. But the 16 filament R&B multiwire could retain about 63% of J_C of straight wire. The lower bending strains on individual filaments of 16 filament multiwire justify this.

Although it is found that the bending strain tolerance is increased with number of filaments, it doesn't guarantee an achievement of a very high tolerance on simply increasing the number of filaments. The highly porous nature of the core and hence a significantly lower density than theoretical density in *in situ* prepared wires, can cause severe damage on the filaments on bending at lower diameters. This is supported by the work of Wang *et al.* where a 36 filamntary MgB_2/Nb/Cu wire showed rapid reduction in J_C with bending than that of a 6-filamentary wire [10]. Therefore to achieve a further increased bending strain tolerance in *in situ* wires, an entirely different approach is required.

6.4 Excess Mg addition: a novel approach to enhance bending strain tolerance of *in situ* PIT MgB_2 wires

6.4.1 The method of excess Mg addition

As described in the previous section, to achieve a major enhancement in electromechanical properties of MgB_2 wire, prepared via in situ PIT method, a serious attention towards minimizing the porosity and hence maximizing the density and grain connectivity of the reacted MgB_2 core inside is necessary. Normally, the density of MgB_2 bulk, wires and tapes prepared via in situ reaction route is as low as around 50 % of the theoretical density (2.62 g/cm^3). the volume reduction during the reaction between Mg and B, lack of proper densification during the filling and higher volatile loss of Mg during the heat treatment above the melting point of Mg are the major reasons for such a disastrous reduction in density of MgB_2 phase. Various attempts to increase the density and connectivity of MgB_2 wires have been reported by different groups. Some of them

suggest to employ diffusion technique or coated conductor technique instead of PIT method [11-15]. The layered core of MgB_2 in wires formed by internal Mg diffusion techniques has shown high density and grain connectivity. But these approaches are not as convenient and scalable as PIT method for long length conductor fabrication. In PIT method, low temperature solid state sintering was found to increase the density and connectivity by several studies. But due to the decreased atomic diffusion rate in solid state, below the melting point of Mg, a long duration of heat treatment is required to form complete MgB_2 phase. To accelerate the phase formation and hence to decrease the reaction time, the methods like ball milling of the starting precursors, addition of metallic sintering aids or use of different Mg-based precursors have been tried and found to be effective [16-21].

There have been reports that a slight excess magnesium addition to compensate anticipated Mg loss improves the normal state properties, grain connectivity and critical current. In an attempt to improve the self-field current carrying capacity by lowering the sintering temperature, we prepared MgB_2 wires heat treated at 600 °C for 5 hours. Though the XRD study revealed the incomplete phase formation and presence of excess residual Mg, the wires showed good current carrying capacity. This showed that presence of excess Mg does not hinder the connectivity and flow of supercurrent in a low temperature synthesized MgB_2. Motivated from this result, in order to elude the excess amount of unreacted amorphous boron corresponding to that of unreacted Mg and to fill the related amount of Mg inside the voids and grain boundaries we increased the stoichiometry of Mg from one to many fold in steps and prepared wires through low temperature processing. The superconducting characterization of these wires gave promising results and brought a new opportunity to develop low cost MgB_2 superconductors with improved self-field transport J_C [22].

The stoichiometry of the wires was varied from (1Mg + 2B) to (7Mg +2B). Figure 6.10 provides the measured transport infield critical current densities at 20 K. The normal state properties, grain connectivity and transport current of these Mg/MgB_2 composite wires were found to be enhanced without much affecting T_C against the expectation. The sample with initial stoichiometry (6Mg + 2B) showed the best J_C value.

The presence of residual Mg in the sample causes a significant reduction in normal state resistivity of the composite, while the MgO content and porosity due to volatile Mg loss are limited by low temperature heat treatment. In short, the overall grain connectivity in the system is improved which enhances the self-field critical current density. The objective of the present work is to study the bending strain tolerance of the optimized sample (6Mg + 2B) from the above study and compare the results with that of the *in situ* MgB_2 PIT wires without excess Mg.

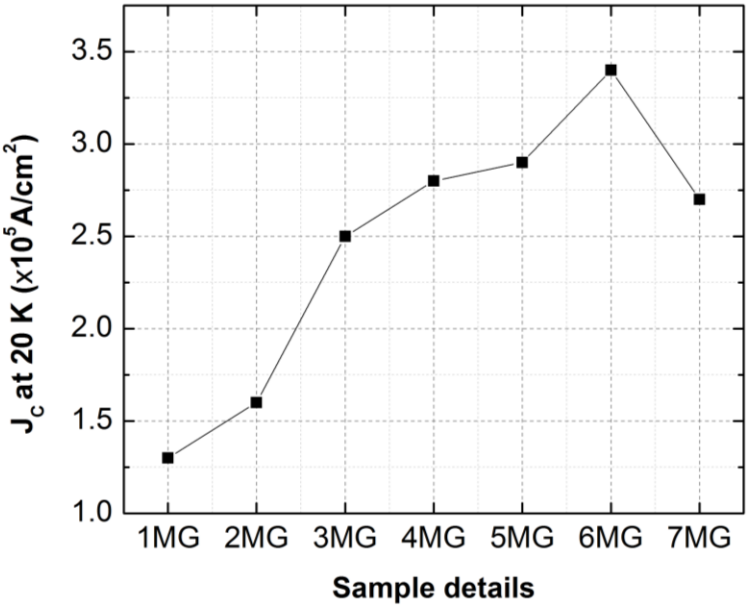

Figure 6.10: Variation in J_C of excess Mg added samples

6.4.2 Evaluation of bending strain tolerance in excess Mg added wire

Although the adverse effect on electromechanical property due to brittle nature of a superconductor can be overcome up to an extent by making multifilamentary wires with very fine filaments, in the case of MgB_2 superconductor, the presence of porosity/voids is a major limitation to this approach. But the method of excess Mg addition is found to be an effective way to increase density and to decrease porosity of MgB_2 wires prepared via in situ method. This gives an opportunity to further improve the bending strain tolerance of MgB_2 superconductor wires. When we analyze the J_C values of excess Mg added wires as discussed in the previous section, the wire with a composition, 6Mg + 2B

(sample 6MG) is found to be have best critical current density at 20 K. Therefore this composition was chosen for detailed study of bending strain tolerance.

Experimental details

Mg powder (<105 µm, 99.8 % purity), amorphous B powder (<44 µm, 99 % purity), and commercially available Fe tubes were used for the in situ PIT wires. Fe tubes of length 10 cm, outer diameter (OD) 6 mm and inner diameter (ID) 4 mm were used for the fabrication of wires. The tubes were filled with homogeneously mixed precursor powder 6Mg + 2B and mechanically compacted. The composite tubes were then groove rolled into wires of 1.67 mm OD. These were cut into short length (10 cm) samples and end sealed. The sealed wires were then heat treated directly in air at 600 °C for 5 hours in a muffle furnace followed by furnace cooling. As a reference, a normal stoichiometric MgB_2 sample was also prepared by heat treating at 650 °C for 2 hours. To prepare R&B set, the reacted wires were bent around cylindrical mandrels of radius 15, 10, 5 and 2.5 cm. The wires which were bent to these radii, prior to heat treatment were labeled as B&R set. A straight wire was also included in each set as a reference for comparison.

The structural and phase analysis of the samples were done using an X-Ray Diffractometer (Philips X'pert Pro) with Cu Kα radiation employing X'Celerator detector and monochromator at the diffracted beam side in the Bragg-Brentano configuration. Samples for the XRD analysis were recovered from the wires by mechanically grinding and peeling off the Fe sheath and powdering the reacted core and the patterns were taken using a zero background holder. Phase identification of the samples was performed using X'Pert Highscore Plus Software in support with ICDD-PDF-2 database. Transport critical current (I_C) measurements at various temperatures were carried out by employing a heavy duty cryocooler-interfaced cryostat using DC four probe resistive method.

Results and discussion

XRD pattern of the superconducting cores of Fe sheathed excess Mg added wire sample, heat treated at 600 °C is shown in figure 6.11. The pattern of stoichiometric MgB_2 sample, heat treated at 650 °C is also presented in the same figure as a reference

pattern for the sake of comparison in which MgB_2 is found to be the main phase with some traces of MgO. The traces of MgO detected in XRD may be due to the higher heat treatment temperature of the sample. XRD patterns of the excess Mg added wire samples, heat treated at 600 °C shows a very large amount of unreacted Mg compared to the reference sample with a hump of MgB_2 main peak. Moreover, absence of the peaks corresponding to Fe and Fe containing compounds indicates that there is no interfacial reaction occurring between the Fe sheath and Mg/B/MgB_2 at these temperatures.

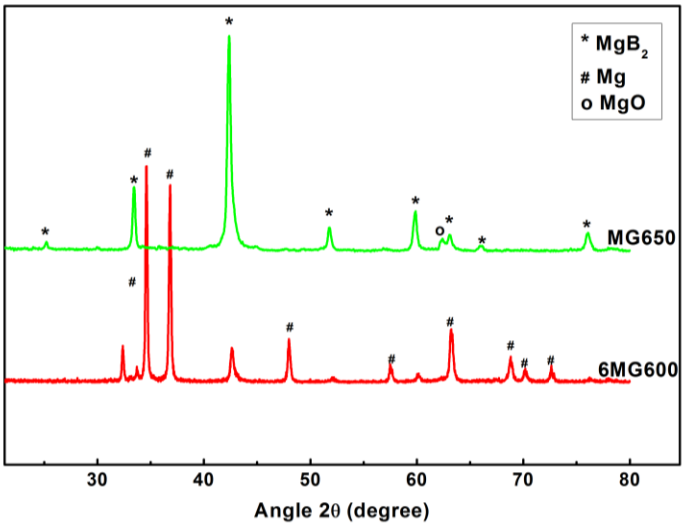

Figure 6.11: XRD patterns of the excess Mg added wire samples heat treated at 600 °C/5 hours (6MG600) and stoichiometric MgB_2 sample heat treated at 650 °C/2 hours (MG650)

In order to understand the effect of bending strain, both B&R and R&B sets of wires bent to different bending diameters were subjected to transport critical current measurements. Bending of all the samples was done at room temperature and the bending strain in percentage, ζ was determined using the equation, $\zeta = \frac{d}{d+D} \times 100$, Here, d is the diameter of wire and D is the bending diameter. The bending strain corresponding to each bending diameter is marked in figure 6.12. As expected, the bending strain becomes higher as the bending radius decreases. The figure shows the plots of self-field transport J_C of the excess Mg added MgB_2 wires (6MG600) as a function of bending diameter and bending strain measured at 20 K. The J_C of straight, stoichiometric sample heat treated at 650 °C is given as a reference for comparison. The presence of residual Mg metal

fraction assists in the enhancement of J_C instead of degrading it. When compare the effect of bending on transport J_C of both B&R and R&B set of wires, degradation in J_C is observed in R&B wires. But about 91 % of the initial J_C is conserved for the R&B wires even at a bending diameter of 2.5 cm, and only 3 % of reduction in J_C is observed at a bending diameter of 5 cm. These values indicate excellent bending strain tolerance even in R&B type excess Mg added wires. In B&R wires, the decrease in bending diameter induces more core compaction of the core which slightly enhances J_C beyond the initial value up to a bending diameter of 5 cm and decreases subsequently.

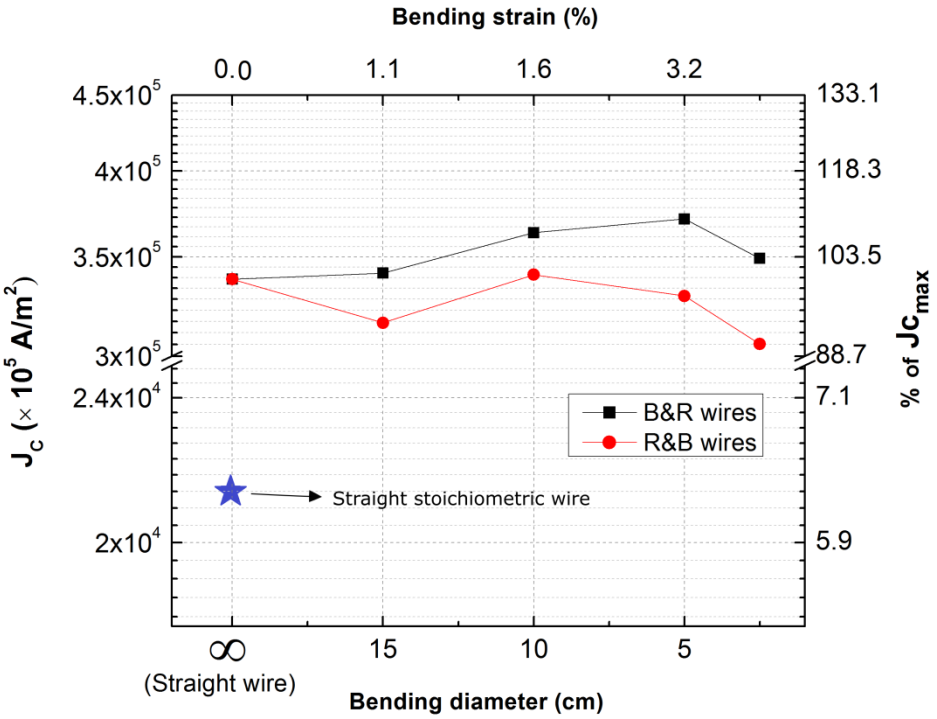

Figure 6.12: Variation of transport J_C with bending diameters for the excess Mg added MgB_2wire (6MG600) both B&R and R&B sets at 20 K

To further investigate the mechanism of improved bending strain tolerance, the microstructure of the excess Mg added wire was studied using an optical microscope. Figure 6.13 shows the optical image of the polished surface of excess Mg added wire. The unreacted-excess Mg is visible as bright metallic grains. These grains are surrounded by thin layer of grey colored MgB_2 formed by solid state diffusion. The remaining black

spots are due to the presence of unreacted B and pores. The solid state diffusion process causes to form 'layered core' of MgB_2 superconductor with thickness of the order of few micrometers.

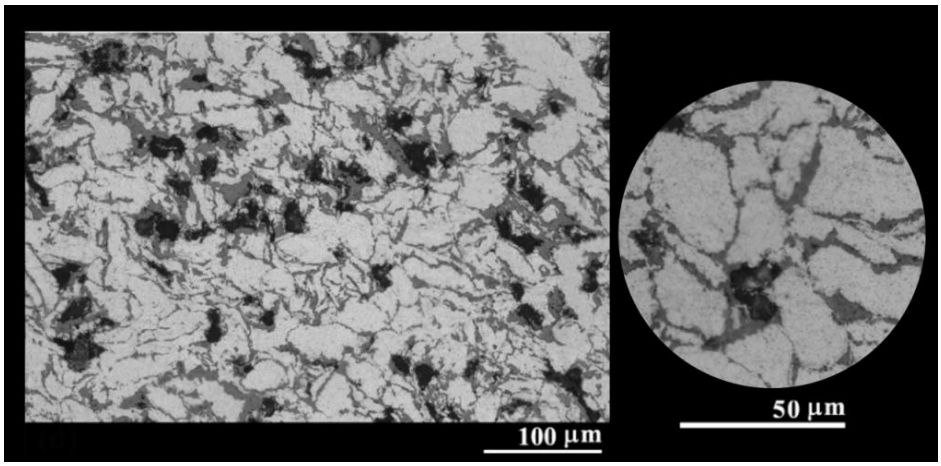

Figure 6.13: Optical image of polished cross-section of excess Mg added MgB_2wire (6MG600)

The observed high transport J_C values in these wires indicate that the formed layers are highly compacted/densified and well-connected from end to end. Therefore, the fine sized layers of MgB_2 embedded in Mg metal matrix with high density and connectivity causes to have a great bending strain tolerance in these wires. The studies on bending strain tolerance of MgB_2 films prepared by HPCVD technique have been reported earlier. Zhuang *et al.* has reported the preparation of MgB_2 films on stainless steel and niobium substrates with remarkable ductility [23, 24]. The thickness of the prepared films ranges from 1 μm to 20 μm, and even at a high degree of bending with radius of curvature 0.5 mm, the superconducting properties were almost unaffected. The remarkable strain tolerance of excess Mg added wire appears like the results obtained in MgB_2 films because of its micrometer sized layered core structure which is formed by solid state diffusion process at a very slow rate.

Conclusions

The method of excess Mg addition is found to be very effective in enhancing both self-field critical current density and electromechanical properties of MgB_2 superconductor wires. The wire with a composition of 6Mg+2B was heat treated at 600

°C for 5 hours to obtain a microstructure wherein micrometer thick, layered cores of MgB_2 embedded in magnesium metal. The metallic matrix formed by Mg holds MgB_2 superconductor layer within, and provides better bending strain tolerance to superconducting current. The J_C of wires of both R&B and B&R sets hardly degrades even at a bending diameter of 5 cm. The high bending strain tolerance in excess Mg added wires resembles that in MgB_2 films of few microns thickness prepared by HPCVD technique. The method of excess Mg addition opens up new avenues to fabricate MgB_2 coils for practical applications even by the R&W approach.

6.5 Summary

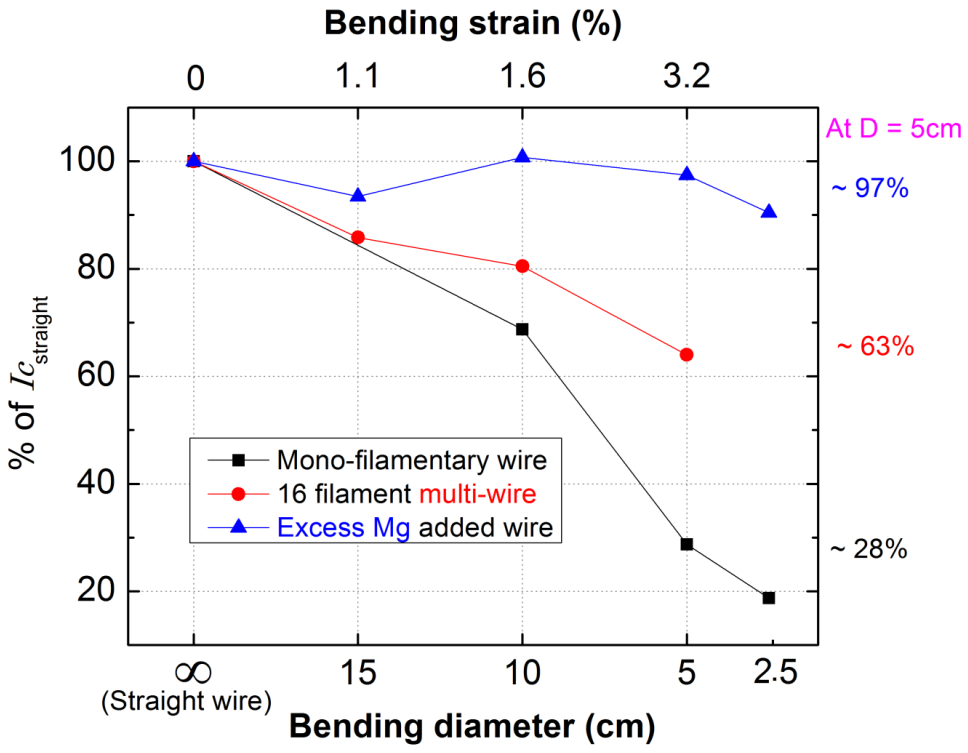

Figure 6.14: Comparison of variation in current carrying capacity of different wires (R&B) under bent strain

Studies on improvement of electromechanical properties of MgB_2 wires were done by making wires of different wire geometry, modifying the superconductor

composition and processing schedule. The effect of bending strain tolerance was investigated by measuring the self-field critical current density of the wires bent to different diameters. The superconducting wires were prepared by *in situ* approach and the studies were conducted on both R&B and B&R samples. Monofilamentary MgB_2/Fe wires exhibited least tolerance in J_C towards the bending due to its highly porous nature and poor grain connectivity. Studies on MgB_2/Fe/Ni multifilamentary wires with Cu stabilizer comprising 4, 8, and 16 showed that the 16-filamentary wire could preserve the initial J_C to very good level. However, the bend strain tolerance of the wires still needs improvement not only for development of coils with smaller diameters but also to retain the maximum possible J_C in all type of bent coils. A novel approach of synthesis of MgB_2 wire was used to further improve the bending strain tolerance in which excess Mg is added in large proportions to the precursors and heat treated at a lower temperature of 600 °C for 5 hours. The method was found to be very effective to increase bending strain tolerance remarkably and yielded superconducting wires with very small reduction in J_C values with bending. As expected, in various approaches tried, the effect of bending on J_C of the B&R set of wires is less significant. The results in R&B set of wires obtained from various approaches to enhance electromechanical properties were summarized in figure 6.14.

REFERENCES

[1] P. J. Lee, *Engineering Superconductivity*: Wiley, 2001.

[2] P. Seidel, *Applied Superconductivity: Handbook on Devices and Applications*: Wliey, 2015.

[3] W. Goldacker, S. I. Schlachter, B. Obst, B. Liu, J. Reiner, and S. Zimmer, "Development and performance of thin steel reinforced MgB_2 wires and low-temperature in situ processing for further improvements," *Superconductor Science & Technology,* vol. 17, pp. S363-S368, May 2004.

[4] A. Hanna, H. Fang, Y. X. Zhou, A. Alessandrini, P. T. Putman, and K. Salama, "Mechanical properties of superconducting MgB_2 wire," *Journal of Materials Processing Technology,* vol. 181, pp. 44-47, Jan 1 2007.

[5] P. Kovac and L. Kopera, "Electromechanical Properties of Filamentary MgB_2 Wires," *Ieee Transactions on Applied Superconductivity,* vol. 22, Feb 2012.

[6] M. Y. Fu, J. X. Chen, Z. K. Jiao, H. Kumakura, K. Togano, L. R. Ding, *et al.*, "Mechanical properties and bending strain effect on Cu-Ni sheathed MgB2 superconducting tape," *Physica C-Superconductivity and Its Applications,* vol. 406, pp. 53-57, Jul 1 2004.

[7] K. Katagiri, R. Takaya, K. Kasaba, K. Tachikawa, Y. Yamada, S. Shimura, *et al.*, "Stress-strain effects on powder-in-tube MgB2 tapes and wires," *Superconductor Science & Technology,* vol. 18, pp. S351-S355, Dec 2005.

[8] P. Kovac, I. Husek, T. Melisek, M. Dhalle, M. Muller, and A. D. Ouden, "The effect of shape and deformation in ex situ MgB_2-W/Fe composite wires," *Superconductor Science & Technology,* vol. 18, pp. 615-622, May 2005.

[9] K. Salama, Y. X. Zhou, M. Hanna, M. Alessandrini, P. T. Putman, and H. Fang, "Electromechanical properties of superconducting MgB2 wire," *Superconductor Science & Technology,* vol. 18, pp. S369-S372, Dec 2005.

[10] Q. Wang, G. Yan, P. Zhang, A. Sulpice, F. Yang, X. Xiong, *et al.*, "Influence of bending strain on mono- and multi-filamentary MgB_2/Nb/Cu wires and tapes," *Physica C-Superconductivity and Its Applications,* vol. 484, pp. 163-166, Jan 2013.

[11] G. Giunchi, "High density MgB_2 obtained by reactive liquid Mg infiltration," *International Journal of Modern Physics B,* vol. 17, pp. 453-460, Mar 10 2003.

[12] V. Ferrando, P. Orgiani, A. V. Pogrebnyakov, J. Chen, Q. Li, J. M. Redwing, *et al.*, "High upper critical field and irreversibility field in MgB_2 coated-conductor fibers," *Applied Physics Letters*, vol. 87, Dec 19 2005.

[13] G. Giunchi, G. Ripamonti, E. Perini, T. Cavallin, and E. Bassani, "Advancements in the reactive liquid Mg infiltration technique to produce long superconducting MgB_2 tubular wires," *IEEE Transactions on Applied Superconductivity*, vol. 17, pp. 2761-2765, Jun 2007.

[14] M. Ranot and W. N. Kang, "MgB_2 coated superconducting tapes with high critical current densities fabricated by hybrid physical-chemical vapor deposition," *Current Applied Physics*, vol. 12, pp. 353-363, Mar 2012.

[15] G. Giunchi, L. Saglietti, A. F. Albisetti, E. Perini, C. Schiavone, G. Ripamonti, *et al.*, "MgB_2 Hollow Wires and Cables Embedded in a Mg Alloy Matrix," *Ieee Transactions on Applied Superconductivity*, vol. 23, Jun 2013.

[16] W. Hassler, C. Rodig, C. Fischer, B. Holzapfel, O. Perner, J. Eckert, *et al.*, "Low temperature preparation of MgB_2 tapes using mechanically alloyed powder," *Superconductor Science & Technology*, vol. 16, pp. 281-284, Feb 2003.

[17] J. H. Kim, S. X. Dou, J. L. Wang, D. Q. Shi, X. Xu, M. S. A. Hossain, *et al.*, "The effects of sintering temperature on superconductivity in MgB_2/Fe wires," *Superconductor Science & Technology*, vol. 20, pp. 448-451, May 2007.

[18] Z. Ma, Y. Liu, L. Yu, and Q. Zhao, "The accelerated formation of MgB_2 phase with high critical current density by Cu and SiC multidoping during the low-temperature sintering process," *Journal of Applied Physics*, vol. 104, Dec 1 2008.

[19] J. C. Grivel, N. H. Andersen, P. G. A. P. Pallewatta, Y. Zhao, and M. von Zimmermann, "Influence of Bi, Se and Te additions on the formation temperature of MgB_2," *Superconductor Science & Technology*, vol. 25, Jan 2012.

[20] L. Yongchang, L. Feng, M. Zongqing, C. Ning, L. Huijun, B. Shaon, *et al.*, "Significantly enhanced critical current density in nano-MgB_2 grains rapidly formed at low temperature with homogeneous carbon doping," *Superconductor Science and Technology*, vol. 28, p. 055005, 2015.

[21] N. Varghese, K. Vinod, S. Rahul, K. M. Devadas, S. Thomas, S. Pradhan, *et al.*, "Influence of nano-Cu additive on MgB_2 phase formation, processing temperature, and transport properties," *Journal of Applied Physics*, vol. 109, Feb 1 2011.

[22] K. M. Devadas, "Studies on development of MgB_2 based superconducting current leads," Ph. D. Thesis, Faculty of Science, Cochin University of Science and Technology (CUSAT), India, 2015.

[23] C. g. Zhuang, L. An, L. p. Chen, L.-l. Ding, K.-c. Zhang, C.-p. Chen, *et al.*, "MgB_2 thick films with remarkable ductility on stainless steel substrate," *Frontiers of Physics in China*, vol. 1, pp. 246-250, 2006// 2006.

[24] Z. Chenggang, Y. Dan, L. Fen, Z. Kaicheng, F. Qingrong, and G. Zizhao, "Study of micron-thick MgB_2 films on niobium substrates," *Superconductor Science and Technology*, vol. 20, p. 287, 2007.

Chapter 7

Summary and Conclusions

7.1 Summary

The main objectives of the present study were to develop cost-effective MgB_2 superconductor wires and to study and improve the in-field critical current density and the electromechanical properties.

The chemical doping method was opted in this work to improve $J_C(H)$ performance of MgB_2 superconductor. In order to study the basic characteristics and properties of doped MgB_2, studies were initially carried out in bulk form of superconductor, before fabricating them into wires. The *in situ* Powder In Sealed Tube (PIST) method was used to prepare doped and undoped MgB_2 in bulk. The carbon was found to be a suitable dopant to increase the $J_C(H)$ by its substitutional effects. Among the two different carbon forms-n-D and n-C-tried, n-C was found to be the best. To further enhance the $J_C(H)$ of MgB_2, co-doping the MgB_2 with two or more dopants was adopted. Instead of doping MgB_2 with nano-SiC, the co-doping with n-C and n-SiO_2 was found to be more effective. In another co-doping study, addition of n-Cu as a co-dopant was studied and found to be advantageous to provide good in-field J_C values.

To prepare MgB_2 in mono and multifilamentary forms, the most popular Powder In Tube (PIT) method was used. For this, Fe was chosen as the most acceptable sheath material among the commonly used sheath materials namely, Fe, Cu, Ni and SS by comparing their properties such as reactivity with Mg and B, malleability, electrical and thermal conductivity and cost. To prepare the multifilamentary wires, Ni was selected as the outer sheath, Fe as the barrier material and OFHC copper was used as the stabilizer material for thermal stability. The studies on enhancement of the $J_C(H)$ of the MgB_2 wires was also done on the basis of the results obtained on the bulk form of the

superconductor. For this, the processing parameters were optimized to obtain the best results in respect of nano-carbon substituted MgB_2. The results of co-doping study in wires were almost in line with that of the bulk samples. The results achieved in this work are at par with the international results and the wires in long length multifilamentary form can be used for practical applications.

Next step was to study and improve the electromechanical properties of MgB_2 wires, with focus on the effect of bending strain on J_C values, by making wires of different wire geometry, modifying the superconductor composition and processing schedule. The effect of bending strain was investigated by measuring the self-field critical current density of the wires bent to different diameters. The studies were conducted on both 'react and bend' and 'bend and react' set of samples. Monofilamentary MgB_2/Fe wires exhibited least tolerance in J_C towards the bending due to its highly porous nature and poor grain connectivity. Studies on MgB_2/Fe/Ni multifilamentary wires with Cu stabilizer and 4, 8, and 16 filament numbers showed that the 16-filamentary wire could preserve the J_C of the straight wires to a very good level. A further improvement was achieved by adopting a novel synthesis route of MgB_2 wire fabrication proposed by our group; in which excess Mg was added in large proportions to the precursors and heat treated at a lower heat treatment temperature of 600 °C for 5 hours. The method was found to be very effective to increase bending strain tolerance remarkably and yielded superconducting wires with very small reduction in J_C values with bending.

7.2 Conclusions

- The effect of carbon doping on the structure and in-field *superconducting* properties of bulk MgB_2 superconductor was studied using two different carbon forms namely, n-C and n-D. The sample with 0.1 at.% of n-C ($MgB_{1.9}C_{0.1}$) was found to be have the best $J_C(H)$ performance

  The carbon substitution and resultant lattice strains helped this sample to improve its $J_C(H)$ behavior. The J_C of the best sample was enhanced by 38 times that of the pure sample at 8 T and 5 K.

- The Co-doping effect of n-C and n-SiO_2 in MgB_2 was studied and the results were compared with pure and mono doped n-C and n-SiC samples. The study showed that the $J_C(H)$ performance of the co-doped sample distinctly dominated the other samples throughout entire range of magnetic field studied. Better carbon substitution, improved grain connectivity as observed from SEM and inferred from high J_C values at low fields and homogeneous distribution of nano-sized Mg_2Si made the co-doped sample to perform better than the others throughout the entire field range of study (0 - 8 T).
- The effect of nano-copper as a metallic co-dopant in MgB_2 was investigated systematically. The J_C of n-Cu doped samples exhibited better $J_C(H)$ values than corresponding their n-Cu deficit samples. The sample co-doped with n-C, n-Ho_2O_3 and n-Cu showed the best J_C performance in the entire field range studied. The poor grain connectivity in n-C + n-Ho_2O_3 doped MgB_2 was rectified by the addition of n-Cu. The variation in *a*-lattice parameter showed that carbon has been more effectively substituted in this sample. A J_C of 0.94×10^4 A/cm^2, which is 65 times higher than that of the pure sample, was obtained for this sample at 8 T and 5 K. The carbon substitution at boron site and intragrain distribution of nano-sized particles like HoB_4 and $MgCu_2$ with good flux pinning ability were responsible for this enhancement.
- MgB_2 monofilamentary wires were prepared by *in situ* PIT method. From the comparative study of the properties of the superconducting wires sheathed with four commonly available and relatively inexpensive sheath materials, namely Cu, Ni, Fe and SS, and heat treated at various temperatures, it was found that the Fe sheath was most suitable for the practical applications. A sintering temperature of 650 °C was found to be optimal for pure MgB_2 wires with Fe sheath. The study was carried out on the basis of applications of the wires using cryogen free cryocoolers. Based on this experimental study, Fe was chosen as the sheath material for the sample preparation for the further studies on MgB_2 superconducting wires.
- Multifilamentary MgB_2 wires were prepared with Ni as the outer sheath and Fe as the barrier material. OFHC copper was used as the stabilizer material for better

thermal stability of the wires. Both self-field and in-field transport characterizations were done on these wires and the results were promising for practical applications.

- Based on the results on carbon doping in bulk MgB_2, 0.1 at.% of nano-carbon was selected to dope in the wires. Since the reaction environment was different from the bulk, the doped wire samples were heat treated at three different temperatures. The transport $J_C(H)$ measurements done up to 8 T at 4.2 K showed that the sample which was heat treated at 750 °C has greater values of J_C than other samples at high magnetic fields. The enhanced H_{C2}, lattice strains and defects created by carbon substitution and the grain boundary pinning were found to be the reasons. With this optimized heat treatment temperature further co-doping studies were taken up. The results of co-doping study in wires were almost the same as in the case of bulk.
- The effect of bending strain on the J_C of MgB_2/Fe monofilamentary wire was studied for both R&B and B&R set of wires. At a bending diameter of 5 cm, only ~ 28 % of the J_C of straight wire was preserved in R&B wire. The porous nature and lower densification in monofilamentary wire were the main reason for such severe reduction. The variation in J_C of B&R set was much lower.
- MgB_2 multifilamentary wires with 4, 8 and16 filaments were prepared and effect of bending strain on J_C was studied. The R&B set of wires showed considerable degradation in J_C with decrease in bending diameter; but the rate of degradation was found to be decreasing with increasing the number of filaments. At 5 cm bending diameter, 16-filamentary wire retained ~ 68 % of initial J_C, whereas the variation in J_C of B&R set was not significant in multi-wires too.
- Excess Mg addition in large proportions was found to be very effective in enhancing both self-field critical current density and electromechanical properties of MgB_2 superconductor wires. The wire with a composition of 6Mg+2B was heat treated at 600 °C for 5 hours to obtain a microstructure wherein micrometer thick, layered cores of MgB_2 embedded in magnesium metal. The metallic matrix formed by Mg held MgB_2 superconductor layer within, and provided better bending strain tolerance to superconducting current. The J_C of wires of both R&B

and B&R sets hardly degraded even at a bending diameter of 5 cm. Only 3 % reduction in J_C was observed in R&B wire bent at 5 cm diameter. The method of excess Mg addition opens up new avenues to fabricate MgB_2 coils for practical applications even by the 'react and wind' approach.

7.3 Future directions

Although promising results were obtained, there remains scope for further investigation on various aspects. A few of them are listed below.

- The n-C is a main ingredient in all co-doping studies in this work. Although it is found to have a major role in enhancing $J_C(H)$, higher heat treatment temperature is needed for effective substitution. Since grain boundary pinning has also a major role in the enhancement of $J_C(H)$ in MgB_2, low temperature heat treatment is preferred to reduce the grain size. This situation could be addressed by exploring suitable hydrocarbon and metallic element combination as dopants.
- Since the density of the samples prepared through in *situ* route is much less than the theoretical density of MgB_2 innovative preparation techniques need to be found out to reduce the porosity.
- More optimization in processing parameters of excess Mg addition is to be done with emphasis on microstructure evolution to exploit maximum output.
- Development of excess Mg added multifilamentary wires and enhancement of in-field transport properties are necessary for high field applications.
- Fabrication and testing of prototype superconductor coils using excess Mg added multifilamentary wires by 'react and wind' approach is needed to evaluate the process and its scalability.

List of Abbreviations

at.%	Atomic percentage
vol.%	Volume percentage
wt.%	Weight percentage
AC	Alternating Current
B&R	Bend and React
BCS	Bardeen Cooper and Schrieffer
BRH	Burned Rice Husk
BSCCO	Bismuth Strontium Calcium Copper Oxide
CNT	Carbon Nano Tube
DC	Direct Current
EDS	Energy Dispersive X-Ray Spectrum
FLL	Flux Line Lattice
FWHM	Full Width at Half Maximum
GL	Ginzburg-Landau
GPIB	General Purpose Interface Board
HGMS	High Gradient Magnetic Separator
HIP	Hot Isostatic Pressing
HPCVD	Hybrid Physical-Chemical Vapour Deposition
HPS	High Pressure Sintering
HTS	High Temperature Superconductor
ICDD	International Center for Diffraction Data
ID	Inside Diameter
IMD	Internal Mg Diffusion
IPR	Institute for Plasma Research
ITER	Thermonuclear Experimental Reactor
JNCASR	Jawaharlal Nehru Centre for Advanced Scientific research
LHC	Large Hadron Collider
LHe	Liquid Helium
LN2	Liquid Nitrogen
LTS	Low Temperature Superconductor
Mg-RLI	Mg-Reactive Liquid Infiltration
MRI	Magnetic Resonance Imaging
NIIST	National Institute for Interdisciplinary Science and Technology
NMR	Nuclear Magnetic Resonance
OD	Outside Diameter
PC	Personal Computer

PDF	Powder Diffraction File
PIST	Powder In Sealed Tube
PIT	Powder In Tube
PPMS	Physical Property Measurement System
R&W	React & Wind
R&W	React & Bend
RE	Rare Earth
REO	Rare Earth Oxide
RRCAT	Raja Ramanna Centre for Advanced Technology
RRR	Residual Resistivity Ratio
RSFQ	Rapid Single Flux Quantum
SEI	Secondary Electron Imaging
SEM	Scanning Electron Microscopy
SFCL	Superconductor Fault Current Limiter
SMES	Superconducting Magnetic Energy Storage
SQUID	Superconducting Quantum Interference Device
SS	Stainless Steel
TEM	Transmission Electron Microscopy
VSM	Vibrating Sample Magnetometer
W&R	Wind and React
XRD	X-Ray Diffraction
YBCO	Yttrium Barium Copper Oxide
ZFC	Zero Field Cooling

List of Symbols

a, b, c	Sample dimensions
a, *c*	Lattice parameters
d	Inter atomic spacing
h, *k*, *l*	Miller indices of crystal planes
Å	Angstrom unit
T	Temperature
I	Current
V	Voltage
M	Magnetization
H	Magnetic field
R	Resistance
ρ	Resistivity
χ	Magnetic Susceptibility
T_C	Critical temperature (Transition temperature)
ΔT_C	Width of Transition (Difference between and T_{Conset} and $T_{Coffset}$)
I_C	Critical Current
J_C	Critical Current density
J_E	Engineering Critical Current density
$J_{C(H)}$	In-field Critical Current density
H_C	Critical Field
H_{C1}	Lower Critical Field
H_{C2}	Upper Critical Field
H_{irr}	Irreversibility Field
F_P	Flux pinning force density
F_{Pmax}	Maximum flux pinning force density
ξ	Coherence length
λ	Penetration depth
Δ(0)	BCS energy gap at 0 K
ω_D	Debye frequency
υ_F	Fermi frequency
κ	Ginzburg-landau parameter
α	Isotope coefficient
ζ	Bending strain

Details of publications

International SCI Journals

1) **Syju Thomas**, S Rahul, K M Devadas, Neson Varghese and U Syamaprasad "Co-addition of nano-carbon and nano-silica: An effective method for improving the in-field properties of magnesium diboride superconductor", Materials Chemistry and Physics 148 (2014) 190.
2) **Syju Thomas**, Neson Varghese, S Rahul, K M Devadas, K Vinod, U Syamaprasad "Enhancement of bending strain tolerance and current carrying property of MgB_2 based multifilamentary wires", Cryogenics 52 (2012) 767.
3) K M Devadas, S Rahul, **Syju Thomas**, Neson Varghese, S Pradhan and U Syamaprasad "An effort toward development of MgB_2-based current leads with 2000-A rating", IEEE Transactions on Applied Superconductivity 24 (2014) 6200205.
4) K M Devadas, S Rahul, **Syju Thomas**, Neson Varghese, A Sundaresan, and U Syamaprasad "Transport properties of sealed MgB_2/Fe/Ni multifilamentary wires heat treated in air", Journal of Alloys and Compounds 509 (2011) 8038.
5) Neson Varghese, K Vinod, S Rahul, P Anees, K M Devadas, **Syju Thomas**, Shipra, A Sundaresan, S B Roy and U Syamaprasad "Effect of carbon substitution on the superconducting properties of nano carbon, diamond and SiC doped MgB_2", Journal of American Ceramics Society 94 (2011) 1133.
6) Neson Varghese, K Vinod, S Rahul, K M Devadas, **Syju Thomas**, S Pradhan, U Syamaprasad "Influence of nano-Cu additive on MgB_2 phase formation, processing temperature and transport properties", Journal of Applied Physics 109, (2011) 033902.
7) S Rahul, N Varghese, K Vinod, K M Devadas , **Syju Thomas**, Anees P ,M K Chattopadhyay, S B Roy, U Syamaprasad "Combined addition of nano diamond and nano SiO_2, an effective method to improve the infield critical current density of MgB_2 superconductor", Materials Research Bulletin 46 (2011) 2036 .
8) K Vinod, Neson Varghese, S Rahul, K M Devadas, **Syju Thomas** U Syamaprasad "On the current transfer length and current sharing in short length MgB_2 wires", Superconductor Science and Technology 23 (2010) 105002 .

Articles presented in International/National Conferences

1. **Syju Thomas**, Rahul S, K M Devadas, Neson Varghese, A sundaresan and U Syamaprasad, "MgB_2 Superconductor with Highly Enhanced In-Field Critical Current Density by Multicomponent Doping", Presented at the *International Conference on Advanced Functional Materials* (ICAFM 2014) held at NIIST, Thiruvananthapuram on February 19-21, 2014
2. **Syju Thomas**, Neson Varghese, S Rahul, K M Devadas K Vinod and U Syamaprasad "Enhancement of bending strain tolerance and current carrying property of MgB_2 based multifilamentary wires", Presented at the *Asian Conference on Applied Superconductivity & Cryogenics* (ACASC 2011*)* held at IUAC, New Delhi on November 16-18, 2011
3. K M Devadas, Neson Varghese, S Rahul, **Syju Thomas**, S Pradhan, P Guruswamy and U Syamaprasad, "Development of MgB_2 based conduction cooled current leads with 1000 A rating", Presented at the *Asian Conference on Applied Superconductivity & Cryogenics* (ACASC 2011) held at IUAC, New Delhi on November 16- 18, 2011
4. Neson Varghese, S Rahul, K M Devadas, **Syju Thomas**, A Sundaresan, S B Roy and U Syamaprasad, "A comparative study on the structural and superconducting properties of carbon variants doped MgB_2", Presented at the *Asian Conference on Applied Superconductivity & Cryogenics* (ACASC 2011) held at IUAC, New Delhi on November 16-18, 2011
5. S Rahul, K M Devadas, **Syju Thomas**, Neson Varghese, K Vinod, S Pradhan, M K Chattopadhyay, S B Roy, and U Syamaprasad, "Transport properties of MgB_2 based multifilamentary wires heat treated in air", Presented at the *Asian Conference on Applied Superconductivity & Cryogenics* (ACASC 2011) held at IUAC, New Delhi on November 16-18, 2011
6. S. Rahul, Neson Varghese, K. Vinod, K. M. Devadas, **Syju Thomas**, P. Anees, M. K. Chattopadhyay, S. B. Roy, R. P. Aloysius and U. Syamaprasad, "Nano diamond and nano SiO_2 – An effective combination to improve the in-field properties of MgB_2 superconductor", Presented at the *55th DAE Solid State Physics Symposium* (DAE SSPS 2010) held at Manipal on December 26-30, 2010
7. K. M. Devadas, Neson Varghese, K. Vinod, S. Rahul, **Syju Thomas**, J. B. Anooja, A. Sundaresan, S.B. Roy and U. Syamaprasad, "Enhanced superconducting properties of MgB_2 by carbon substitution using carbon containing nano additives", Presented at the *55th DAE Solid State Physics Symposium* (DAE SSPS 2010) held at Manipal on December 26-30, 2010
8. Neson Varghese, K. Vinod, S. Rahul, K. M. Devadas, **Syju Thomas**, P. M. Aswathy, S. Pradhan and U. Syamaprasad, "Lowering the sintering temperature of MgB_2/Fe wires with high transport current by nano-Cu doping", Presented at the *55th DAE Solid State Physics Symposium* (DAE SSPS 2010) held at Manipal on December 26-30, 2010